Published for SISSA by Springer

Received: December 17, 2024
Accepted: March 20, 2025
Published: May 6, 2025

Test of lepton flavour universality in W-boson decays into electrons and τ-leptons using pp collisions at $\sqrt{s} = 13$ TeV with the ATLAS detector

The ATLAS collaboration

E-mail: atlas.publications@cern.ch

Abstract: A measurement of the ratio of the branching fractions, $R_{\tau/e} = B(W \to \tau\nu)/B(W \to e\nu)$, is performed using a sample of W bosons originating from top-quark decays to final states containing τ-leptons or electrons. This measurement uses pp collisions at $\sqrt{s} = 13$ TeV, collected by the ATLAS experiment at the Large Hadron Collider during Run 2, corresponding to an integrated luminosity of 140 fb^{-1}. The $W \to \tau\nu_\tau$ (with $\tau \to e\nu_e\nu_\tau$) and $W \to e\nu_e$ decays are distinguished using the differences in the impact parameter distributions and transverse momentum spectra of the electrons. The measured ratio of branching fractions $R_{\tau/e} = 0.975 \pm 0.012\,(\text{stat.}) \pm 0.020\,(\text{syst.})$, is consistent with the Standard Model assumption of lepton flavour universality in W-boson decays.

Keywords: Flavour Physics, Hadron-Hadron Scattering, Tau Physics

ArXiv ePrint: 2412.11989

https://doi.org/10.1007/JHEP05(2025)038

JHEP05(2025)038

Contents

1 Introduction

The Standard Model (SM) [1–3] posits that the electroweak interactions of charged leptons (electrons, muons and τ-leptons) are identical. This feature, known as lepton flavour universality (LFU), is one of the foundational principles of the SM. Differences in the rates of electroweak processes among charged leptons are induced only via their mass differences, manifesting in phase space and radiative effects. Any violation of LFU would be an unambiguous signal of physics beyond the SM and would help to identify the principles that can be used to build a more comprehensive theory.

LFU has been extensively tested by measuring the couplings of the different generations of leptons to the W boson. Such studies have been performed in decays of τ-leptons, charged π and K mesons [4], and in leptonic decays of the W bosons [5]. No significant deviations from LFU have been observed in the charged-current decays of τ-leptons, π and K mesons, with experimental precision reaching about 0.1–0.2%. The precision of LFU tests in the decays of on-shell W bosons is lower. The ratios of the branching fractions of the W-boson decays into leptons are consistent with LFU, and the world-average values have a precision of 0.6–2%. Despite higher experimental uncertainties, probes of LFU in decays of on-shell W bosons offer sensitivity to different possible new physics effects compared to the decays of light particles [6–8].

The ratio of branching fractions $R_{\tau/\mu} \equiv B(W \to \tau\nu_\tau)/B(W \to \mu\nu_\mu)$ was measured at the LEP collider [9] and at the Large Hadron Collider (LHC) by the ATLAS [10] and CMS [11] collaborations. The measurements at LEP deviate from unity by more than two standard deviations, but the more precise subsequent measurements from ATLAS and CMS agree with the SM expectation. The Particle Data Group (PDG) average of all the measurements of $R_{\tau/\mu}$, accounting for the tension between them, is 1.002 ± 0.020 [5]. Recently,

JHEP05(2025)038

the ATLAS collaboration published a measurement of $R_{\mu/e} \equiv B(W \to \mu\nu_\mu)/B(W \to e\nu_e) = 0.9995 \pm 0.0044$ [12] with an improved precision compared to the current world average $R_{\mu/e} = 1.002 \pm 0.006$ [5]. The combined LEP result of $R_{\tau/e} \equiv B(W \to \tau\nu_\tau)/B(W \to e\nu_e) = 1.063 \pm 0.027$ deviates from the SM by more than two standard deviations like the LEP $R_{\tau/\mu}$ measurement [9]. The result of the CMS collaboration $R_{\tau/e} = 0.994 \pm 0.021$ [11] agrees with the SM expectation and differs from the corresponding LEP measurement.

This paper presents the first measurement of the ratio $R_{\tau/e}$ with the ATLAS detector using top-quark decays as a source of W bosons. The analysis complements the previous ATLAS measurement of $R_{\tau/\mu}$ and $R_{\mu/e}$ in W-boson decays by including another decay channel. Top-quark pair-production yields a clean source of W bosons, owing to the large $t\bar{t}$ production cross-section relative to expected background processes and efficient triggering. The SM predicts that the top quark decays almost exclusively into a Wb final state, and thus a measurement of the ratio of branching fractions $B(t \to \tau\nu b)/B(t \to e\nu b)$ provides a measurement of $R_{\tau/e}$. For the τ-lepton selection, the leptonic decay $\tau \to e\nu_e\nu_\tau$ is chosen over hadronic τ decays due to the smaller experimental uncertainties associated with the leptonic channel. In addition, selecting the electron in both the $W \to \tau\nu_\tau$ and $W \to e\nu_e$ final states results in a substantial reduction of the systematic uncertainties in the ratio $R_{\tau/e}$.

This paper is organised as follows. Section 2 presents the ATLAS detector, followed by a description of the data and Monte Carlo simulation samples used in the analysis in section 3. Section 4 details the physical objects and event selection criteria. The calibration of the signal modelling is discussed in section 5, and section 6 describes the estimate of background contributions. The statistical analysis and systematic uncertainties are covered in section 7, with the results and conclusions presented in sections 8 and 9, respectively.

2 ATLAS detector

The ATLAS detector [13] at the LHC covers nearly the entire solid angle around the collision point.[1] It consists of an inner tracking detector surrounded by a thin superconducting solenoid, electromagnetic and hadronic calorimeters, and a muon spectrometer incorporating three large superconducting air-core toroidal magnets.

The inner-detector system (ID) is immersed in a 2 T axial magnetic field and provides charged-particle tracking in the range of $|\eta| < 2.5$. The high-granularity silicon pixel detector covers the vertex region and typically provides four measurements per track, the first hit generally being in the insertable B-layer (IBL) installed before Run 2 [14, 15]. It is followed by the SemiConductor Tracker (SCT), which usually provides eight measurements per track. These silicon detectors are complemented by the transition radiation tracker (TRT), which enables radially extended track reconstruction up to $|\eta| = 2.0$. The TRT also provides

[1] ATLAS uses a right-handed coordinate system with its origin at the nominal interaction point (IP) in the centre of the detector and the z-axis along the beam pipe. The x-axis points from the IP to the centre of the LHC ring, and the y-axis points upwards. Polar coordinates (r, ϕ) are used in the transverse plane, ϕ being the azimuthal angle around the z-axis. The pseudorapidity is defined in terms of the polar angle θ as $\eta = -\ln\tan(\theta/2)$ and is equal to the rapidity $y = \frac{1}{2}\ln\left(\frac{E+p_z}{E-p_z}\right)$ in the relativistic limit. Angular distance is measured in units of $\Delta R \equiv \sqrt{(\Delta y)^2 + (\Delta\phi)^2}$. The transverse momentum p_{T} is defined as the projection of the momentum of a particle on the plane perpendicular to the beam pipe in the centre of ATLAS detector.

electron identification information based on the fraction of hits (typically 30 in total) above a higher energy-deposit threshold arising from transition radiation.

The calorimeter system covers the pseudorapidity range $|\eta| < 4.9$. Within the region $|\eta| < 3.2$, electromagnetic calorimetry is provided by barrel and endcap high-granularity lead/liquid-argon (LAr) calorimeters, with an additional thin LAr presampler covering $|\eta| < 1.8$ to correct for energy loss in material upstream of the calorimeters. Hadronic calorimetry is provided by the steel/scintillator-tile calorimeter, segmented into three barrel structures within $|\eta| < 1.7$, and two copper/LAr hadronic endcap calorimeters. The solid angle coverage is completed with forward copper/LAr and tungsten/LAr calorimeter modules optimised for electromagnetic and hadronic energy measurements, respectively.

The muon spectrometer (MS) comprises separate trigger and high-precision tracking chambers measuring the deflection of muons in a magnetic field generated by the superconducting air-core toroidal magnets. The field integral of the toroids ranges between 2.0 and 6.0 T m across most of the detector. Three layers of precision chambers, each consisting of layers of monitored drift tubes, cover the region $|\eta| < 2.7$, complemented by cathode-strip chambers in the forward region, where the background is highest. The muon trigger system covers the range $|\eta| < 2.4$ with resistive-plate chambers in the barrel, and thin-gap chambers in the endcap regions.

The luminosity is measured mainly by the LUCID–2 [16] detector that records Cherenkov light produced in the quartz windows of photomultipliers located close to the beampipe.

Events are selected by the first-level trigger system implemented in custom hardware, followed by selections made by algorithms implemented in software in the high-level trigger [17]. The first-level trigger accepts events from the 40 MHz bunch crossings at a rate below 100 kHz, which the high-level trigger further reduces to record complete events to disk at about 1 kHz.

A software suite [18] is used in data simulation, in the reconstruction and analysis of real and simulated data, in detector operations, and in the trigger and data acquisition systems of the experiment.

3 Data and simulated events samples

The measurement uses *pp* collision data recorded by the ATLAS detector from 2015 to 2018 at a centre-of-mass energy of $\sqrt{s} = 13$ TeV. Each recorded event includes on average 33 additional inelastic collisions because of the high instantaneous luminosity of the LHC. These background collisions are referred to as *pile-up*. After the application of data-quality requirements [19], the data sample corresponds to an integrated luminosity of $140.1 \pm 1.2\,\mathrm{fb}^{-1}$ [20].

Samples of simulated events were produced using Monte Carlo (MC) techniques to model different SM processes. After event generation of the process of interest for each sample, the detector response was modelled using either the full ATLAS detector simulation based on Geant4 toolkit [21] or a fast simulation that relied on a parametrisation of the calorimeter response [22]. The effect of pile-up was modelled by overlaying the simulated hard-scattering event with inelastic *pp* collisions generated with Pythia 8.186 [23] using the NNPDF2.3lo [24] set of parton distribution functions (PDF) and the A3 set of tuned parameters [25]. The data and MC simulated events were passed through the same reconstruction and analysis procedures.

JHEP05(2025)038

For all MC samples simulating the production of top quarks, the mass of the top quark was set to $m_{\text{top}} = 172.5$ GeV. The mass of the Higgs boson was set to 125 GeV. In all samples where PYTHIA was used to simulate the parton shower (PS) and hadronisation, it used the A14 set of tuned parameters [26] and the NNPDF2.3LO set of PDFs. In all samples where the PYTHIA or HERWIG [27, 28] generators were used to simulate the PS and hadronisation, the decays of bottom and charm hadrons were simulated using the EVTGEN program [29].

The production of $t\bar{t}$ events was modelled using the POWHEG BOX v2 [30–33] generator, which provides matrix elements (ME) at next-to-leading order (NLO) in the strong coupling constant α_s, and the NNPDF3.0NLO [34] PDF set. The h_{damp} parameter, which effectively regulates the high-transverse momentum (p_T) radiation against which the $t\bar{t}$ system recoils, was set to $1.5\, m_{\text{top}}$ [35]. The functional form of the renormalisation and factorisation scales was set to $\sqrt{m_{\text{top}}^2 + p_T^2}$. The events were passed through PYTHIA 8.230 [36] for the PS and hadronisation.

An additional re-weighting was applied to the $t\bar{t}$ events to match the calculations at next-to-next-to-leading-order (NNLO) in α_s and NLO in α_{EW} [37]. The applied weights are based on the parton-level distributions, after final state radiation, and are derived as a function of the top-quark and anti-top-quark p_T, and the mass and transverse momentum of the $t\bar{t}$ system. The re-weighting improves the agreement between data and MC simulation.

The $t\bar{t}$ sample was normalised to the cross-section prediction at NNLO in α_s including the resummation of next-to-next-to-leading logarithmic (NNLL) soft-gluon terms calculated using TOP++ 2.0 [38–44]. For pp collisions at a centre-of-mass energy of $\sqrt{s} = 13$ TeV, this cross-section corresponds to $\sigma(t\bar{t})_{\text{NNLO+NNLL}} = 832 \pm 45$ pb. The uncertainties in the cross-section due to the PDF and α_s were calculated using the PDF4LHC15 prescription [45] with the MSTW2008NNLO [46, 47], CT10NNLO [48, 49] and NNPDF2.3LO PDF sets in the five-flavour scheme, and were added in quadrature to the effect of the scale uncertainty.

In addition to $t\bar{t}$ events, the contribution of the Wt and $t\bar{t}+X$ ($X = W, Z, H$) production processes are treated as signal. For the Wt process, the leptons (electron or τ-lepton) coming from the top-quark and W-boson decays are included in the analysis as in both cases they are produced in the decays of a real W boson.

Single-top Wt associated production was modelled using POWHEG BOX v2 and PYTHIA 8.230. The renormalisation and factorisation scales were set to m_{top}. A diagram removal scheme [50] was employed to handle the interference with $t\bar{t}$ production [35]. The inclusive cross-section of Wt production was corrected to the theory prediction calculated at NLO in α_s with NNLL soft-gluon corrections [51, 52] yielding $\sigma(Wt)_{\text{NLO+NNLL}} = 71.7 \pm 3.8$ pb. The uncertainty in the cross-section due to the PDF was calculated using the MSTW2008NNLO PDF set, and was added in quadrature to the uncertainty of $\sigma(Wt)$.

The production of $t\bar{t}V$ ($V = W, Z$) events was modelled using the MADGRAPH5_AMC@NLO 2.3.3 [53] generator, which provided MEs at NLO in α_s with the NNPDF3.0NLO PDF set. The functional form of the renormalisation and factorisation scales was set to $0.5 \times \sum_i \sqrt{m_i^2 + p_{T,i}^2}$, where the sum runs over all the particles generated from the ME calculation. Top quarks were decayed at leading-order (LO) using MADSPIN [54, 55]. The events were passed through PYTHIA 8.210 for the PS and hadronisation. The cross-sections were calculated at NLO in α_s and NLO in α_{EW}

accuracy using MadGraph5_aMC@NLO as reported in ref. [56]. In the case of $t\bar{t}l^+l^-$ ($l = e, \mu, \tau$), the cross-section was scaled by an off-shell correction estimated at the one-loop level in α_s. The predicted values at $\sqrt{s} = 13\,\text{TeV}$ are $0.88^{+0.09}_{-0.11}$ pb and $0.60^{+0.08}_{-0.07}$ pb for $t\bar{t}Z$ and $t\bar{t}W$, respectively, where the uncertainties were estimated from variations of α_s and the renormalisation and factorisation scales.

The production of $t\bar{t}H$ events was modelled using the Powheg Box v2 [30–33, 57] generator. The functional form of the renormalisation and factorisation scales was set to $\sqrt[3]{m_T(t) \cdot m_T(\bar{t}) \cdot m_T(H)}$, where $m_T = \sqrt{m^2 + p_T^2}$ is the transverse mass of a generated particle, m is its mass, and p_T is its transverse momentum. The events were passed through Pythia 8.230. The cross-section was calculated at NLO in α_s and NLO in α_{EW} accuracy using MadGraph5_aMC@NLO as reported in ref. [56]. The predicted value at $\sqrt{s} = 13\,\text{TeV}$ is 507^{+35}_{-50} fb, where the uncertainties were estimated from variations of α_s and the renormalisation and factorisation scales.

The background for this analysis comes from two main sources. The first is the production of Z bosons decaying to pairs of leptons. The second source includes all processes in which the probe electrons do not come from the decays of real W or Z bosons. Such electrons are referred to as *fake* electrons.

The production of most V+jets ($V = Z, W$) events was simulated with the Sherpa 2.2.11 [58] generator. For the simulation of $Z \to \tau^+\tau^-$ events Sherpa 2.2.14 was used. The simulation setup involved MEs with NLO accuracy in α_s for up to two partons, and LO accuracy for up to four partons calculated with the Comix [59] and OpenLoops [60–62] libraries. The default Sherpa PS [63] based on Catani-Seymour dipole factorisation and the cluster hadronisation model [64] were used. They employed the dedicated set of tuned parameters developed by the Sherpa authors and the NNPDF3.0nnlo [34] PDF set. The NLO MEs for a given jet multiplicity were matched to the PS using a colour-exact variant of the MC@NLO algorithm [65]. Different jet multiplicities were then merged into an inclusive sample using an improved CKKW matching procedure [66, 67] which was extended to NLO accuracy using the MEPS@NLO prescription [68].

The production of diboson final states (VV) was simulated with the Sherpa 2.2.1 or 2.2.2 generator depending on the process, including off-shell effects and Higgs boson contributions, where appropriate. Fully leptonic final states and semileptonic final states, where one boson decays leptonically and the other hadronically, were generated using MEs at NLO in α_s for up to one additional parton and at LO in α_s for up to three additional parton emissions. Samples for the loop-induced processes $gg \to VV$ were generated using LO-accurate MEs for up to one additional parton emission for both the cases of fully leptonic and semileptonic final states. The ME calculations were matched and merged with the Sherpa PS based on Catani-Seymour dipole factorisation [59, 63] using the MEPS@NLO prescription [65–68]. The virtual QCD corrections were provided by the OpenLoops library [60–62]. The NNPDF3.0nnlo set of PDFs was used, along with the dedicated set of tuned PS parameters developed by the Sherpa authors.

Events featuring at least one fake lepton originate from $t\bar{t}$, $t\bar{t} + X$ ($X = W, Z, H$), or Wt production processes. The simulation of such events was described above. Single-top-quark s- and t-channel production can also produce dilepton events with at least one fake lepton. These processes were modelled using the Powheg Box v2 [31–33, 69] generator. The functional form of the renormalisation and factorisation scales was set to $\sqrt{m_b^2 + p_{\mathrm{T},b}^2}$ for t-channel following the recommendation of ref. [69], and to m_{top} for s-channel. The events were processed through Pythia 8.230.

Any possible contribution of other sources of fake leptons was taken into account in the correction factors measured using data as explained in section 6.

The uncertainties related to the modelling of the signal and background production were estimated by comparing the baseline MC samples described above with different MC generators or a modified configuration of the baseline MC generators. More details of these studies are given in section 7. Here, the description of the alternative MC samples is given.

The uncertainty due to the choice of the PS and hadronisation model used in $t\bar{t}$ and Wt production was evaluated with a sample generated with Powheg Box v2 for the hard-scatter simulation but passed through Herwig 7.1.3 for the PS and hadronisation. The samples employ the Herwig 7.1 default set of tuned parameters and the MMHT2014lo [70] PDF set.

The baseline $t\bar{t}$ and Wt samples were generated with $h_{\mathrm{damp}} = 1.5\ m_{\mathrm{top}}$. A variation of the h_{damp} value to 3.0 m_{top} was used to evaluate the systematic uncertainty related to this parameter.

The NLO matching uncertainty was evaluated by comparing the baseline $t\bar{t}$ and Wt samples with alternative samples obtained by setting the $\mathtt{pT}_{\mathrm{hard}}$ parameter of Pythia 8 to one (the default value is zero). This parameter regulates the definition of the vetoed region of the showering, important to avoid holes or overlap in the phase space filled by Powheg and Pythia. This follows the recommendation of refs. [71, 72].

An additional source of uncertainty in the PS is the modelling of the recoil for gluons emitted from b-quarks in the $t \to Wb$ process. The baseline $t\bar{t}$ sample employs a scheme where partons recoil against b-quarks. An alternative sample was generated with identical settings to the baseline ones, except for a modified recoil scheme. Here, the gluon emissions from the PS of the b-quark were made to recoil against the top quark itself. This scheme changes the modelling of second and subsequent gluon emissions.

The baseline Powheg+Pythia 8 sample of Wt production was generated using the diagram removal scheme to model the interference between the $t\bar{t}$ and Wt production. To evaluate the corresponding uncertainty, the baseline simulation was compared with an alternative sample generated using the diagram subtraction scheme [35, 50].

To estimate the systematic uncertainty related to the electron reconstruction efficiency, an alternative sample of $Z(\to e^+e^-)+$ jets events was used, which was simulated with MadGraph5_aMC@NLO 2.2.2 [53], using MEs at NLO in α_{s} with up to four final-state partons. The ME calculation employed the NNPDF2.3lo set of PDFs. Events were passed through Pythia 8.186 for the modelling of the PS and hadronisation. The overlap between ME and PS emissions was removed using the CKKW-L merging procedure [73, 74]. The Z+jets samples were normalised to a NNLO prediction [75].

4 Event reconstruction and selection

A sample of $t\bar{t}$ events, in which the W bosons from both t and $\bar{t}$ quarks decay to leptons, is selected for the measurement. With this selection, the tag-and-probe approach is used.

One charged lepton (muon or electron) from the decay of the $t\bar{t}$ pair is used as the *tag*. The other lepton (electron), which is called the *probe*, is used in an unbiased way to determine whether the electron is directly produced in the decay $W \to e\nu_e$ or via an intermediate decay $W \to \tau\nu_\tau \to e\nu_e\nu_\tau\nu_\tau$. In the first case, the probe electrons are called *prompt* and denoted by $W \to e$, while in the second case they are denoted by $W \to \tau \to e$.

To distinguish between electrons from $W \to e$ and $W \to \tau \to e$ decays, the analysis exploits differences in the p_{T} spectra of the probe electrons together with the displacement of the intermediate τ-lepton decays from the pp collision point (primary vertex) owing to the τ-lepton lifetime. The quantity reflecting the displacement of the vertex of the τ-lepton decay from the primary vertex is the transverse impact parameter (d_0) of the electron track with respect to the beamline. This quantity is defined as the distance of closest approach of the extrapolated track to the beamline in the transverse plane. Electrons originating from the $W \to \tau\nu_\tau \to e\nu_e\nu_\tau\nu_\tau$ decays generally have lower p_{T} due to energy lost to undetected neutrinos. These electrons also have on average a larger $|d_0|$ because of the non-zero lifetime of the τ-lepton. In contrast, the electrons from prompt decays are produced directly at the primary vertex, and therefore their measured value of d_0 depends mainly on the detector resolution.

Electrons are reconstructed using the clusters of energy deposits in the electromagnetic calorimeter matched to tracks in the ID. They must pass the *tight* (for both isolation and quality) requirements of refs. [76, 77]. Muons are reconstructed by combining tracks from the ID with matching tracks reconstructed in the MS. They must pass the *medium* quality and *tight* isolation criteria defined in ref. [78]. The charged tracks of the selected electrons and muons must be consistent with the primary vertex and have $|d_0| < 0.5$ mm. These requirements reduce the contribution of fake leptons, which becomes large compared to the signal for $|d_0| > 0.5$ mm. The pseudorapidity of the electromagnetic cluster associated with the electron (η_{cl}) must be $|\eta_{\mathrm{cl}}| < 2.47$. The electrons with $1.37 < |\eta_{\mathrm{cl}}| < 1.52$ are not used in the analysis to exclude the transition region between the barrel and endcap electromagnetic calorimeters. The pseudorapidity of the selected muons must be $|\eta| < 2.5$. All these requirements are applied to both tag and probe leptons. The tag lepton must pass a suite of single-muon or single-electron triggers [79–81]. No trigger requirement for the probe electron is applied. The lowest electron p_{T} trigger threshold is 24 GeV in 2015 and 26 GeV in 2016–2018. The lowest muon p_{T} trigger threshold is 20 GeV in 2015 and 26 GeV in 2016–2018. The efficiency of the triggers reached the plateau for electrons with $p_{\mathrm{T}} > 27$ GeV and muons with $p_{\mathrm{T}} > 27.3$ GeV. Consequently, the tag electrons must have $p_{\mathrm{T}} > 27$ GeV and tag muons must have $p_{\mathrm{T}} > 27.3$ GeV. The probe electrons must have $7 < p_{\mathrm{T}} < 250$ GeV. The fraction of electrons with $p_{\mathrm{T}} > 250$ GeV from $W \to \tau\nu_\tau$ is much smaller than from other sources, and the upper cut on p_{T} of probe electrons is applied to simplify the measurement without loss in accuracy.

Jets are reconstructed using the anti-k_t algorithm [82, 83] with a radius parameter R = 0.4 applied to particle flow objects based on tracks and topological clusters calibrated as specified in ref. [84]. The jet energy scale and resolution are calibrated using simulations with in situ corrections obtained from data [85]. Jets are required to have $p_{\mathrm{T}} > 25$ GeV and $|\eta| < 2.5$. To reduce the pile-up contribution, an additional requirement for jets with $p_{\mathrm{T}} < 60$ GeV and $|\eta| < 2.4$ is applied based on a dedicated jet vertex tagger (JVT) algorithm which is designed to discriminate between jets produced in the hard-scatter process and those from pile-up [86].

JHEP05(2025)038

To avoid double counting electrons and muons within jets, an overlap removal procedure is implemented. Specifically, all electrons that share a track with another electron are removed, as are electrons sharing a track with a muon. Additionally, the closest jet found within a $\Delta R = 0.2$ of a reconstructed electron is removed. Any electron subsequently found within $\Delta R = 0.4$ of a jet is also removed. Any jet with fewer than three tracks associated to it and found within $\Delta R = 0.2$ of a muon is removed. Any muon subsequently found within $\Delta R = 0.4$ of a jet is removed.

Jets likely to contain b hadrons are identified as b-jets using the `DL1r` algorithm [87], which employs a deep neural network. Such jets are referred to as *b-tagged* in the following. The network utilises distinctive features of b-hadrons, such as the impact parameters of tracks and the displaced vertices reconstructed in the ID. The b-tagging efficiency in simulated $t\bar{t}$ events is approximately 70%.

Events containing exactly one tag lepton (muon or electron), one probe electron, and at least two b-tagged jets are selected for this measurement. The tag and probe leptons must have opposite electric charge. The events with μ_{tag} and e_{probe}, and with e_{tag} and e_{probe} are analysed separately. These channels are referred to as μe and ee, respectively. To further refine the selection, several criteria based on the invariant mass of the tag and probe leptons ($m_{\ell\ell}$) are applied. Only events with $m_{\ell\ell} > 15\,\text{GeV}$ are selected to suppress the contribution from fake probe electrons. Additionally, the ee channel events with $|m_{e^+e^-} - m_Z| < 5\,\text{GeV}$ are excluded, to remove events that could come from Z-boson production.[2] Finally, the ee events where both electrons satisfied the tag criteria are analysed twice, with each electron considered in turn the tag or probe.

The sample of events passing this selection is referred to as *nominal* in the following.

5 Electron impact parameter calibration

The impact parameter d_0 is one of the two quantities used to separate the electrons produced in τ-lepton decays from other sources. An accurate calibration of the d_0 distribution in simulation is essential for the measurement of $R_{\tau/e}$. The impact parameter d_0 is measured relative to the beamline. Therefore, the shape of the d_0 distribution of prompt electrons is mainly determined by the detector resolution and the precision of the beamspot measurement, and can be obtained in data using the $Z \to e^+e^-$ decay. A clean sample of such events is obtained by requiring that two electrons satisfy the same criteria as in the nominal event selection, but with the invariant mass of the e^+e^- pair satisfying $|m_{e^+e^-} - m_Z| < 10\,\text{GeV}$. At least two jets are required in the event to reproduce the track activity around the electron as in the nominal sample. However, no b-tagging condition must be fulfilled. This selection results in a sample of 4.3 million electrons, which is referred to in the following as the Z data sample. The contribution of non-prompt electrons is estimated by using the MC simulation to be about 0.4%. By using the Z data sample to calibrate the d_0 distribution of prompt electrons, the uncertainties due to the shape of the d_0 distribution are considerably reduced.

The d_0 distribution depends on the electron p_{T} and η. Consequently, the shape of the d_0 distribution of prompt electrons is determined separately in 39 kinematic bins of p_{T} and

[2] The mass of Z boson is taken to be $m_Z = 91.188\,\text{GeV}$ [5].

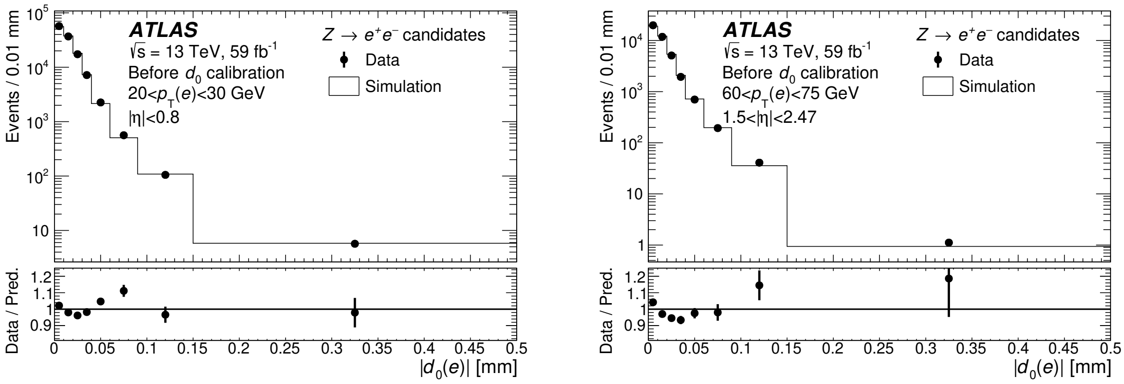

(a) (b)

Figure 1. Example distributions of $|d_0|$ of the probe electrons for two kinematic bins in the Z data and simulation samples (before $|d_0|$ calibration) collected in the 2018 data-taking period. The data are represented by black markers and the simulation prediction as the histogram. Only the statistical uncertainties in the data are shown. The distribution of the simulated events in each kinematic bin is normalised to the number of data events in that bin. The bottom panels show the ratio of the data to the simulation prediction.

$|\eta|$. These bins are obtained by dividing the p_{T} range of 7–250 GeV into 13 bins and the $|\eta|$ range of 0–2.47 into three bins. The boundaries are optimised to have reasonable statistics in each bin. Figure 1 shows the comparison of $|d_0|$ distributions in data and MC simulation in two kinematic bins before the $|d_0|$ calibration is applied.

For the measurement of $R_{\tau/e}$, the d_0 distribution in each kinematic bin is taken from the Z data sample after subtracting the contribution of non-prompt electrons estimated from MC simulation. The resulting distributions $T_{ij}^{\mathrm{pr}}(d_0)$, which are referred to as d_0 *templates*, are normalised to unity. Here the indices i and j refer to the p_{T} and $|\eta|$ bins, respectively. Separate templates are used for data collected in different years (2015–2016, 2017, and 2018) because of the variation of the beam conditions and the alignment of the ID from year to year.

The d_0 distribution of prompt electrons with p_{T} in a range $p_{\mathrm{T}}^{\mathrm{min}} \leq p_{\mathrm{T}} < p_{\mathrm{T}}^{\mathrm{max}}$ is computed as

$$D^{\mathrm{pr}}(d_0, p_{\mathrm{T}}^{\mathrm{min}}, p_{\mathrm{T}}^{\mathrm{max}}) = \sum_{i=i_{\mathrm{min}}}^{i_{\mathrm{max}}} \sum_{j=1}^{3} f_{ij}^{\mathrm{pr}}\, T_{ij}^{\mathrm{pr}}(d_0). \tag{5.1}$$

Here, f_{ij}^{pr} is the fraction of prompt probe electrons produced in the $W \to e$ decay and contained in the kinematic bin ij relative to the total number of prompt probe electrons from the $W \to e$ decay in all bins. The outer sum ranges from i_{min} to i_{max}, the indices of the bins containing $p_{\mathrm{T}}^{\mathrm{min}}$ and $p_{\mathrm{T}}^{\mathrm{max}}$. The values of $p_{\mathrm{T}}^{\mathrm{min}}$ and $p_{\mathrm{T}}^{\mathrm{max}}$ correspond to the definition of p_{T} bins used for the measurement of $R_{\tau/e}$ ($7 < p_{\mathrm{T}} < 10$ GeV, $10 < p_{\mathrm{T}} < 20$ GeV, and $20 < p_{\mathrm{T}} < 250$ GeV) as defined in section 7. The same method and d_0 templates are used to obtain the d_0 distribution of prompt electrons from other sources (i.e., non-resonant Drell-Yan production of e^+e^- and VV production), with the fractions f_{ij} being computed from MC simulation for each source separately. Figure 2 shows the comparison of $|d_0|$ distributions of the probe electrons with $20 < p_{\mathrm{T}} < 250$ GeV in the nominal sample before and after

JHEP05(2025)038

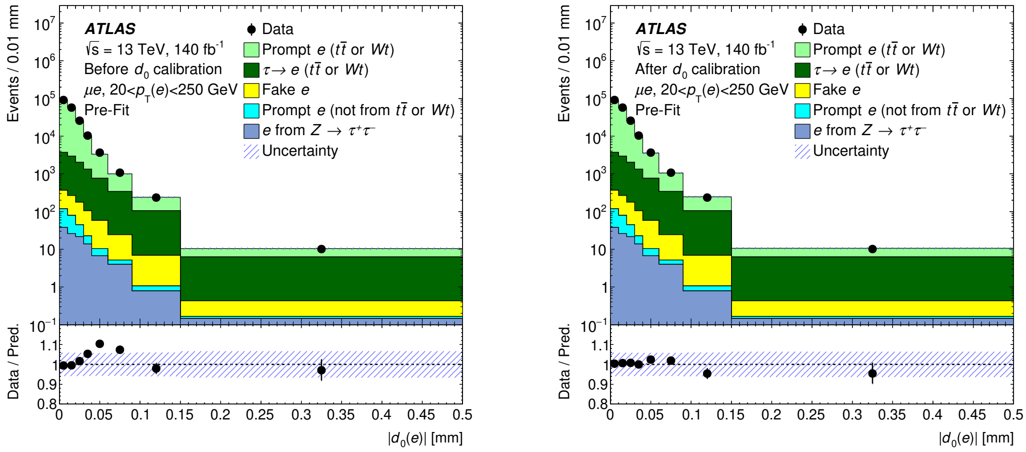

(a) (b)

Figure 2. Distributions of $|d_0|$ for the μe channel of the nominal sample for $20 < p_{\mathrm{T}}(e) < 250\,\mathrm{GeV}$ (a) before and (b) after the d_0 calibration is applied. The data are represented by black markers. The different contributions to the nominal sample, are shown by stacked histograms. The bottom panels show the ratio of the data to the simulation prediction. The systematic uncertainties in the prediction are represented by the blue hatched bands.

the d_0 calibration is applied. A significant improvement in the agreement between data and MC simulation is observed.

The d_0 templates of electrons from $W \to \tau \to e$ decays are determined using simulated events and corrected for the difference in resolution of d_0 in data and simulation following the method employed in ref. [10]. For these electrons, the d_0 distribution is the convolution of the d_0 resolution and the d_0 distribution due to the lifetime of the τ-lepton. This lifetime is known with good precision [88]. Therefore, only the correction of d_0 resolution is necessary to calibrate the d_0 templates of electrons from $W \to \tau \to e$ decays in simulation. To quantify the difference in resolution of d_0 in data and simulation, the $|d_0|$ distribution of the probe electrons in the Z data sample is fitted using a Gaussian function with the mean fixed at zero. The fit is performed in each kinematic bin in the range of $|d_0| < 0.02\,\mathrm{mm}$. For $p_{\mathrm{T}} = 20\,\mathrm{GeV}$, the d_0 resolution is about $15\,\mu\mathrm{m}$. The d_0 resolution is determined separately for 2015–2016, 2017, and 2018 data-taking periods. The d_0 templates of the electrons from τ-lepton decays in the MC simulation are corrected using the measured $|d_0|$ resolution. The corrected templates are then used to measure $R_{\tau/e}$. The resulting correction due to the d_0 resolution is small and varies within 1% for different values of d_0. The d_0 templates of fake electrons are similarly taken from simulated events and corrected using the d_0 resolution from data events with corrections also at the 1% level.

6 Background estimation

Drell-Yan production of an e^+e^- pair in association with jets is a large background at small values of $|d_0|$. The resonant $Z \to e^+e^-$ decay is suppressed by applying a selection on the e^+e^- invariant mass $|m_{e^+e^-} - m_Z| > 5\,\mathrm{GeV}$. However, non-resonant e^+e^- production is

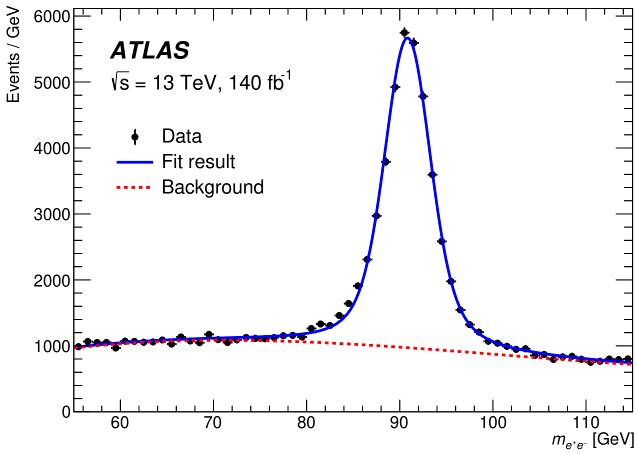

Figure 3. Distribution of the invariant mass of the electron-positron system, $m_{e^+e^-}$, in the control sample. The data are represented by black markers. The result of the fit by the sum of the Voigt profile for the Z-boson peak and the second-degree Chebyshev polynomial for the background is shown by the solid line. The dashed line corresponds to the parametrisation of the background contribution.

an irreducible background. Its contribution is determined using a control sample of e^+e^- events containing the resonant $Z \to e^+e^-$ contribution. This sample is obtained by removing the Z-mass window veto ($|m_{e^+e^-} - m_Z| > 5$ GeV), whilst keeping all other requirements as specified in section 4. Figure 3 shows the $m_{e^+e^-}$ distribution for the data control sample in the range of $55 < m_{e^+e^-} < 115$ GeV which is used to determine the $Z \to e^+e^-$ contribution.

The control sample in data and MC simulation is partitioned into three subsamples, depending on p_{T} of the probe electron ($7 < p_{\mathrm{T}} < 10$ GeV, $10 < p_{\mathrm{T}} < 20$ GeV, and $20 < p_{\mathrm{T}} < 250$ GeV). This binning in p_{T} matches the one used in the measurement of $R_{\tau/e}$, as detailed in section 7. A binned extended maximum-likelihood fit [89] of the $m_{e^+e^-}$ distribution in the range of $55 < m_{e^+e^-} < 115$ GeV is used to estimate the number of Z+jets events in each p_{T} bin i, $N_{Z,i}$, of the control sample. The distribution is modelled by the function

$$F(m_{e^+e^-}\,|\,m_Z, \Gamma_Z, s, N_{Z,i}, N_{\mathrm{bkg},i}) = N_{Z,i}\,V(m_{e^+e^-}\,|\,m_Z, \Gamma_Z, s) + N_{\mathrm{bkg},i}\,P(m_{e^+e^-}). \tag{6.1}$$

Here, $V(m_{e^+e^-}\,|\,m_Z, \Gamma_Z, s)$ is the Voigt profile [90] describing the $Z \to e^+e^-$ signal and $P(m_{e^+e^-})$ is the second-degree Chebyshev polynomial corresponding to the background under the Z-boson peak. The parameters $N_{Z,i}$ and $N_{\mathrm{bkg},i}$ are the numbers of Z and background events, respectively. The parameters m_Z and Γ_Z are the mass and width of the Z boson, respectively, and s is the standard deviation of the mass resolution. The Z boson's width is fixed to the PDG value $\Gamma_Z = 2.4955$ GeV [5], while the other parameters in eq. (6.1) are varied freely in the fit.

The numbers of $Z \to e^+e^-$ events in data and MC, $N_{\mathrm{Z},i}^{\mathrm{data}}$ and $N_{\mathrm{Z},i}^{\mathrm{MC}}$, are obtained from the fit to the $m_{e^+e^-}$ distribution in data and MC simulation, respectively. The simulated non-resonant Drell-Yan contribution in the nominal sample is then scaled in each p_{T} bin i by the factor $C_i^Z \equiv N_{\mathrm{Z},i}^{\mathrm{data}}/N_{\mathrm{Z,i}}^{\mathrm{MC}}$. The scaling factors C_i^Z are also applied to the $Z(\to \tau^+\tau^-)$+jets sample, which contributes to both μe and ee channels.

The values of C_i^Z in all p_{T} groups are found to be statistically consistent across all p_{T} bins. The average value of C_i^Z is 1.117 ± 0.013, where the uncertainty reflects the limited size of the data and simulation samples.

The solid blue line in figure 3 shows the result of the fit to the full data control sample using the model function specified in eq. (6.1). The parametrisation of the background, which comes mainly from $t\bar{t}$ and Wt production, is shown as the dashed line.

Fake electrons are another important source of background. They mainly arise from two processes: the decay of b- or c-hadrons, and photon conversions. The number of fake electrons in the nominal sample in simulation is corrected by a factor derived from the comparison of data and simulation. A control sample is defined by applying the nominal selections, but requiring two leptons with the same electric charge. The fake electrons contribute to both the nominal (i.e., opposite-sign) and control (i.e., same-sign) samples, while the contribution of non-fake leptons to the same-sign sample is reduced. For electrons with $p_{\mathrm{T}} < 10\,\mathrm{GeV}$ the fraction of fake electrons in the same-sign sample is about 97%, and for electrons with $20 < p_{\mathrm{T}} < 250\,\mathrm{GeV}$ it is about 50%. The extrapolation of the correction factor from the same-sign to opposite-sign sample is evaluated from simulated events.

In addition to the fake electrons from hadron decays and photon conversions, prompt electrons from W- and Z-boson decays also contribute to the same-sign sample, especially at high p_{T} and small values of $|d_0|$. The main processes yielding prompt same-sign electrons are $t\bar{t} + V$ and VV production, where the leptons from the V boson and one of the top-quark decays can have the same electric charge. There is also a 3% contribution of events with a wrong measurement of the charge of the electron due to bremsstrahlung.

The correction factors for the number of fake electrons from hadron decays (C^{HAD}), from photon conversions (C^{PH}), and for the number of prompt electrons (C^{PR}), are derived from the comparison of the number of same-sign events as a function of probe lepton p_{T} in data and simulation. In addition to the events with probe electrons, the same-sign events with probe muons are also used. The probe muons are selected using the same requirements as the tag muons but changing the p_{T} condition to $5 < p_{\mathrm{T}}(\mu) < 250\,\mathrm{GeV}$. No trigger requirements are applied to the probe muons. The addition of the events with a probe muon increases the statistical precision of the correction factors. The same C^{PR} value is applied to the events with prompt probe muons and electrons, and the same C^{HAD} value is applied to the events with fake muons and electrons from hadron decays. It was verified that the separate treatment of electrons and muons from these sources had no statistically significant impact on the result.

The same-sign sample is divided into 12 groups depending on the channel (ee, μe, $e\mu$, and $\mu\mu$) and p_{T} of the probe lepton ($p_{\mathrm{T}} < 10\,\mathrm{GeV}$, $10 < p_{\mathrm{T}} < 20\,\mathrm{GeV}$, and $20 < p_{\mathrm{T}} < 250\,\mathrm{GeV}$), and a binned maximum-likelihood fit is performed to these groups. The free parameters in the fit are C^{HAD}, C^{PH}, and C^{PR}. The statistical and systematic uncertainties related to the limited size of the simulation samples are taken into account. Other systematic uncertainties are discussed in section 7. Figure 4 shows the results of the fit. A good agreement between data and simulation is obtained for all 12 groups of same-sign events with the p-value of the global goodness of the fit [91] being equal to 0.7. The obtained values of C^{HAD}, C^{PH}, and C^{PR} are 1.41 ± 0.03, 0.84 ± 0.05, and 1.45 ± 0.08, respectively.

Figure 5 shows the p_{T} and $|d_0|$ distributions of the probe electrons after the fit to the same-sign data. A reasonably good agreement between data and simulation is observed

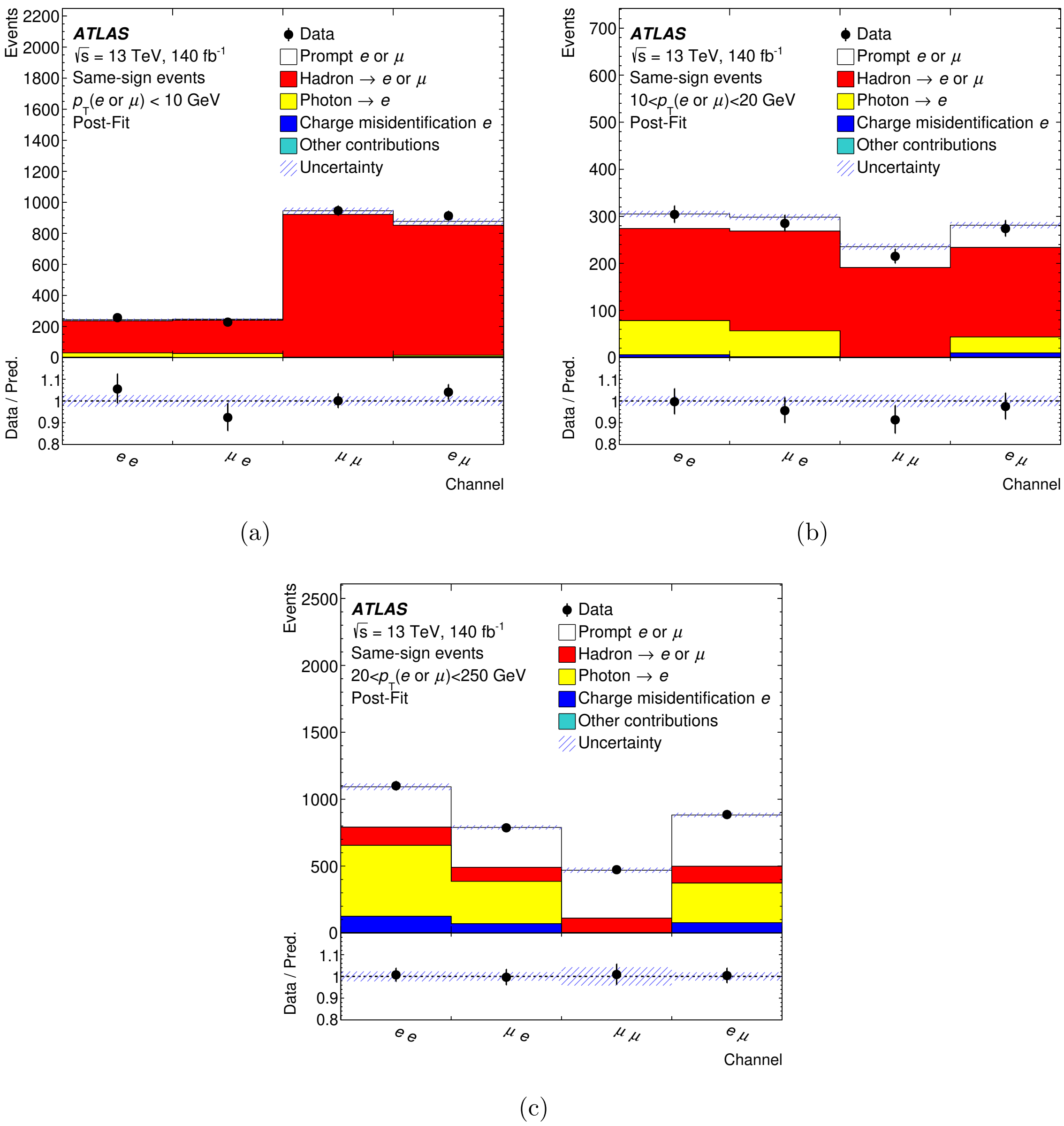

Figure 4. Number of same-sign events in the ee, μe, $e\mu$, and $\mu\mu$ channels where the first lepton is the tag lepton and the second is the probe lepton. The sub-figures correspond to (a) $p_{\mathrm{T}} < 10\,\mathrm{GeV}$, (b) $10 < p_{\mathrm{T}} < 20\,\mathrm{GeV}$, and (c) $20 < p_{\mathrm{T}} < 250\,\mathrm{GeV}$ of the probe lepton (electron or muon). The data are represented by black markers and the different components contributing to the sample, taken from simulation after the fit ('Post-Fit'), are shown by stacked histograms. The component 'Other contributions' contains events with both fake leptons or with charge misidentification of both leptons. Distributions are shown after the fit to the same-sign data has been performed. The systematic uncertainties related to the limited size of the simulation samples are included in the fit, and represented by the blue hatched bands. The bottom panels show the ratio of the data to the simulation prediction.

after applying the measured correction factors. The remaining differences are in the regions where the contribution of prompt electrons from $t\bar{t}V$ and VV production is dominant. These differences are taken into account by the uncertainties in the $t\bar{t}V$ and VV production together with the systematic uncertainties of fake-lepton contribution.

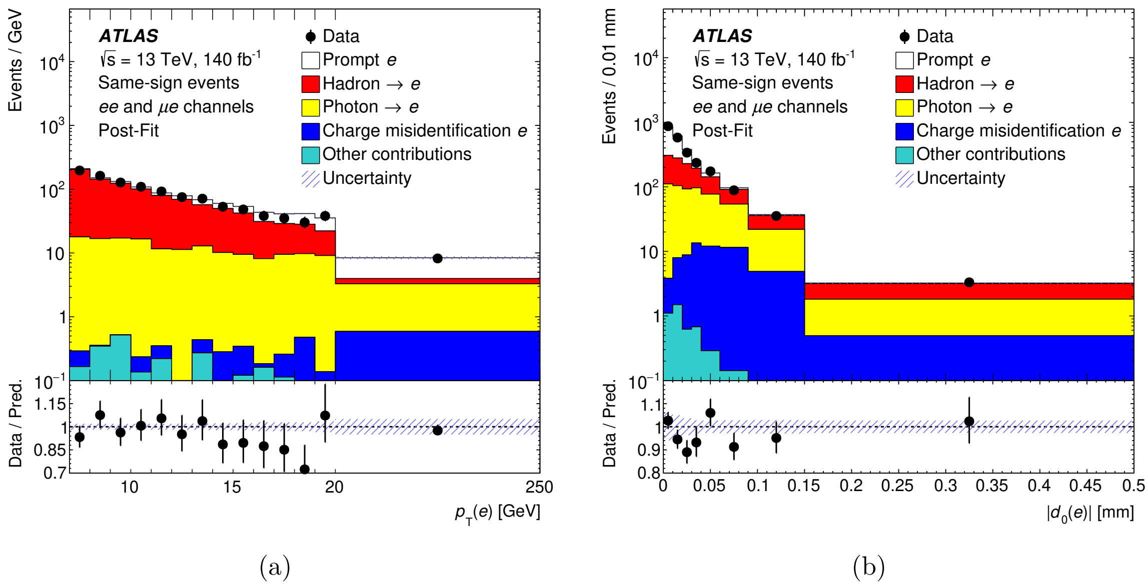

Figure 5. Distributions of (a) p_{T} and (b) $|d_0|$ of the probe electrons for the sum of the μe and ee channels of the same-sign sample. The last bin in the p_{T} distribution includes all events with $20 < p_{\mathrm{T}}(e) < 250\,\mathrm{GeV}$. The data are represented by black markers and the different components contributing to the sample, taken from simulation after the fit ('Post-Fit'), are shown by stacked histograms. The component 'Other contributions' contains events with both fake leptons or with charge misidentification of both leptons. Distributions are shown after the fit to the same-sign data has been performed. The systematic uncertainties related to the limited size of the simulation samples and the cross-section of $t\bar{t}V$ production are represented by the blue hatched bands. The bottom panels show the ratio of the data to the simulation prediction.

7 Statistical analysis and systematic uncertainties

To measure $R_{\tau/e}$, a two-dimensional binned template profile likelihood fit is performed to the p_{T} and $|d_0|$ distributions. The bin boundaries are optimised to provide the best sensitivity to $R_{\tau/e}$ given the available data. This optimisation resulted in three bins in p_{T} ($7 < p_{\mathrm{T}} < 10\,\mathrm{GeV}$, $10 < p_{\mathrm{T}} < 20\,\mathrm{GeV}$, and $20 < p_{\mathrm{T}} < 250\,\mathrm{GeV}$) and eight bins in $|d_0|$ ($|d_0| < 0.01\,\mathrm{mm}$, $0.01 < |d_0| < 0.02\,\mathrm{mm}$, $0.02 < |d_0| < 0.03\,\mathrm{mm}$, $0.03 < |d_0| < 0.04\,\mathrm{mm}$, $0.04 < |d_0| < 0.06\,\mathrm{mm}$, $0.06 < |d_0| < 0.09\,\mathrm{mm}$, $0.09 < |d_0| < 0.15\,\mathrm{mm}$, $0.15 < |d_0| < 0.5\,\mathrm{mm}$) in both the ee and μe channels. In total 48 bins are used in the fit.

The fit is set up such that a negative-log-likelihood minimization is performed with the parameter of interest, $R_{\tau/e}$, two other unknown parameters k_{sig} and $k(\mu/e)$ defined below, and systematic uncertainties included as nuisance parameters (NP), $\boldsymbol{\theta}$. The likelihood function is defined as a product of Poisson probabilities for each bin in each channel and a probability density function for systematic uncertainties

$$L(\boldsymbol{n}, \boldsymbol{\theta}^0 | R_{\tau/e}, k_{\mathrm{sig}}, k(\mu/e), \boldsymbol{\theta}) = \prod_{i \in \mathrm{bins}} P(n_i | R_{\tau/e}, k_{\mathrm{sig}}, k(\mu/e), \boldsymbol{\theta}) \times \prod_{j \in \mathrm{NPs}} G(\theta_j^0 | \theta_j). \tag{7.1}$$

Here n_i is the number of events in bin i and G is a Gaussian distribution that constrains the nuisance parameter θ_j to the nominal value θ_j^0.

The scaling factors $R_{\tau/e}$, k_{sig}, $k(\mu/e)$ and more than 300 nuisance parameters representing various statistical and systematic uncertainties are varied in the fit. The parameter of interest $R_{\tau/e}$ is applied to the $W \to \tau \to e$ events. The SM value of $R_{\tau/e} = 1$ is set in the MC simulation. The parameter k_{sig} is the normalisation scaling factor of the $t\bar{t}$ and Wt processes contributing to the signal. It is applied to both the $W \to \tau \to e$ and $W \to e$ components of the signal. The parameter $k(\mu/e)$ takes into account any residual difference in the modelling of the selection efficiencies of the tag muon and electron. It is applied to both the signal and background contributions to the μe channel.

The fit is performed after applying the correction factors to the main components of the background events as explained in section 6. Other background processes are normalised to their theoretical cross-sections.

The main systematic uncertainties in $R_{\tau/e}$ are discussed in detail below.

For the measurement of $R_{\tau/e}$ the $t\bar{t}$ simulation with NNLO re-weighting is used as explained in section 3. The uncertainty due to re-weighting of the NNLO matrix element calculations is estimated by comparing the result with and without this re-weighting applied.

The uncertainties related to the modelling of $t\bar{t}$ and Wt signals are estimated by comparing the baseline Powheg + Pythia 8 generator to alternative MC generators of $t\bar{t}$ and Wt production or to modified configurations of the baseline MC generators. The NNLO re-weighting is available only for some of the alternative MC generators. For consistency, the systematic uncertainties related to the $t\bar{t}$ and Wt modelling are derived from the comparison of the baseline and alternative MC generators without NNLO re-weighting.

To evaluate the uncertainty of $t\bar{t}$ production due to the h_{damp} parameter, the PS and hadronisation model, the NLO matching, and the gluon recoil scheme, the templates obtained with the Powheg+Pythia 8 generator are compared with the simulation obtained with the alternative MC samples described in section 3.

To estimate the sensitivity of $t\bar{t}$ production to the amount of parton radiation and potential missing higher-order QCD corrections, the renormalisation and factorisation scales of the baseline MC generator are varied up by a factor of 2.0 and down by a factor of 0.5 from the default values. The uncertainties in initial-state-radiation (ISR) are estimated by using the Var3c eigen-tune variations of the A14 tune [26]. The impact of final-state-radiation (FSR) uncertainties is evaluated using weights which vary the renormalisation scale for QCD emission in the FSR by factors of 0.5 and 2.0, respectively. The difference between up and down variations divided by two is taken as a symmetric uncertainty related to these variations of the MC generators.

The modelling uncertainties of Wt production related to the PS and hadronisation model, h_{damp} parameter, NLO matching, ISR and FSR are estimated similarly to $t\bar{t}$ events. The uncertainty related to the interference between the $t\bar{t}$ and Wt processes is evaluated by comparing the baseline Wt simulation, which was generated using the diagram removal scheme, and the alternative MC sample generated using the diagram subtraction scheme [35, 50] as described in section 3.

The uncertainty of 5% in the Wt cross-section is included as a separate contribution to the systematic uncertainty. The relative uncertainties of the $t\bar{t}V$ and VV production cross-section are set to 15% and 30%, respectively. The relative uncertainties in the t-

and s-channel single-top-quark production are set to 5%. These uncertainties produce a negligible impact on $R_{\tau/e}$.

To estimate the systematic uncertainty due to the proton PDFs, 30 nuisance parameters corresponding to 30 different variations of PDF defined by the PDF4LHC15 set [45] are included in the fit.

The modelling uncertainties are estimated separately for $t\bar{t}$ and Wt processes, and treated as correlated between these processes and between $W \to e$ and $W \to \tau \to e$ contributions.

To build the d_0 templates of prompt electrons from $W \to e$ decays, the Z sample containing mainly $Z \to e^+e^-$ events is used as explained in section 5. The electrons from these two processes originate in the hard-scatter primary vertex and therefore their d_0 distributions are expected to be the same. However, second-order effects related to track reconstruction and differences in kinematics of electrons coming from Z-boson decay and from $t\bar{t}$ result in residual differences between the templates employed in the fit and the actual d_0 distributions. To evaluate the impact of this difference on the result, the d_0 templates are modified as

$$T'_{ij}(d_0) = N\, T^{\mathrm{pr}}_{ij}(d_0)\frac{D^{W\to e}_{ij}(d_0)}{D^{Z}_{ij}(d_0)}. \tag{7.2}$$

Here, $D^{Z}_{ij}(d_0)$ and $D^{W\to e}_{ij}(d_0)$ are the normalised d_0 distributions of prompt electrons produced in $Z \to e^+e^-$ and $t\bar{t}$ processes, respectively, which are obtained in simulation. The coefficient N normalises the modified templates $T'_{ij}(d_0)$ to unity. The difference in the value of $R_{\tau/e}$ obtained with the $T'_{ij}(d_0)$ and $T^{\mathrm{pr}}_{ij}(d_0)$ templates is taken as the systematic uncertainty due to the calibration of d_0 of prompt electrons.

Three sources of uncertainty in the evaluation of the correction factors to the number of fake electrons are considered. These include the limited size of the same-sign sample, the choice of PS and hadronisation model, and the possible variation of the fraction of electrons from photon conversion. The uncertainty due to the parton shower and hadronisation model is obtained by comparing the expected number of fake electrons evaluated using the baseline Pythia and alternative Herwig algorithms. The fraction of electrons from photon conversions is evaluated using the MC simulation. The effect of the uncertainty in this quantity is estimated by using the fraction in the same-sign sample instead of the nominal opposite-sign sample when measuring $R_{\tau/e}$.

The electron energy scale and resolution, the reconstruction, isolation, and identification efficiencies and their corresponding uncertainties are measured using $Z \to e^+e^-$ and $J/\psi \to e^+e^-$ events [76, 77, 92]. In particular, J/ψ events are used to measure the identification efficiency for electrons with $p_{\mathrm{T}} < 20\,\mathrm{GeV}$. The reconstruction efficiency is not measured for electrons with $p_{\mathrm{T}} < 15\,\mathrm{GeV}$ with the standard tag-and-probe method because of large backgrounds which make the measurement unreliable. The agreement between data and MC in p_{T} dependence of electron efficiency is essential for this measurement. This agreement is tested using the Z sample of events described in section 5. The dominant contribution to this sample originates from $Z \to e^+e^-$ events accompanied with two or more jets. Following this study, an additional correction to the efficiency of electrons with small p_{T} is found to be necessary. The corresponding correction factors are derived from the ratio of the p_{T}

distribution of probe electrons in the Z sample in data and simulation. They are determined separately for 2015–2016, 2017, and 2018 data-taking periods. The systematic uncertainty due to the additional efficiency correction is evaluated using the comparison of the correction factors obtained with the baseline SHERPA MC generator and an alternative sample generated with MADGRAPH5_AMC@NLO. It is verified that the variation of the correction factors in events with different numbers of jets is within the assigned systematic uncertainty.

Muon reconstruction, identification, and isolation efficiencies, as well as muon momentum scale and resolution, are obtained using the prescriptions specified in refs. [78, 93]. The size of the corresponding uncertainties are derived using $J/\psi \to \mu^+\mu^-$ events for muons with $p_{\mathrm{T}} < 15\,\mathrm{GeV}$ and $Z \to \mu^+\mu^-$ events for muons with $p_{\mathrm{T}} > 15\,\mathrm{GeV}$.

The lepton trigger efficiencies are measured in $Z \to e^+e^-$ and $Z \to \mu^+\mu^-$ events using tag-and-probe techniques [80, 81], and are varied within the corresponding uncertainties.

The jet energy scale and resolution are evaluated using simulation and *in situ* measurements [85]. For the jet energy scale uncertainty, 35 independent nuisance parameters are used, and 13 nuisance parameters are taken into account for the jet energy resolution. The uncertainties in the jet b-tagging efficiency and rate of b-tagged background are estimated by using the semileptonic and dileptonic $t\bar{t}$ events, as well as Z+jets events [94–96]. The simulated pile-up events are weighted to reproduce the distribution of the average number of inelastic interactions per bunch crossing observed in the data. The associated uncertainty is included as a nuisance parameter in the measurement of $R_{\tau/e}$. The uncertainty associated with the use of the JVT algorithm is estimated by using the results of the study presented in ref. [86].

The uncertainty in the integrated luminosity is 0.83% [20], obtained using the LUCID-2 detector for the primary luminosity measurements, complemented by measurements using the inner detector and calorimeters. This uncertainty has a negligible impact on $R_{\tau/e}$.

The measurement of $R_{\tau/e}$ depends on $B(\tau \to e\nu_e\nu_\tau)$, which has been measured to be $(17.82 \pm 0.04)\%$ [5]. The dependence on this branching fraction is included as an additional uncertainty. The limited size of the MC samples is treated as a separate contribution to the systematic uncertainty following the Barlow-Beeston approach [97].

8 Results

The numbers of observed events in the μe and ee channels and in different p_{T} bins, together with the fitted number of events from different sources, are given in tables 1 and 2. The number of events in simulation agrees with that in data across different channels and p_{T} bins.

Figures 6 and 7 show the distribution in data and in simulation of $|d_0|$ in the six regions after the fit. Good agreement between data and simulation is observed, both in the total yield and differential shape. The p-value of the global goodness of the fit [91] is 87%. These figures also demonstrate the separation between the signal and background processes. The electrons from $W \to e$ dominate at high p_{T} and small $|d_0|$, while the electrons from $W \to \tau \to e$ dominate at high $|d_0|$. The fake electrons mainly contribute at small p_{T}.

The measured value of $R_{\tau/e}$ is

$$R_{\tau/e} = 0.975 \pm 0.012\,(\text{stat.}) \pm 0.020\,(\text{syst.}). \tag{8.1}$$

	μe $7 < p_T < 10$ GeV	μe $10 < p_T < 20$ GeV	μe $20 < p_T < 250$ GeV
Prompt $e(t\bar{t})$	1278 ± 28	13370 ± 150	178000 ± 1000
e from τ $(t\bar{t})$	1092 ± 32	4490 ± 100	11670 ± 290
Prompt $e(Wt)$	34 ± 6	340 ± 60	5300 ± 900
e from τ (Wt)	28.0 ± 2.5	119 ± 16	380 ± 110
Prompt e (not from $t\bar{t}$ or Wt)	5.2 ± 1.5	23 ± 7	180 ± 50
e from $Z \to \tau^+\tau^-$	19.9 ± 0.4	85.4 ± 1.4	132.9 ± 2.2
Fake e	317 ± 22	380 ± 33	840 ± 60
Total predicted	2770 ± 40	18800 ± 120	196500 ± 400
Data	2768	18783	196552

Table 1. Number of events in the μe channel from different sources, as estimated by the fit to the data, compared with the observed yield. Uncertainties include the statistical and systematic contributions. The uncertainty in the total expected number of events can be smaller than the uncertainties of the individual contributions because of correlations between them resulting from the fit.

	ee $7 < p_T < 10$ GeV	ee $10 < p_T < 20$ GeV	ee $20 < p_T < 250$ GeV
Prompt $e(t\bar{t})$	1238 ± 35	12210 ± 130	160300 ± 900
e from τ $(t\bar{t})$	1051 ± 30	4060 ± 100	10490 ± 260
Prompt $e(Wt)$	35 ± 7	320 ± 50	5000 ± 700
e from τ (Wt)	30 ± 4	116 ± 13	340 ± 100
e from $Z \to e^+e^-$	240 ± 50	1770 ± 120	12380 ± 200
Prompt e (not from $t\bar{t}$ or Wt)	11.7 ± 3.5	59 ± 17	560 ± 170
e from $Z \to \tau^+\tau^-$	19.7 ± 0.4	69.7 ± 0.9	105.3 ± 1.3
Fake e	302 ± 20	374 ± 32	810 ± 50
Total predicted	2930 ± 50	18970 ± 120	190000 ± 400
Data	2928	19047	189945

Table 2. Number of events in the ee channel from different sources, as estimated by the fit to the data, compared with the observed yield. Uncertainties include the statistical and systematic contributions. The uncertainty in the total expected number of events can be smaller than the uncertainties of the individual contributions because of correlations between them resulting from the fit.

The values of k_{sig} and $k(\mu/e)$ obtained in the fit are $k_{\text{sig}} = 1.03 \pm 0.06$ and $k(\mu/e) = 0.986 \pm 0.010$ with uncertainties that include both statistical and systematic components. Both k_{sig} and $k(\mu/e)$ are consistent with unity within less than two standard deviations. Fixing $k(\mu/e)$ to unity in the fit has a negligible impact on the $R_{\tau/e}$ result, both central value and uncertainties.

Consistent results are found when performing the measurement separately for the 2015–2016, 2017 and 2018 data-taking periods, as well as for the individual channels and p_T bins. Table 3 shows the results for the different p_T bins.

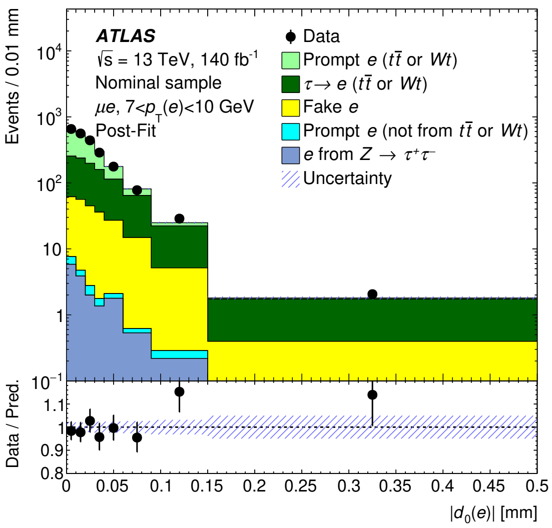

(a)

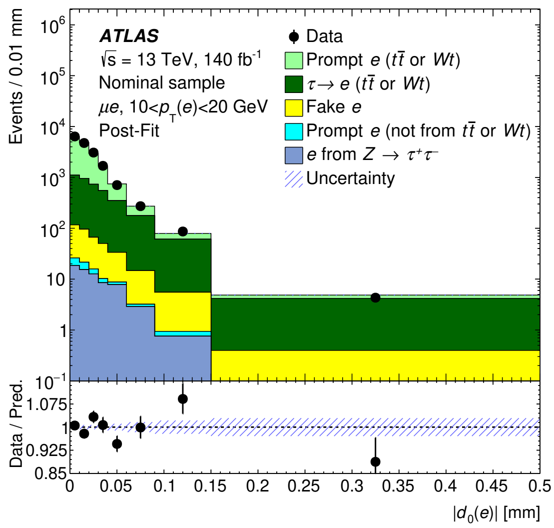

(b)

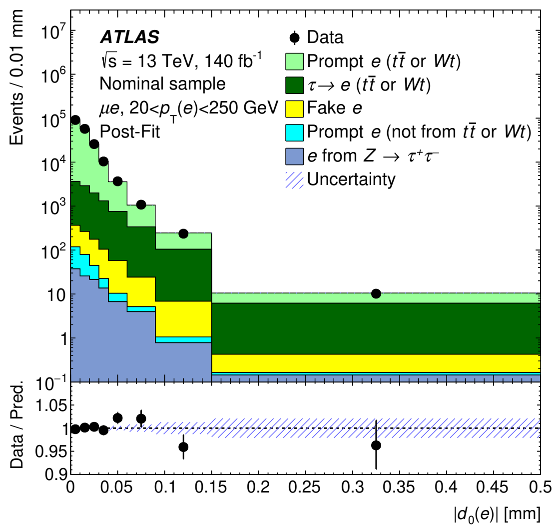

(c)

Figure 6. Distributions of $|d_0|$ for the μe channel of the nominal sample in different p_{T} bins. The data are represented by black markers. The different contributions to the nominal sample, taken from simulation after the fit ('Post-Fit'), are shown by stacked histograms. The bottom panels show the ratio of the data to the simulation prediction after the fit. The systematic uncertainties in the prediction with the constraints from the fit and the correlation between the nuisance parameters applied are represented by the blue hatched bands.

A breakdown of uncertainties grouped into categories is shown in table 4. Many systematic uncertainties are treated as correlated between the $W \to e$ and $W \to \tau \to e$ contributions. These include the uncertainties in the jet reconstruction, selection of b-jets, and trigger efficiencies. The impact of such correlated uncertainties on $R_{\tau/e}$ is reduced. The remaining dominant uncertainties are related to the modelling of $t\bar{t}$ production, the calibration of d_0 distributions (section 5), the evaluation of the background (section 6), and electron

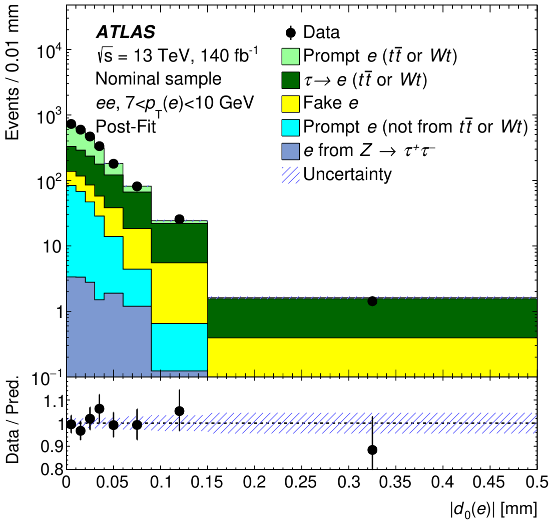

(a)

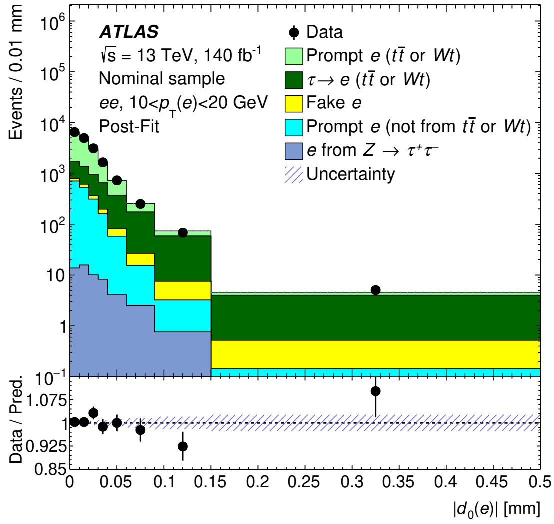

(b)

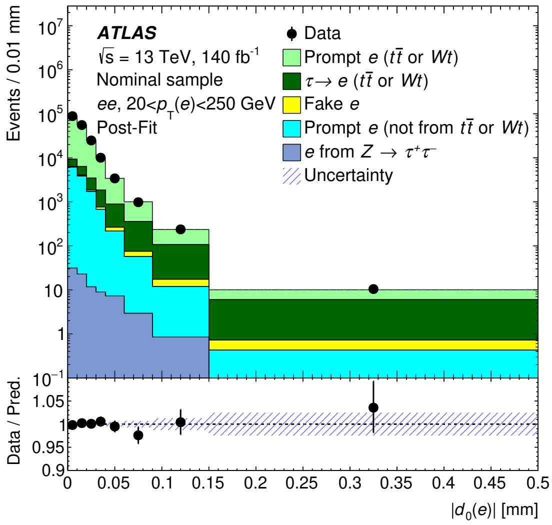

(c)

Figure 7. Distributions of $|d_0|$ for the ee channel of the nominal sample in different p_{T} bins. The data are represented by black markers. The different contributions to the nominal sample, taken from simulation after the fit ('Post-Fit'), are shown by stacked histograms. The bottom panels show the ratio of the data to the simulation prediction after the fit. The systematic uncertainties in the prediction with the constraints from the fit and the correlation between the nuisance parameters applied are represented by the blue hatched bands.

reconstruction, identification, and isolation. The largest impact on $R_{\tau/e}$ in the modelling group of uncertainties comes from NNLO re-weighting, the variation of PS and hadronisation model, the amount of parton radiation, and h_{damp} parameter.

Figure 8 provides a comparison of this result to other measurements of $R_{\tau/e}$. A similar precision is achieved to that of the CMS result [11]. This new measurement agrees with the SM expectation of lepton flavour universality and with the previous measurement of $R_{\tau/e}$ by

JHEP05(2025)038

p_T bin	$R_{\tau/e}$
$7 < p_T < 10$ GeV	1.13 ± 0.11 (stat) ± 0.07 (syst)
$10 < p_T < 20$ GeV	0.93 ± 0.04 (stat) ± 0.02 (syst)
$20 < p_T < 250$ GeV	0.98 ± 0.04 (stat) ± 0.02 (syst)

Table 3. Measured values of $R_{\tau/e}$ in the different p_T bins.

Uncertainty group	$\sigma(R_{\tau/e})$
Modelling of $t\bar{t}$ and Wt	0.011
d_0 calibration	0.006
Background estimation	0.005
Electron reconstruction, identification, and isolation	0.005
Electron energy scale	0.003
Electron energy resolution	0.002
Jet energy resolution	0.004
Jet energy scale	0.003
Jet b-tagging	0.002
Muon reconstruction, identification, and isolation	0.001
Other sources	0.002
Variation of k_{sig} and $k(\mu/e)$	0.003
Finite size of simulated samples	0.003
$B(W \to \tau\nu_\tau \to e\nu_e\nu_\tau\nu_\tau)$	0.002
Total systematical uncertainty	0.020
Data statistical uncertainty	0.012
Total uncertainty	0.024

Table 4. Breakdown of statistical and systematic uncertainties in the fit to data. Different individual components used in the fit are combined into categories. The size of the impact each group of uncertainties has on $R_{\tau/e}$, which is denoted by $\sigma(R_{\tau/e})$ and shown in the second column, is assessed by subtracting in quadrature the uncertainty from the nominal fit and the fit with the relevant nuisance parameters fixed to their post-fit values. The group 'Other sources' includes the uncertainties due to trigger, JVT, luminosity, and pile-up.

the CMS collaboration. It however differs from the combination of LEP measurements [9] by more than two standard deviations.

9 Conclusion

The value of $R_{\tau/e} = B(W \to \tau\nu_\tau)/B(W \to e\nu_e)$ has been measured using the decays of the top quark to final states containing τ-leptons or electrons. A sample of pp collisions at $\sqrt{s} = 13$ TeV collected by the ATLAS experiment in Run 2 and corresponding to 140 fb^{-1} was used in the analysis. The leptonic decay $\tau \to e\nu_e\nu_\tau$ was used for the τ-lepton selection. The decays

JHEP05(2025)038

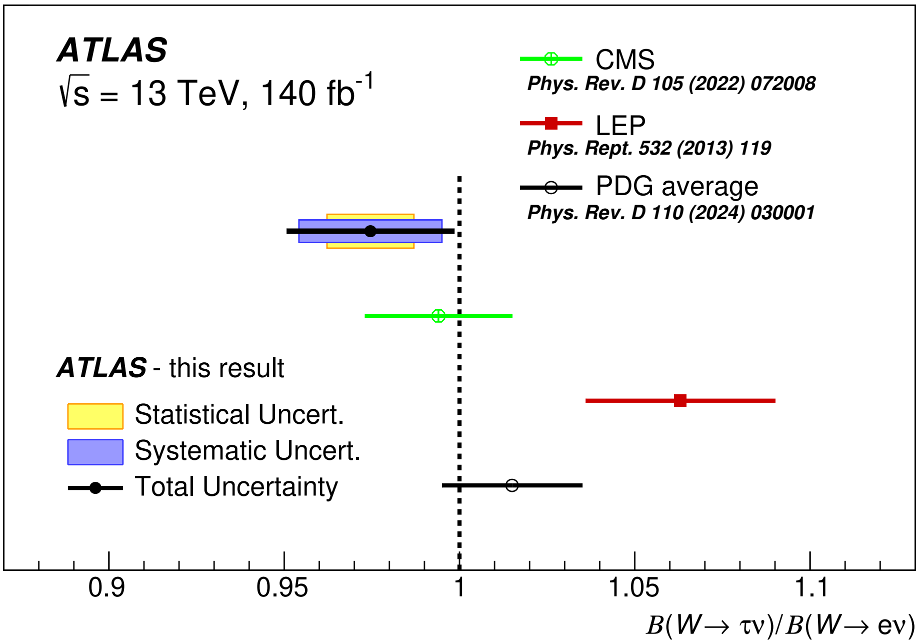

Figure 8. Summary of measurements of $R_{\tau/e} = B(W \to \tau\nu_\tau)/B(W \to e\nu_e)$. The $R_{\tau/e}$ value measured in this publication is shown together with the corresponding statistical and systematic uncertainties. It is compared with other measurements and the average value from the PDG [5]. The vertical dashed line at unity indicates the Standard Model assumption of equal branching fractions to all lepton flavours.

$W \to \tau\nu_\tau \to e\nu_e\nu_\tau\nu_\tau$ and $W \to e\nu_e$ were distinguished by exploiting differences in the impact parameter and transverse momentum distributions of the electrons. The dominant systematic uncertainties are related to the modelling of $t\bar{t}$ and Wt production, the impact parameter calibration, the estimate of the background, and electron reconstruction, identification, and isolation requirements. The resulting value of $R_{\tau/e} = 0.975 \pm 0.012\,(\text{stat}) \pm 0.020\,(\text{syst})$ is consistent with the Standard Model assumption of lepton flavour universality. The precision of this measurement is comparable to that of the LEP combination and that of the CMS collaboration, and will further reduce the uncertainty in the world-average result for $R_{\tau/e}$.

Acknowledgments

We thank CERN for the very successful operation of the LHC and its injectors, as well as the support staff at CERN and at our institutions worldwide without whom ATLAS could not be operated efficiently.

The crucial computing support from all WLCG partners is acknowledged gratefully, in particular from CERN, the ATLAS Tier-1 facilities at TRIUMF/SFU (Canada), NDGF (Denmark, Norway, Sweden), CC-IN2P3 (France), KIT/GridKA (Germany), INFN-CNAF (Italy), NL-T1 (Netherlands), PIC (Spain), RAL (U.K.) and BNL (U.S.A.), the Tier-2 facilities worldwide and large non-WLCG resource providers. Major contributors of computing resources are listed in ref. [98].

We gratefully acknowledge the support of ANPCyT, Argentina; YerPhI, Armenia; ARC, Australia; BMWFW and FWF, Austria; ANAS, Azerbaijan; CNPq and FAPESP, Brazil; NSERC, NRC and CFI, Canada; CERN; ANID, Chile; CAS, MOST and NSFC, China; Minciencias, Colombia; MEYS CR, Czech Republic; DNRF and DNSRC, Denmark; IN2P3-CNRS and CEA-DRF/IRFU, France; SRNSFG, Georgia; BMBF, HGF and MPG, Germany; GSRI, Greece; RGC and Hong Kong SAR, China; ICHEP and Academy of Sciences and Humanities, Israel; INFN, Italy; MEXT and JSPS, Japan; CNRST, Morocco; NWO, Netherlands; RCN, Norway; MNiSW, Poland; FCT, Portugal; MNE/IFA, Romania; MSTDI, Serbia; MSSR, Slovakia; ARIS and MVZI, Slovenia; DSI/NRF, South Africa; MICIU/AEI, Spain; SRC and Wallenberg Foundation, Sweden; SERI, SNSF and Cantons of Bern and Geneva, Switzerland; NSTC, Taipei; TENMAK, Türkiye; STFC/UKRI, United Kingdom; DOE and NSF, United States of America.

Individual groups and members have received support from BCKDF, CANARIE, CRC and DRAC, Canada; CERN-CZ, FORTE and PRIMUS, Czech Republic; COST, ERC, ERDF, Horizon 2020, ICSC-NextGenerationEU and Marie Skłodowska-Curie Actions, European Union; Investissements d'Avenir Labex, Investissements d'Avenir Idex and ANR, France; DFG and AvH Foundation, Germany; Herakleitos, Thales and Aristeia programmes co-financed by EU-ESF and the Greek NSRF, Greece; BSF-NSF and MINERVA, Israel; NCN and NAWA, Poland; La Caixa Banking Foundation, CERCA Programme Generalitat de Catalunya and PROMETEO and GenT Programmes Generalitat Valenciana, Spain; Göran Gustafssons Stiftelse, Sweden; The Royal Society and Leverhulme Trust, United Kingdom.

In addition, individual members wish to acknowledge support from Armenia: Yerevan Physics Institute (FAPERJ); CERN: European Organization for Nuclear Research (CERN PJAS); Chile: Agencia Nacional de Investigación y Desarrollo (FONDECYT 1230812, FONDECYT 1230987, FONDECYT 1240864); China: Chinese Ministry of Science and Technology (MOST-2023YFA1605700, MOST-2023YFA1609300), National Natural Science Foundation of China (NSFC - 12175119, NSFC 12275265, NSFC-12075060); Czech Republic: Czech Science Foundation (GACR - 24-11373S), Ministry of Education Youth and Sports (FORTE CZ.02.01.01/00/22_008/0004632), PRIMUS Research Programme (PRIMUS/21/SCI/017); EU: H2020 European Research Council (ERC - 101002463); European Union: European Research Council (ERC - 948254, ERC 101089007), European Union, Future Artificial Intelligence Research (FAIR-NextGenerationEU PE00000013), Italian Center for High Performance Computing, Big Data and Quantum Computing (ICSC, NextGenerationEU); France: Agence Nationale de la Recherche (ANR-20-CE31-0013, ANR-21-CE31-0013, ANR-21-CE31-0022, ANR-22-EDIR-0002); Germany: Baden-Württemberg Stiftung (BW Stiftung-Postdoc Eliteprogramme), Deutsche Forschungsgemeinschaft (DFG - 469666862, DFG - CR 312/5-2); Italy: Istituto Nazionale di Fisica Nucleare (ICSC, NextGenerationEU), Ministero dell'Università e della Ricerca (PRIN - 20223N7F8K - PNRR M4.C2.1.1); Japan: Japan Society for the Promotion of Science (JSPS KAKENHI JP22H01227, JSPS KAKENHI JP22H04944, JSPS KAKENHI JP22KK0227, JSPS KAKENHI JP23KK0245); Netherlands: Netherlands Organisation for Scientific Research (NWO Veni 2020 - VI.Veni.202.179); Norway: Research Council of Norway (RCN-314472); Poland: Ministry of Science and Higher Education (IDUB AGH, POB8, D4 no. 9722), Polish National Agency for Academic Exchange (PPN/PPO/2020/1/00002/U/00001), Polish National Science

Centre (NCN 2021/42/E/ST2/00350, NCN OPUS 2023/51/B/ST2/02507, NCN OPUS nr 2022/47/B/ST2/03059, NCN UMO-2019/34/E/ST2/00393, NCN & H2020 MSCA 945339, UMO-2020/37/B/ST2/01043, UMO-2021/40/C/ST2/00187, UMO-2022/47/O/ST2/00148, UMO-2023/49/B/ST2/04085, UMO-2023/51/B/ST2/00920); Slovenia: Slovenian Research Agency (ARIS grant J1-3010); Spain: Generalitat Valenciana (Artemisa, FEDER, IDIFEDER/2018/048), Ministry of Science and Innovation (MCIN & NextGenEU PCI2022-135018-2, MICIN & FEDER PID2021-125273NB, RYC2019-028510-I, RYC2020-030254-I, RYC2021-031273-I, RYC2022-038164-I); Sweden: Carl Trygger Foundation (Carl Trygger Foundation CTS 22:2312), Swedish Research Council (Swedish Research Council 2023-04654, VR 2018-00482, VR 2022-03845, VR 2022-04683, VR 2023-03403, VR grant 2021-03651), Knut and Alice Wallenberg Foundation (KAW 2018.0458, KAW 2019.0447, KAW 2022.0358); Switzerland: Swiss National Science Foundation (SNSF - PCEFP2_194658); United Kingdom: Leverhulme Trust (Leverhulme Trust RPG-2020-004), Royal Society (NIF-R1-231091); United States of America: U.S. Department of Energy (ECA DE-AC02-76SF00515), Neubauer Family Foundation.

Data Availability Statement. This article has no associated data or the data will not be deposited.

Code Availability Statement. This article has no associated code or the code will not be deposited.

References

[1] S.L. Glashow, *Partial Symmetries of Weak Interactions*, *Nucl. Phys.* **22** (1961) 579 [INSPIRE].

[2] S. Weinberg, *A Model of Leptons*, *Phys. Rev. Lett.* **19** (1967) 1264 [INSPIRE].

[3] A. Salam, *Weak and Electromagnetic Interactions*, *Conf. Proc. C* **680519** (1968) 367 [INSPIRE].

[4] A. Pich, *Precision Tau Physics*, *Prog. Part. Nucl. Phys.* **75** (2014) 41 [arXiv:1310.7922] [INSPIRE].

[5] Particle Data Group, *Review of particle physics*, *Phys. Rev. D* **110** (2024) 030001 [INSPIRE].

[6] A. Crivellin, M. Kirk, T. Kitahara and F. Mescia, *Global fit of modified quark couplings to EW gauge bosons and vector-like quarks in light of the Cabibbo angle anomaly*, *JHEP* **03** (2023) 234 [arXiv:2212.06862] [INSPIRE].

[7] L. Allwicher, G. Isidori, J.M. Lizana, N. Selimović and B.A. Stefanek, *Third-family quark-lepton Unification and electroweak precision tests*, *JHEP* **05** (2023) 179 [arXiv:2302.11584] [INSPIRE].

[8] A. Abada, J. Kriewald, E. Pinsard, S. Rosauro-Alcaraz and A.M. Teixeira, *Heavy neutral lepton corrections to SM boson decays: lepton flavour universality violation in low-scale seesaw realisations*, *Eur. Phys. J. C* **84** (2024) 149 [arXiv:2307.02558] [INSPIRE].

JHEP05(2025)038

[9] ALEPH, DELPHI, L3, OPAL and LEP Electroweak collaborations, *Electroweak Measurements in Electron-Positron Collisions at W-Boson-Pair Energies at LEP*, Phys. Rep. **532** (2013) 119 [arXiv:1302.3415] [INSPIRE].

[10] ATLAS collaboration, *Test of the universality of τ and μ lepton couplings in W-boson decays with the ATLAS detector*, Nat. Phys. **17** (2021) 813 [arXiv:2007.14040] [INSPIRE].

[11] CMS collaboration, *Precision measurement of the W boson decay branching fractions in proton-proton collisions at $\sqrt{s} = 13$ TeV*, Phys. Rev. D **105** (2022) 072008 [arXiv:2201.07861] [INSPIRE].

[12] ATLAS collaboration, *Precise test of lepton flavour universality in W-boson decays into muons and electrons in pp collisions at $\sqrt{s} = 13$ TeV with the ATLAS detector*, Eur. Phys. J. C **84** (2024) 993 [arXiv:2403.02133] [INSPIRE].

[13] ATLAS collaboration, *The ATLAS Experiment at the CERN Large Hadron Collider*, 2008 *JINST* **3** S08003 [INSPIRE].

[14] ATLAS collaboration, *ATLAS Insertable B-Layer Technical Design Report*, CERN-LHCC-2010-013 (2010).

[15] B. Abbott et al., *Production and Integration of the ATLAS Insertable B-Layer*, 2018 *JINST* **13** T05008 [arXiv:1803.00844] [INSPIRE].

[16] G. Avoni et al., *The new LUCID-2 detector for luminosity measurement and monitoring in ATLAS*, 2018 *JINST* **13** P07017 [INSPIRE].

[17] ATLAS collaboration, *Performance of the ATLAS Trigger System in 2015*, Eur. Phys. J. C **77** (2017) 317 [arXiv:1611.09661] [INSPIRE].

[18] ATLAS collaboration, *Software and computing for Run 3 of the ATLAS experiment at the LHC*, Eur. Phys. J. C **85** (2025) 234 [arXiv:2404.06335] [INSPIRE].

[19] ATLAS collaboration, *ATLAS data quality operations and performance for 2015–2018 data-taking*, 2020 *JINST* **15** P04003 [arXiv:1911.04632] [INSPIRE].

[20] ATLAS collaboration, *Luminosity determination in pp collisions at $\sqrt{s} = 13$ TeV using the ATLAS detector at the LHC*, Eur. Phys. J. C **83** (2023) 982 [arXiv:2212.09379] [INSPIRE].

[21] GEANT4 collaboration, *GEANT4 — A Simulation Toolkit*, Nucl. Instrum. Meth. A **506** (2003) 250 [INSPIRE].

[22] ATLAS collaboration, *The ATLAS Simulation Infrastructure*, Eur. Phys. J. C **70** (2010) 823 [arXiv:1005.4568] [INSPIRE].

[23] T. Sjöstrand, S. Mrenna and P. Skands, *A Brief Introduction to PYTHIA 8.1*, Comput. Phys. Commun. **178** (2008) 852 [arXiv:0710.3820] [INSPIRE].

[24] NNPDF collaboration, *Parton distributions with LHC data*, Nucl. Phys. B **867** (2013) 244 [arXiv:1207.1303] [INSPIRE].

[25] ATLAS collaboration, *The Pythia 8 A3 tune description of ATLAS minimum bias and inelastic measurements incorporating the Donnachie-Landshoff diffractive model*, ATL-PHYS-PUB-2016-017 (2016).

[26] ATLAS collaboration, *ATLAS Pythia 8 tunes to 7 TeV data*, ATL-PHYS-PUB-2014-021 (2014).

[27] M. Bähr et al., *Herwig++ Physics and Manual*, Eur. Phys. J. C **58** (2008) 639 [arXiv:0803.0883] [INSPIRE].

[28] J. Bellm et al., *Herwig 7.1 Release Note*, arXiv:1705.06919 [INSPIRE].

[29] D.J. Lange, *The EvtGen particle decay simulation package*, *Nucl. Instrum. Meth. A* **462** (2001) 152 [INSPIRE].

[30] S. Frixione, G. Ridolfi and P. Nason, *A Positive-weight next-to-leading-order Monte Carlo for heavy flavour hadroproduction*, *JHEP* **09** (2007) 126 [arXiv:0707.3088] [INSPIRE].

[31] P. Nason, *A New method for combining NLO QCD with shower Monte Carlo algorithms*, *JHEP* **11** (2004) 040 [hep-ph/0409146] [INSPIRE].

[32] S. Frixione, P. Nason and C. Oleari, *Matching NLO QCD computations with Parton Shower simulations: the POWHEG method*, *JHEP* **11** (2007) 070 [arXiv:0709.2092] [INSPIRE].

[33] S. Alioli, P. Nason, C. Oleari and E. Re, *A general framework for implementing NLO calculations in shower Monte Carlo programs: the POWHEG BOX*, *JHEP* **06** (2010) 043 [arXiv:1002.2581] [INSPIRE].

[34] NNPDF collaboration, *Parton distributions for the LHC Run II*, *JHEP* **04** (2015) 040 [arXiv:1410.8849] [INSPIRE].

[35] ATLAS collaboration, *Studies on top-quark Monte Carlo modelling for Top2016*, ATL-PHYS-PUB-2016-020 (2016).

[36] T. Sjöstrand et al., *An introduction to PYTHIA 8.2*, *Comput. Phys. Commun.* **191** (2015) 159 [arXiv:1410.3012] [INSPIRE].

[37] M. Czakon, D. Heymes, A. Mitov, D. Pagani, I. Tsinikos and M. Zaro, *Top-pair production at the LHC through NNLO QCD and NLO EW*, *JHEP* **10** (2017) 186 [arXiv:1705.04105] [INSPIRE].

[38] M. Beneke, P. Falgari, S. Klein and C. Schwinn, *Hadronic top-quark pair production with NNLL threshold resummation*, *Nucl. Phys. B* **855** (2012) 695 [arXiv:1109.1536] [INSPIRE].

[39] M. Cacciari, M. Czakon, M. Mangano, A. Mitov and P. Nason, *Top-pair production at hadron colliders with next-to-next-to-leading logarithmic soft-gluon resummation*, *Phys. Lett. B* **710** (2012) 612 [arXiv:1111.5869] [INSPIRE].

[40] P. Bärnreuther, M. Czakon and A. Mitov, *Percent Level Precision Physics at the Tevatron: First Genuine NNLO QCD Corrections to $q\bar{q} \to t\bar{t} + X$*, *Phys. Rev. Lett.* **109** (2012) 132001 [arXiv:1204.5201] [INSPIRE].

[41] M. Czakon and A. Mitov, *NNLO corrections to top-pair production at hadron colliders: the all-fermionic scattering channels*, *JHEP* **12** (2012) 054 [arXiv:1207.0236] [INSPIRE].

[42] M. Czakon and A. Mitov, *NNLO corrections to top pair production at hadron colliders: the quark-gluon reaction*, *JHEP* **01** (2013) 080 [arXiv:1210.6832] [INSPIRE].

[43] M. Czakon, P. Fiedler and A. Mitov, *Total Top-Quark Pair-Production Cross Section at Hadron Colliders Through $O(\alpha_S^4)$*, *Phys. Rev. Lett.* **110** (2013) 252004 [arXiv:1303.6254] [INSPIRE].

[44] M. Czakon and A. Mitov, *Top++: A Program for the Calculation of the Top-Pair Cross-Section at Hadron Colliders*, *Comput. Phys. Commun.* **185** (2014) 2930 [arXiv:1112.5675] [INSPIRE].

[45] J. Butterworth et al., *PDF4LHC recommendations for LHC Run II*, *J. Phys. G* **43** (2016) 023001 [arXiv:1510.03865] [INSPIRE].

[46] A.D. Martin, W.J. Stirling, R.S. Thorne and G. Watt, *Parton distributions for the LHC*, *Eur. Phys. J. C* **63** (2009) 189 [arXiv:0901.0002] [INSPIRE].

[47] A.D. Martin, W.J. Stirling, R.S. Thorne and G. Watt, *Uncertainties on α_S in global PDF analyses and implications for predicted hadronic cross sections*, *Eur. Phys. J. C* **64** (2009) 653 [arXiv:0905.3531] [INSPIRE].

[48] H.-L. Lai et al., *New parton distributions for collider physics*, *Phys. Rev. D* **82** (2010) 074024 [arXiv:1007.2241] [INSPIRE].

[49] J. Gao et al., *CT10 next-to-next-to-leading order global analysis of QCD*, *Phys. Rev. D* **89** (2014) 033009 [arXiv:1302.6246] [INSPIRE].

[50] S. Frixione, E. Laenen, P. Motylinski, C. White and B.R. Webber, *Single-top hadroproduction in association with a W boson*, *JHEP* **07** (2008) 029 [arXiv:0805.3067] [INSPIRE].

[51] N. Kidonakis, *Two-loop soft anomalous dimensions for single top quark associated production with a W^- or H^-*, *Phys. Rev. D* **82** (2010) 054018 [arXiv:1005.4451] [INSPIRE].

[52] N. Kidonakis, *Top Quark Production*, in the proceedings of the *Helmholtz International Summer School on Physics of Heavy Quarks and Hadrons (HQ 2013)*, Dubna, Russian Federation, 15–28 July 2013, pp. 139–168 [DOI:10.3204/DESY-PROC-2013-03/Kidonakis] [arXiv:1311.0283] [INSPIRE].

[53] J. Alwall et al., *The automated computation of tree-level and next-to-leading order differential cross sections, and their matching to parton shower simulations*, *JHEP* **07** (2014) 079 [arXiv:1405.0301] [INSPIRE].

[54] S. Frixione, E. Laenen, P. Motylinski and B.R. Webber, *Angular correlations of lepton pairs from vector boson and top quark decays in Monte Carlo simulations*, *JHEP* **04** (2007) 081 [hep-ph/0702198] [INSPIRE].

[55] P. Artoisenet, R. Frederix, O. Mattelaer and R. Rietkerk, *Automatic spin-entangled decays of heavy resonances in Monte Carlo simulations*, *JHEP* **03** (2013) 015 [arXiv:1212.3460] [INSPIRE].

[56] LHC Higgs Cross Section Working Group, *Handbook of LHC Higgs Cross Sections: 4. Deciphering the Nature of the Higgs Sector*, arXiv:1610.07922 [DOI:10.23731/CYRM-2017-002] [INSPIRE].

[57] H.B. Hartanto, B. Jäger, L. Reina and D. Wackeroth, *Higgs boson production in association with top quarks in the POWHEG BOX*, *Phys. Rev. D* **91** (2015) 094003 [arXiv:1501.04498] [INSPIRE].

[58] E. Bothmann et al., *Event Generation with Sherpa 2.2*, *SciPost Phys.* **7** (2019) 034 [arXiv:1905.09127] [INSPIRE].

[59] T. Gleisberg and S. Höche, *Comix, a new matrix element generator*, *JHEP* **12** (2008) 039 [arXiv:0808.3674] [INSPIRE].

[60] F. Buccioni et al., *OpenLoops 2*, *Eur. Phys. J. C* **79** (2019) 866 [arXiv:1907.13071] [INSPIRE].

[61] F. Cascioli, P. Maierhöfer and S. Pozzorini, *Scattering Amplitudes with Open Loops*, *Phys. Rev. Lett.* **108** (2012) 111601 [arXiv:1111.5206] [INSPIRE].

[62] A. Denner, S. Dittmaier and L. Hofer, *Collier: a fortran-based Complex One-Loop LIbrary in Extended Regularizations*, *Comput. Phys. Commun.* **212** (2017) 220 [arXiv:1604.06792] [INSPIRE].

[63] S. Schumann and F. Krauss, *A Parton shower algorithm based on Catani-Seymour dipole factorisation*, *JHEP* **03** (2008) 038 [arXiv:0709.1027] [INSPIRE].

[64] J.-C. Winter, F. Krauss and G. Soff, *A Modified cluster hadronization model*, *Eur. Phys. J. C* **36** (2004) 381 [hep-ph/0311085] [INSPIRE].

[65] S. Höche, F. Krauss, M. Schönherr and F. Siegert, *A critical appraisal of NLO+PS matching methods*, *JHEP* **09** (2012) 049 [arXiv:1111.1220] [INSPIRE].

JHEP05(2025)038

[66] S. Catani, F. Krauss, B.R. Webber and R. Kuhn, *QCD matrix elements + parton showers*, *JHEP* **11** (2001) 063 [hep-ph/0109231] [INSPIRE].

[67] S. Höche, F. Krauss, S. Schumann and F. Siegert, *QCD matrix elements and truncated showers*, *JHEP* **05** (2009) 053 [arXiv:0903.1219] [INSPIRE].

[68] S. Höche, F. Krauss, M. Schönherr and F. Siegert, *QCD matrix elements + parton showers: The NLO case*, *JHEP* **04** (2013) 027 [arXiv:1207.5030] [INSPIRE].

[69] R. Frederix, E. Re and P. Torrielli, *Single-top t-channel hadroproduction in the four-flavour scheme with POWHEG and aMC@NLO*, *JHEP* **09** (2012) 130 [arXiv:1207.5391] [INSPIRE].

[70] L.A. Harland-Lang, A.D. Martin, P. Motylinski and R.S. Thorne, *Parton distributions in the LHC era: MMHT 2014 PDFs*, *Eur. Phys. J. C* **75** (2015) 204 [arXiv:1412.3989] [INSPIRE].

[71] S. Höche, S. Mrenna, S. Payne, C.T. Preuss and P. Skands, *A Study of QCD Radiation in VBF Higgs Production with Vincia and Pythia*, *SciPost Phys.* **12** (2022) 010 [arXiv:2106.10987] [INSPIRE].

[72] ATLAS collaboration, *Studies on the improvement of the matching uncertainty definition in top-quark processes simulated with Powheg+Pythia 8*, ATL-PHYS-PUB-2023-029 (2023).

[73] L. Lönnblad, *Correcting the color dipole cascade model with fixed order matrix elements*, *JHEP* **05** (2002) 046 [hep-ph/0112284] [INSPIRE].

[74] L. Lönnblad and S. Prestel, *Matching Tree-Level Matrix Elements with Interleaved Showers*, *JHEP* **03** (2012) 019 [arXiv:1109.4829] [INSPIRE].

[75] C. Anastasiou, L.J. Dixon, K. Melnikov and F. Petriello, *High precision QCD at hadron colliders: Electroweak gauge boson rapidity distributions at NNLO*, *Phys. Rev. D* **69** (2004) 094008 [hep-ph/0312266] [INSPIRE].

[76] ATLAS collaboration, *Electron and photon performance measurements with the ATLAS detector using the 2015–2017 LHC proton-proton collision data*, 2019 *JINST* **14** P12006 [arXiv:1908.00005] [INSPIRE].

[77] ATLAS collaboration, *Electron and photon efficiencies in LHC Run 2 with the ATLAS experiment*, *JHEP* **05** (2024) 162 [arXiv:2308.13362] [INSPIRE].

[78] ATLAS collaboration, *Muon reconstruction and identification efficiency in ATLAS using the full Run 2 pp collision data set at* $\sqrt{s} = 13$ *TeV*, *Eur. Phys. J. C* **81** (2021) 578 [arXiv:2012.00578] [INSPIRE].

[79] ATLAS collaboration, *The ATLAS inner detector trigger performance in pp collisions at* 13 *TeV during LHC Run 2*, *Eur. Phys. J. C* **82** (2022) 206 [arXiv:2107.02485] [INSPIRE].

[80] ATLAS collaboration, *Performance of electron and photon triggers in ATLAS during LHC Run 2*, *Eur. Phys. J. C* **80** (2020) 47 [arXiv:1909.00761] [INSPIRE].

[81] ATLAS collaboration, *Performance of the ATLAS muon triggers in Run 2*, 2020 *JINST* **15** P09015 [arXiv:2004.13447] [INSPIRE].

[82] M. Cacciari, G.P. Salam and G. Soyez, *The anti-k_t jet clustering algorithm*, *JHEP* **04** (2008) 063 [arXiv:0802.1189] [INSPIRE].

[83] M. Cacciari, G.P. Salam and G. Soyez, *FastJet User Manual*, *Eur. Phys. J. C* **72** (2012) 1896 [arXiv:1111.6097] [INSPIRE].

[84] ATLAS collaboration, *Jet reconstruction and performance using particle flow with the ATLAS Detector*, *Eur. Phys. J. C* **77** (2017) 466 [arXiv:1703.10485] [INSPIRE].

[85] ATLAS collaboration, *Jet energy scale and resolution measured in proton-proton collisions at* $\sqrt{s} = 13$ *TeV with the ATLAS detector*, *Eur. Phys. J. C* **81** (2021) 689 [arXiv:2007.02645] [INSPIRE].

[86] ATLAS collaboration, *Performance of pile-up mitigation techniques for jets in pp collisions at* $\sqrt{s} = 8$ *TeV using the ATLAS detector*, *Eur. Phys. J. C* **76** (2016) 581 [arXiv:1510.03823] [INSPIRE].

[87] ATLAS collaboration, *ATLAS flavour-tagging algorithms for the LHC Run 2 pp collision dataset*, *Eur. Phys. J. C* **83** (2023) 681 [arXiv:2211.16345] [INSPIRE].

[88] BELLE collaboration, *Measurement of the* τ*-lepton lifetime at Belle*, *Phys. Rev. Lett.* **112** (2014) 031801 [arXiv:1310.8503] [INSPIRE].

[89] R.J. Barlow, *Extended maximum likelihood*, *Nucl. Instrum. Meth. A* **297** (1990) 496 [INSPIRE].

[90] W. Voigt, *Über das Gesetz der Intensitätsverteilung innerhalb der Linien eines Gasspektrums*, in *Sitzungsberichte* **25**, Königlich Bayerische Akademie der Wissenschaften, Munich, German (1912), pp. 603–620.

[91] R.D. Cousins, *Generalization of chisquare goodness-of-fit test for binned data using saturated models, with application to histograms*, http://www.physics.ucla.edu/~cousins/stats/cousins_saturated.pdf.

[92] ATLAS collaboration, *Electron and photon energy calibration with the ATLAS detector using LHC Run 2 data*, 2024 *JINST* **19** P02009 [arXiv:2309.05471] [INSPIRE].

[93] ATLAS collaboration, *Studies of the muon momentum calibration and performance of the ATLAS detector with pp collisions at* $\sqrt{s} = 13$ *TeV*, *Eur. Phys. J. C* **83** (2023) 686 [arXiv:2212.07338] [INSPIRE].

[94] ATLAS collaboration, *ATLAS b-jet identification performance and efficiency measurement with* $t\bar{t}$ *events in pp collisions at* $\sqrt{s} = 13$ *TeV*, *Eur. Phys. J. C* **79** (2019) 970 [arXiv:1907.05120] [INSPIRE].

[95] ATLAS collaboration, *Measurement of the c-jet mistagging efficiency in* $t\bar{t}$ *events using pp collision data at* $\sqrt{s} = 13$ *TeV collected with the ATLAS detector*, *Eur. Phys. J. C* **82** (2022) 95 [arXiv:2109.10627] [INSPIRE].

[96] ATLAS collaboration, *Calibration of the light-flavour jet mistagging efficiency of the b-tagging algorithms with Z+jets events using* $139\,fb^{-1}$ *of ATLAS proton-proton collision data at* $\sqrt{s} = 13$ *TeV*, *Eur. Phys. J. C* **83** (2023) 728 [arXiv:2301.06319] [INSPIRE].

[97] R.J. Barlow and C. Beeston, *Fitting using finite Monte Carlo samples*, *Comput. Phys. Commun.* **77** (1993) 219 [INSPIRE].

[98] ATLAS collaboration, *ATLAS Computing Acknowledgements*, ATL-SOFT-PUB-2023-001 (2023).

The ATLAS collaboration

G. Aad[105], E. Aakvaag[17], B. Abbott[124], S. Abdelhameed[120a], K. Abeling[57], N.J. Abicht[51], S.H. Abidi[30], M. Aboelela[46], A. Aboulhorma[36e], H. Abramowicz[156], Y. Abulaiti[121], B.S. Acharya[71a,71b,m], A. Ackermann[65a], C. Adam Bourdarios[4], L. Adamczyk[88a], S.V. Addepalli[148], M.J. Addison[104], J. Adelman[119], A. Adiguzel[22c], T. Adye[138], A.A. Affolder[140], Y. Afik[41], M.N. Agaras[13], A. Aggarwal[103], C. Agheorghiesei[28c], F. Ahmadov[40,ab], S. Ahuja[98], X. Ai[64e], G. Aielli[78a,78b], A. Aikot[168], M. Ait Tamlihat[36e], B. Aitbenchikh[36a], M. Akbiyik[103], T.P.A. Åkesson[101], A.V. Akimov[150], D. Akiyama[173], N.N. Akolkar[25], S. Aktas[22a], K. Al Khoury[43], G.L. Alberghi[24b], J. Albert[170], P. Albicocco[55], G.L. Albouy[62], S. Alderweireldt[54], Z.L. Alegria[125], M. Aleksa[37], I.N. Aleksandrov[40], C. Alexa[28b], T. Alexopoulos[10], F. Alfonsi[24b], M. Algren[58], M. Alhroob[172], B. Ali[136], H.M.J. Ali[94,v], S. Ali[32], S.W. Alibocus[95], M. Aliev[34c], G. Alimonti[73a], W. Alkakhi[57], C. Allaire[68], B.M.M. Allbrooke[151], J.S. Allen[104], J.F. Allen[54], C.A. Allendes Flores[141f], P.P. Allport[21], A. Aloisio[74a,74b], F. Alonso[93], C. Alpigiani[143], Z.M.K. Alsolami[94], M. Alvarez Estevez[102], A. Alvarez Fernandez[103], M. Alves Cardoso[58], M.G. Alviggi[74a,74b], M. Aly[104], Y. Amaral Coutinho[85b], A. Ambler[107], C. Amelung[37], M. Amerl[104], C.G. Ames[112], D. Amidei[109], B. Amini[56], K.J. Amirie[159], S.P. Amor Dos Santos[134a], K.R. Amos[168], D. Amperiadou[157], S. An[86], V. Ananiev[129], C. Anastopoulos[144], T. Andeen[11], J.K. Anders[37], A.C. Anderson[61], A. Andreazza[73a,73b], S. Angelidakis[9], A. Angerami[43], A.V. Anisenkov[39], A. Annovi[76a], C. Antel[58], E. Antipov[150], M. Antonelli[55], F. Anulli[77a], M. Aoki[86], T. Aoki[158], M.A. Aparo[151], L. Aperio Bella[50], C. Appelt[156], A. Apyan[27], S.J. Arbiol Val[89], C. Arcangeletti[55], A.T.H. Arce[53], J-F. Arguin[111], S. Argyropoulos[157], J.-H. Arling[50], O. Arnaez[4], H. Arnold[150], G. Artoni[77a,77b], H. Asada[114], K. Asai[122], S. Asai[158], N.A. Asbah[37], R.A. Ashby Pickering[172], K. Assamagan[30], R. Astalos[29a], K.S.V. Astrand[101], S. Atashi[163], R.J. Atkin[34a], H. Atmani[36f], P.A. Atmasiddha[132], K. Augsten[136], A.D. Auriol[21], V.A. Austrup[104], G. Avolio[37], K. Axiotis[58], G. Azuelos[111,af], D. Babal[29b], H. Bachacou[139], K. Bachas[157,q], A. Bachiu[35], E. Bachmann[52], A. Badea[41], T.M. Baer[109], P. Bagnaia[77a,77b], M. Bahmani[19], D. Bahner[56], K. Bai[127], J.T. Baines[138], L. Baines[97], O.K. Baker[177], E. Bakos[16], D. Bakshi Gupta[8], L.E. Balabram Filho[85b], V. Balakrishnan[124], R. Balasubramanian[4], E.M. Baldin[39], P. Balek[88a], E. Ballabene[24b,24a], F. Balli[139], L.M. Baltes[65a], W.K. Balunas[33], J. Balz[103], I. Bamwidhi[120b], E. Banas[89], M. Bandieramonte[133], A. Bandyopadhyay[25], S. Bansal[25], L. Barak[156], M. Barakat[50], E.L. Barberio[108], D. Barberis[59b,59a], M. Barbero[105], M.Z. Barel[118], T. Barillari[113], M-S. Barisits[37], T. Barklow[148], P. Baron[126], D.A. Baron Moreno[104], A. Baroncelli[64a], A.J. Barr[130], J.D. Barr[99], F. Barreiro[102], J. Barreiro Guimarães da Costa[14], M.G. Barros Teixeira[134a], S. Barsov[39], F. Bartels[65a], R. Bartoldus[148], A.E. Barton[94], P. Bartos[29a], A. Basan[103], M. Baselga[51], A. Bassalat[68,b], M.J. Basso[160a], S. Bataju[46], R. Bate[169], R.L. Bates[61], S. Batlamous[102], B. Batool[146], M. Battaglia[140], D. Battulga[19], M. Bauce[77a,77b], M. Bauer[81], P. Bauer[25], L.T. Bazzano Hurrell[31], J.B. Beacham[53], T. Beau[131], J.Y. Beaucamp[93], P.H. Beauchemin[162], P. Bechtle[25], H.P. Beck[20,p], K. Becker[172], A.J. Beddall[84], V.A. Bednyakov[40], C.P. Bee[150], L.J. Beemster[16], T.A. Beermann[37],

JHEP05(2025)038

M. Begalli[85d], M. Begel[30], J.K. Behr[50], J.F. Beirer[37], F. Beisiegel[25], M. Belfkir[120b], G. Bella[156], L. Bellagamba[24b], A. Bellerive[35], P. Bellos[21], K. Beloborodov[39], D. Benchekroun[36a], F. Bendebba[36a], Y. Benhammou[156], K.C. Benkendorfer[63], L. Beresford[50], M. Beretta[55], E. Bergeaas Kuutmann[166], N. Berger[4], B. Bergmann[136], J. Beringer[18a], G. Bernardi[5], C. Bernius[148], F.U. Bernlochner[25], F. Bernon[37], A. Berrocal Guardia[13], T. Berry[98], P. Berta[137], A. Berthold[52], S. Bethke[113], A. Betti[77a,77b], A.J. Bevan[97], N.K. Bhalla[56], S. Bharthuar[113], S. Bhatta[150], D.S. Bhattacharya[171], P. Bhattarai[148], Z.M. Bhatti[121], K.D. Bhide[56], V.S. Bhopatkar[125], R.M. Bianchi[133], G. Bianco[24b,24a], O. Biebel[112], M. Biglietti[79a], C.S. Billingsley[46], Y. Bimgdi[36f], M. Bindi[57], A. Bingham[176], A. Bingul[22b], C. Bini[77a,77b], G.A. Bird[33], M. Birman[174], M. Biros[137], S. Biryukov[151], T. Bisanz[51], E. Bisceglie[45b,45a], J.P. Biswal[138], D. Biswas[146], I. Bloch[50], A. Blue[61], U. Blumenschein[97], J. Blumenthal[103], V.S. Bobrovnikov[39], M. Boehler[56], B. Boehm[171], D. Bogavac[37], A.G. Bogdanchikov[39], L.S. Boggia[131], C. Bohm[49a], V. Boisvert[98], P. Bokan[37], T. Bold[88a], M. Bomben[5], M. Bona[97], M. Boonekamp[139], A.G. Borbély[61], I.S. Bordulev[39], G. Borissov[94], D. Bortoletto[130], D. Boscherini[24b], M. Bosman[13], K. Bouaouda[36a], N. Bouchhar[168], L. Boudet[4], J. Boudreau[133], E.V. Bouhova-Thacker[94], D. Boumediene[42], R. Bouquet[59b,59a], A. Boveia[123], J. Boyd[37], D. Boye[30], I.R. Boyko[40], L. Bozianu[58], J. Bracinik[21], N. Brahimi[4], G. Brandt[176], O. Brandt[33], B. Brau[106], J.E. Brau[127], R. Brener[174], L. Brenner[118], R. Brenner[166], S. Bressler[174], G. Brianti[80a,80b], D. Britton[61], D. Britzger[113], I. Brock[25], R. Brock[110], G. Brooijmans[43], A.J. Brooks[70], E.M. Brooks[160b], E. Brost[30], L.M. Brown[170], L.E. Bruce[63], T.L. Bruckler[130], P.A. Bruckman de Renstrom[89], B. Brüers[50], A. Bruni[24b], G. Bruni[24b], D. Brunner[49a,49b], M. Bruschi[24b], N. Bruscino[77a,77b], T. Buanes[17], Q. Buat[143], D. Buchin[113], A.G. Buckley[61], O. Bulekov[39], B.A. Bullard[148], S. Burdin[95], C.D. Burgard[51], A.M. Burger[37], B. Burghgrave[8], O. Burlayenko[56], J. Burleson[167], J.T.P. Burr[33], J.C. Burzynski[147], E.L. Busch[43], V. Büscher[103], P.J. Bussey[61], J.M. Butler[26], C.M. Buttar[61], J.M. Butterworth[99], W. Buttinger[138], C.J. Buxo Vazquez[110], A.R. Buzykaev[39], S. Cabrera Urbán[168], L. Cadamuro[68], D. Caforio[60], H. Cai[133], Y. Cai[14,115c], Y. Cai[115a], V.M.M. Cairo[37], O. Cakir[3a], N. Calace[37], P. Calafiura[18a], G. Calderini[131], P. Calfayan[35], G. Callea[61], L.P. Caloba[85b], D. Calvet[42], S. Calvet[42], R. Camacho Toro[131], S. Camarda[37], D. Camarero Munoz[27], P. Camarri[78a,78b], M.T. Camerlingo[74a,74b], D. Cameron[37], C. Camincher[170], M. Campanelli[99], A. Camplani[44], V. Canale[74a,74b], A.C. Canbay[3a], E. Canonero[98], J. Cantero[168], Y. Cao[167], F. Capocasa[27], M. Capua[45b,45a], A. Carbone[73a,73b], R. Cardarelli[78a], J.C.J. Cardenas[8], M.P. Cardiff[27], G. Carducci[45b,45a], T. Carli[37], G. Carlino[74a], J.I. Carlotto[13], B.T. Carlson[133,r], E.M. Carlson[170,160a], J. Carmignani[95], L. Carminati[73a,73b], A. Carnelli[139], M. Carnesale[37], S. Caron[117], E. Carquin[141f], I.B. Carr[108], S. Carrá[73a], G. Carratta[24b,24a], A.M. Carroll[127], M.P. Casado[13,i], M. Caspar[50], F.L. Castillo[4], L. Castillo Garcia[13], V. Castillo Gimenez[168], N.F. Castro[134a,134e], A. Catinaccio[37], J.R. Catmore[129], T. Cavaliere[4], V. Cavaliere[30], L.J. Caviedes Betancourt[23b], Y.C. Cekmecelioglu[50], E. Celebi[84], S. Cella[37], V. Cepaitis[58], K. Cerny[126], A.S. Cerqueira[85a], A. Cerri[151], L. Cerrito[78a,78b], F. Cerutti[18a],

B. Cervato[146], A. Cervelli[24b], G. Cesarini[55], S.A. Cetin[84], P.M. Chabrillat[131], D. Chakraborty[119], J. Chan[18a], W.Y. Chan[158], J.D. Chapman[33], E. Chapon[139], B. Chargeishvili[154b], D.G. Charlton[21], M. Chatterjee[20], C. Chauhan[137], Y. Che[115a], S. Chekanov[6], S.V. Chekulaev[160a], G.A. Chelkov[40,a], A. Chen[109], B. Chen[156], B. Chen[170], H. Chen[115a], H. Chen[30], J. Chen[64c], J. Chen[147], M. Chen[130], S. Chen[90], S.J. Chen[115a], X. Chen[64c], X. Chen[15,ae], Y. Chen[64a], C.L. Cheng[175], H.C. Cheng[66a], S. Cheong[148], A. Cheplakov[40], E. Cheremushkina[50], E. Cherepanova[118], R. Cherkaoui El Moursli[36e], E. Cheu[7], K. Cheung[67], L. Chevalier[139], V. Chiarella[55], G. Chiarelli[76a], N. Chiedde[105], G. Chiodini[72a], A.S. Chisholm[21], A. Chitan[28b], M. Chitishvili[168], M.V. Chizhov[40,s], K. Choi[11], Y. Chou[143], E.Y.S. Chow[117], K.L. Chu[174], M.C. Chu[66a], X. Chu[14,115c], Z. Chubinidze[55], J. Chudoba[135], J.J. Chwastowski[89], D. Cieri[113], K.M. Ciesla[88a], V. Cindro[96], A. Ciocio[18a], F. Cirotto[74a,74b], Z.H. Citron[174], M. Citterio[73a], D.A. Ciubotaru[28b], A. Clark[58], P.J. Clark[54], N. Clarke Hall[99], C. Clarry[159], J.M. Clavijo Columbie[50], S.E. Clawson[50], C. Clement[49a,49b], Y. Coadou[105], M. Cobal[71a,71c], A. Coccaro[59b], R.F. Coelho Barrue[134a], R. Coelho Lopes De Sa[106], S. Coelli[73a], L.S. Colangeli[159], B. Cole[43], J. Collot[62], P. Conde Muiño[134a,134g], M.P. Connell[34c], S.H. Connell[34c], E.I. Conroy[130], F. Conventi[74a,ag], H.G. Cooke[21], A.M. Cooper-Sarkar[130], F.A. Corchia[24b,24a], A. Cordeiro Oudot Choi[131], L.D. Corpe[42], M. Corradi[77a,77b], F. Corriveau[107,aa], A. Cortes-Gonzalez[19], M.J. Costa[168], F. Costanza[4], D. Costanzo[144], B.M. Cote[123], J. Couthures[4], G. Cowan[98], K. Cranmer[175], L. Cremer[51], D. Cremonini[24b,24a], S. Crépé-Renaudin[62], F. Crescioli[131], M. Cristinziani[146], M. Cristoforetti[80a,80b], V. Croft[118], J.E. Crosby[125], G. Crosetti[45b,45a], A. Cueto[102], H. Cui[99], Z. Cui[7], W.R. Cunningham[61], F. Curcio[168], J.R. Curran[54], P. Czodrowski[37], M.J. Da Cunha Sargedas De Sousa[59b,59a], J.V. Da Fonseca Pinto[85b], C. Da Via[104], W. Dabrowski[88a], T. Dado[37], S. Dahbi[153], T. Dai[109], D. Dal Santo[20], C. Dallapiccola[106], M. Dam[44], G. D'amen[30], V. D'Amico[112], J. Damp[103], J.R. Dandoy[35], D. Dannheim[37], M. Danninger[147], V. Dao[150], G. Darbo[59b], S.J. Das[30], F. Dattola[50], S. D'Auria[73a,73b], A. D'Avanzo[74a,74b], C. David[34a], T. Davidek[137], I. Dawson[97], H.A. Day-hall[136], K. De[8], C. De Almeida Rossi[159], R. De Asmundis[74a], N. De Biase[50], S. De Castro[24b,24a], N. De Groot[117], P. de Jong[118], H. De la Torre[119], A. De Maria[115a], A. De Salvo[77a], U. De Sanctis[78a,78b], F. De Santis[72a,72b], A. De Santo[151], J.B. De Vivie De Regie[62], J. Debevc[96], D.V. Dedovich[40], J. Degens[95], A.M. Deiana[46], F. Del Corso[24b,24a], J. Del Peso[102], L. Delagrange[131], F. Deliot[139], C.M. Delitzsch[51], M. Della Pietra[74a,74b], D. Della Volpe[58], A. Dell'Acqua[37], L. Dell'Asta[73a,73b], M. Delmastro[4], C.C. Delogu[103], P.A. Delsart[62], S. Demers[177], M. Demichev[40], S.P. Denisov[39], H. Denizli[22a], L. D'Eramo[42], D. Derendarz[89], F. Derue[131], P. Dervan[95], K. Desch[25], C. Deutsch[25], F.A. Di Bello[59b,59a], A. Di Ciaccio[78a,78b], L. Di Ciaccio[4], A. Di Domenico[77a,77b], C. Di Donato[74a,74b], A. Di Girolamo[37], G. Di Gregorio[37], A. Di Luca[80a,80b], B. Di Micco[79a,79b], R. Di Nardo[79a,79b], K.F. Di Petrillo[41], M. Diamantopoulou[35], F.A. Dias[118], T. Dias Do Vale[147], M.A. Diaz[141a,141b], A.R. Didenko[40], M. Didenko[168], E.B. Diehl[109], S. Díez Cornell[50], C. Diez Pardos[146], C. Dimitriadi[166], A. Dimitrievska[21], J. Dingfelder[25], T. Dingley[130], I-M. Dinu[28b], S.J. Dittmeier[65b], F. Dittus[37],

JHEP05(2025)038

M. Divisek[137], B. Dixit[95], F. Djama[105], T. Djobava[154b], C. Doglioni[104,101], A. Dohnalova[29a], Z. Dolezal[137], K. Domijan[88a], K.M. Dona[41], M. Donadelli[85d], B. Dong[110], J. Donini[42], A. D'Onofrio[74a,74b], M. D'Onofrio[95], J. Dopke[138], A. Doria[74a], N. Dos Santos Fernandes[134a], P. Dougan[104], M.T. Dova[93], A.T. Doyle[61], M.A. Draguet[130], M.P. Drescher[57], E. Dreyer[174], I. Drivas-koulouris[10], M. Drnevich[121], M. Drozdova[58], D. Du[64a], T.A. du Pree[118], F. Dubinin[39], M. Dubovsky[29a], E. Duchovni[174], G. Duckeck[112], O.A. Ducu[28b], D. Duda[54], A. Dudarev[37], E.R. Duden[27], M. D'uffizi[104], L. Duflot[68], M. Dührssen[37], I. Duminica[28g], A.E. Dumitriu[28b], M. Dunford[65a], S. Dungs[51], K. Dunne[49a,49b], A. Duperrin[105], H. Duran Yildiz[3a], M. Düren[60], A. Durglishvili[154b], D. Duvnjak[35], B.L. Dwyer[119], G.I. Dyckes[18a], M. Dyndal[88a], B.S. Dziedzic[37], Z.O. Earnshaw[151], G.H. Eberwein[130], B. Eckerova[29a], S. Eggebrecht[57], E. Egidio Purcino De Souza[85e], L.F. Ehrke[58], G. Eigen[17], K. Einsweiler[18a], T. Ekelof[166], P.A. Ekman[101], S. El Farkh[36b], Y. El Ghazali[64a], H. El Jarrari[37], A. El Moussaouy[36a], V. Ellajosyula[166], M. Ellert[166], F. Ellinghaus[176], N. Ellis[37], J. Elmsheuser[30], M. Elsawy[120a], M. Elsing[37], D. Emeliyanov[138], Y. Enari[86], I. Ene[18a], S. Epari[13], P.A. Erland[89], D. Ernani Martins Neto[89], M. Errenst[176], M. Escalier[68], C. Escobar[168], E. Etzion[156], G. Evans[134a,134b], H. Evans[70], L.S. Evans[98], A. Ezhilov[39], S. Ezzarqtouni[36a], F. Fabbri[24b,24a], L. Fabbri[24b,24a], G. Facini[99], V. Fadeyev[140], R.M. Fakhrutdinov[39], D. Fakoudis[103], S. Falciano[77a], L.F. Falda Ulhoa Coelho[134a], F. Fallavollita[113], G. Falsetti[45b,45a], J. Faltova[137], C. Fan[167], K.Y. Fan[66b], Y. Fan[14], Y. Fang[14,115c], M. Fanti[73a,73b], M. Faraj[71a,71b], Z. Farazpay[100], A. Farbin[8], A. Farilla[79a], T. Farooque[110], J.N. Farr[177], S.M. Farrington[138,54], F. Fassi[36e], D. Fassouliotis[9], M. Faucci Giannelli[78a,78b], W.J. Fawcett[33], L. Fayard[68], P. Federic[137], P. Federicova[135], O.L. Fedin[39,a], M. Feickert[175], L. Feligioni[105], D.E. Fellers[127], C. Feng[64b], Z. Feng[118], M.J. Fenton[163], L. Ferencz[50], R.A.M. Ferguson[94], P. Fernandez Martinez[69], M.J.V. Fernoux[105], J. Ferrando[94], A. Ferrari[166], P. Ferrari[118,117], R. Ferrari[75a], D. Ferrere[58], C. Ferretti[109], M.P. Fewell[1], D. Fiacco[77a,77b], F. Fiedler[103], P. Fiedler[136], S. Filimonov[39], A. Filipčič[96], E.K. Filmer[160a], F. Filthaut[117], M.C.N. Fiolhais[134a,134c,c], L. Fiorini[168], W.C. Fisher[110], T. Fitschen[104], P.M. Fitzhugh[139], I. Fleck[146], P. Fleischmann[109], T. Flick[176], M. Flores[34d,ac], L.R. Flores Castillo[66a], L. Flores Sanz De Acedo[37], F.M. Follega[80a,80b], N. Fomin[33], J.H. Foo[159], A. Formica[139], A.C. Forti[104], E. Fortin[37], A.W. Fortman[18a], M.G. Foti[18a], L. Fountas[9,j], D. Fournier[68], H. Fox[94], P. Francavilla[76a,76b], S. Francescato[63], S. Franchellucci[58], M. Franchini[24b,24a], S. Franchino[65a], D. Francis[37], L. Franco[117], V. Franco Lima[37], L. Franconi[50], M. Franklin[63], G. Frattari[27], Y.Y. Frid[156], J. Friend[61], N. Fritzsche[37], A. Froch[58], D. Froidevaux[37], J.A. Frost[130], Y. Fu[64a], S. Fuenzalida Garrido[141f], M. Fujimoto[105], K.Y. Fung[66a], E. Furtado De Simas Filho[85e], M. Furukawa[158], J. Fuster[168], A. Gaa[57], A. Gabrielli[24b,24a], A. Gabrielli[159], P. Gadow[37], G. Gagliardi[59b,59a], L.G. Gagnon[18a], S. Gaid[165], S. Galantzan[156], J. Gallagher[1], E.J. Gallas[130], A.L. Gallen[166], B.J. Gallop[138], K.K. Gan[123], S. Ganguly[158], Y. Gao[54], F.M. Garay Walls[141a,141b], B. Garcia[30], C. García[168], A. Garcia Alonso[118], A.G. Garcia Caffaro[177], J.E. García Navarro[168], M. Garcia-Sciveres[18a], G.L. Gardner[132], R.W. Gardner[41], N. Garelli[162], R.B. Garg[148], J.M. Gargan[54], C.A. Garner[159], C.M. Garvey[34a], V.K. Gassmann[162], G. Gaudio[75a], V. Gautam[13], P. Gauzzi[77a,77b], J. Gavranovic[96], I.L. Gavrilenko[39], A. Gavrilyuk[39], C. Gay[169], G. Gaycken[127], E.N. Gazis[10], A.A. Geanta[28b], A. Gekow[123], C. Gemme[59b], M.H. Genest[62], A.D. Gentry[116], S. George[98], W.F. George[21], T. Geralis[48], A.A. Gerwin[124], P. Gessinger-Befurt[37], M.E. Geyik[176], M. Ghani[172], K. Ghorbanian[97], A. Ghosal[146], A. Ghosh[163], A. Ghosh[7], B. Giacobbe[24b], S. Giagu[77a,77b], T. Giani[118], A. Giannini[64a], S.M. Gibson[98], M. Gignac[140], D.T. Gil[88b], A.K. Gilbert[88a], B.J. Gilbert[43], D. Gillberg[35], G. Gilles[118], L. Ginabat[131], D.M. Gingrich[2,af], M.P. Giordani[71a,71c], P.F. Giraud[139], G. Giugliarelli[71a,71c], D. Giugni[73a], F. Giuli[78a,78b], I. Gkialas[9,j], L.K. Gladilin[39], C. Glasman[102], G.R. Gledhill[127], G. Glemža[50], M. Glisic[127], I. Gnesi[45b], Y. Go[30], M. Goblirsch-Kolb[37], B. Gocke[51], D. Godin[111], B. Gokturk[22a], S. Goldfarb[108], T. Golling[58], M.G.D. Gololo[34g], D. Golubkov[39], J.P. Gombas[110], A. Gomes[134a,134b], G. Gomes Da Silva[146], A.J. Gomez Delegido[168], R. Gonçalo[134a], L. Gonella[21], A. Gongadze[154c], F. Gonnella[21], J.L. Gonski[148], R.Y. González Andana[54], S. González de la Hoz[168], R. Gonzalez Lopez[95], C. Gonzalez Renteria[18a], M.V. Gonzalez Rodrigues[50], R. Gonzalez Suarez[166], S. Gonzalez-Sevilla[58], L. Goossens[37], B. Gorini[37], E. Gorini[72a,72b], A. Gorišek[96], T.C. Gosart[132], A.T. Goshaw[53], M.I. Gostkin[40], S. Goswami[125], C.A. Gottardo[37], S.A. Gotz[112], M. Gouighri[36b], V. Goumarre[50], A.G. Goussiou[143], N. Govender[34c], R.P. Grabarczyk[130], I. Grabowska-Bold[88a], K. Graham[35], E. Gramstad[129], S. Grancagnolo[72a,72b], C.M. Grant[1,139], P.M. Gravila[28f], F.G. Gravili[72a,72b], H.M. Gray[18a], M. Greco[72a,72b], M.J. Green[1], C. Grefe[25], A.S. Grefsrud[17], I.M. Gregor[50], K.T. Greif[163], P. Grenier[148], S.G. Grewe[113], A.A. Grillo[140], K. Grimm[32], S. Grinstein[13,w], J.-F. Grivaz[68], E. Gross[174], J. Grosse-Knetter[57], L. Guan[109], J.G.R. Guerrero Rojas[168], G. Guerrieri[37], R. Gugel[103], J.A.M. Guhit[109], A. Guida[19], E. Guilloton[172], S. Guindon[37], F. Guo[14,115c], J. Guo[64c], L. Guo[50], L. Guo[14,u], Y. Guo[109], A. Gupta[51], R. Gupta[133], S. Gurbuz[25], S.S. Gurdasani[56], G. Gustavino[77a,77b], P. Gutierrez[124], L.F. Gutierrez Zagazeta[132], M. Gutsche[52], C. Gutschow[99], C. Gwenlan[130], C.B. Gwilliam[95], E.S. Haaland[129], A. Haas[121], M. Habedank[61], C. Haber[18a], H.K. Hadavand[8], A. Hadef[52], A.I. Hagan[94], J.J. Hahn[146], E.H. Haines[99], M. Haleem[171], J. Haley[125], G.D. Hallewell[105], L. Halser[20], K. Hamano[170], M. Hamer[25], E.J. Hampshire[98], J. Han[64b], L. Han[115a], L. Han[64a], S. Han[18a], Y.F. Han[159], K. Hanagaki[86], M. Hance[140], D.A. Hangal[43], H. Hanif[147], M.D. Hank[132], J.B. Hansen[44], P.H. Hansen[44], D. Harada[58], T. Harenberg[176], S. Harkusha[178], M.L. Harris[106], Y.T. Harris[25], J. Harrison[13], N.M. Harrison[123], P.F. Harrison[172], N.M. Hartman[113], N.M. Hartmann[112], R.Z. Hasan[98,138], Y. Hasegawa[145], F. Haslbeck[130], S. Hassan[17], R. Hauser[110], C.M. Hawkes[21], R.J. Hawkings[37], Y. Hayashi[158], D. Hayden[110], C. Hayes[109], R.L. Hayes[118], C.P. Hays[130], J.M. Hays[97], H.S. Hayward[95], F. He[64a], M. He[14,115c], Y. He[50], Y. He[99], N.B. Heatley[97], V. Hedberg[101], A.L. Heggelund[129], C. Heidegger[56], K.K. Heidegger[56], J. Heilman[35], S. Heim[50], T. Heim[18a], J.G. Heinlein[132], J.J. Heinrich[127], L. Heinrich[113,ad], J. Hejbal[135], A. Held[175], S. Hellesund[17], C.M. Helling[169], S. Hellman[49a,49b], R.C.W. Henderson[94], L. Henkelmann[33], A.M. Henriques Correia[37], H. Herde[101], Y. Hernández Jiménez[150], L.M. Herrmann[25], T. Herrmann[52], G. Herten[56], R. Hertenberger[112], L. Hervas[37], M.E. Hesping[103], N.P. Hessey[160a], J. Hessler[113], M. Hidaoui[36b], N. Hidic[137], E. Hill[159],

JHEP05(2025)038

S.J. Hillier[21], J.R. Hinds[110], F. Hinterkeuser[25], M. Hirose[128], S. Hirose[161], D. Hirschbuehl[176], T.G. Hitchings[104], B. Hiti[96], J. Hobbs[150], R. Hobincu[28e], N. Hod[174], M.C. Hodgkinson[144], B.H. Hodkinson[130], A. Hoecker[37], D.D. Hofer[109], J. Hofer[168], T. Holm[25], M. Holzbock[37], L.B.A.H. Hommels[33], B.P. Honan[104], J.J. Hong[70], J. Hong[64c], T.M. Hong[133], B.H. Hooberman[167], W.H. Hopkins[6], M.C. Hoppesch[167], Y. Horii[114], M.E. Horstmann[113], S. Hou[153], M.R. Housenga[167], A.S. Howard[96], J. Howarth[61], J. Hoya[6], M. Hrabovsky[126], A. Hrynevich[50], T. Hryn'ova[4], P.J. Hsu[67], S.-C. Hsu[143], T. Hsu[68], M. Hu[18a], Q. Hu[64a], S. Huang[33], X. Huang[14,115c], Y. Huang[144], Y. Huang[103], Y. Huang[14], Z. Huang[104], Z. Hubacek[136], M. Huebner[25], F. Huegging[25], T.B. Huffman[130], M. Hufnagel Maranha De Faria[85a], C.A. Hugli[50], M. Huhtinen[37], S.K. Huiberts[17], R. Hulsken[107], N. Huseynov[12,g], J. Huston[110], J. Huth[63], R. Hyneman[7], G. Iacobucci[58], G. Iakovidis[30], L. Iconomidou-Fayard[68], J.P. Iddon[37], P. Iengo[74a,74b], R. Iguchi[158], Y. Iiyama[158], T. Iizawa[130], Y. Ikegami[86], D. Iliadis[157], N. Ilic[159], H. Imam[85c], G. Inacio Goncalves[85d], T. Ingebretsen Carlson[49a,49b], J.M. Inglis[97], G. Introzzi[75a,75b], M. Iodice[79a], V. Ippolito[77a,77b], R.K. Irwin[95], M. Ishino[158], W. Islam[175], C. Issever[19], S. Istin[22a,ak], H. Ito[173], R. Iuppa[80a,80b], A. Ivina[174], J.M. Izen[47], V. Izzo[74a], P. Jacka[135], P. Jackson[1], C.S. Jagfeld[112], G. Jain[160a], P. Jain[50], K. Jakobs[56], T. Jakoubek[174], J. Jamieson[61], W. Jang[158], M. Javurkova[106], P. Jawahar[104], L. Jeanty[127], J. Jejelava[154a], P. Jenni[56,f], C.E. Jessiman[35], C. Jia[64b], H. Jia[169], J. Jia[150], X. Jia[14,115c], Z. Jia[115a], C. Jiang[54], S. Jiggins[50], J. Jimenez Pena[13], S. Jin[115a], A. Jinaru[28b], O. Jinnouchi[142], P. Johansson[144], K.A. Johns[7], J.W. Johnson[140], F.A. Jolly[50], D.M. Jones[151], E. Jones[50], K.S. Jones[8], P. Jones[33], R.W.L. Jones[94], T.J. Jones[95], H.L. Joos[57,37], R. Joshi[123], J. Jovicevic[16], X. Ju[18a], J.J. Junggeburth[37], T. Junkermann[65a], A. Juste Rozas[13,w], M.K. Juzek[89], S. Kabana[141e], A. Kaczmarska[89], M. Kado[113], H. Kagan[123], M. Kagan[148], A. Kahn[132], C. Kahra[103], T. Kaji[158], E. Kajomovitz[155], N. Kakati[174], I. Kalaitzidou[56], C.W. Kalderon[30], N.J. Kang[140], D. Kar[34g], K. Karava[130], M.J. Kareem[160b], E. Karentzos[25], O. Karkout[118], S.N. Karpov[40], Z.M. Karpova[40], V. Kartvelishvili[94], A.N. Karyukhin[39], E. Kasimi[157], J. Katzy[50], S. Kaur[35], K. Kawade[145], M.P. Kawale[124], C. Kawamoto[90], T. Kawamoto[64a], E.F. Kay[37], F.I. Kaya[162], S. Kazakos[110], V.F. Kazanin[39], Y. Ke[150], J.M. Keaveney[34a], R. Keeler[170], G.V. Kehris[63], J.S. Keller[35], J.J. Kempster[151], O. Kepka[135], J. Kerr[160b], B.P. Kerridge[138], S. Kersten[176], B.P. Kerševan[96], L. Keszeghova[29a], S. Ketabchi Haghighat[159], R.A. Khan[133], A. Khanov[125], A.G. Kharlamov[39], T. Kharlamova[39], E.E. Khoda[143], M. Kholodenko[134a], T.J. Khoo[19], G. Khoriauli[171], J. Khubua[154b,*], Y.A.R. Khwaira[131], B. Kibirige[34g], D. Kim[6], D.W. Kim[49a,49b], Y.K. Kim[41], N. Kimura[99], M.K. Kingston[57], A. Kirchhoff[57], C. Kirfel[25], F. Kirfel[25], J. Kirk[138], A.E. Kiryunin[113], S. Kita[161], C. Kitsaki[10], O. Kivernyk[25], M. Klassen[162], C. Klein[35], L. Klein[171], M.H. Klein[46], S.B. Klein[58], U. Klein[95], A. Klimentov[30], T. Klioutchnikova[37], P. Kluit[118], S. Kluth[113], E. Kneringer[81], T.M. Knight[159], A. Knue[51], D. Kobylianskii[174], S.F. Koch[130], M. Kocian[148], P. Kodyš[137], D.M. Koeck[127], P.T. Koenig[25], T. Koffas[35], O. Kolay[52], I. Koletsou[4], T. Komarek[89], K. Köneke[57], A.X.Y. Kong[1], T. Kono[122], N. Konstantinidis[99], P. Kontaxakis[58], B. Konya[101], R. Kopeliansky[43], S. Koperny[88a],

JHEP05(2025)038

K. Korcyl[89], K. Kordas[157,e], A. Korn[99], S. Korn[57], I. Korolkov[13], N. Korotkova[39], B. Kortman[118], O. Kortner[113], S. Kortner[113], W.H. Kostecka[119], V.V. Kostyukhin[146], A. Kotsokechagia[37], A. Kotwal[53], A. Koulouris[37], A. Kourkoumeli-Charalampidi[75a,75b], C. Kourkoumelis[9], E. Kourlitis[113,ad], O. Kovanda[127], R. Kowalewski[170], W. Kozanecki[127], A.S. Kozhin[39], V.A. Kramarenko[39], G. Kramberger[96], P. Kramer[25], M.W. Krasny[131], A. Krasznahorkay[37], A.C. Kraus[119], J.W. Kraus[176], J.A. Kremer[50], T. Kresse[52], L. Kretschmann[176], J. Kretzschmar[95], K. Kreul[19], P. Krieger[159], K. Krizka[21], K. Kroeninger[51], H. Kroha[113], J. Kroll[135], J. Kroll[132], K.S. Krowpman[110], U. Kruchonak[40], H. Krüger[25], N. Krumnack[83], M.C. Kruse[53], O. Kuchinskaia[39], S. Kuday[3a], S. Kuehn[37], R. Kuesters[56], T. Kuhl[50], V. Kukhtin[40], Y. Kulchitsky[40], S. Kuleshov[141d,141b], M. Kumar[34g], N. Kumari[50], P. Kumari[160b], A. Kupco[135], T. Kupfer[51], A. Kupich[39], O. Kuprash[56], H. Kurashige[87], L.L. Kurchaninov[160a], O. Kurdysh[68], Y.A. Kurochkin[38], A. Kurova[39], M. Kuze[142], A.K. Kvam[106], J. Kvita[126], T. Kwan[107], N.G. Kyriacou[109], L.A.O. Laatu[105], C. Lacasta[168], F. Lacava[77a,77b], H. Lacker[19], D. Lacour[131], N.N. Lad[99], E. Ladygin[40], A. Lafarge[42], B. Laforge[131], T. Lagouri[177], F.Z. Lahbabi[36a], S. Lai[57], J.E. Lambert[170], S. Lammers[70], W. Lampl[7], C. Lampoudis[157,e], G. Lamprinoudis[103], A.N. Lancaster[119], E. Lançon[30], U. Landgraf[56], M.P.J. Landon[97], V.S. Lang[56], O.K.B. Langrekken[129], A.J. Lankford[163], F. Lanni[37], K. Lantzsch[25], A. Lanza[75a], M. Lanzac Berrocal[168], J.F. Laporte[139], T. Lari[73a], F. Lasagni Manghi[24b], M. Lassnig[37], V. Latonova[135], S.D. Lawlor[144], Z. Lawrence[104], R. Lazaridou[172], M. Lazzaroni[73a,73b], H.D.M. Le[110], E.M. Le Boulicaut[177], L.T. Le Pottier[18a], B. Leban[24b,24a], A. Lebedev[83], M. LeBlanc[104], F. Ledroit-Guillon[62], S.C. Lee[153], S. Lee[49a,49b], T.F. Lee[95], L.L. Leeuw[34c,ai], M. Lefebvre[170], C. Leggett[18a], G. Lehmann Miotto[37], M. Leigh[58], W.A. Leight[106], W. Leinonen[117], A. Leisos[157,t], M.A.L. Leite[85c], C.E. Leitgeb[19], R. Leitner[137], K.J.C. Leney[46], T. Lenz[25], S. Leone[76a], C. Leonidopoulos[54], A. Leopold[149], R. Les[110], C.G. Lester[33], M. Levchenko[39], J. Levêque[4], L.J. Levinson[174], G. Levrini[24b,24a], M.P. Lewicki[89], C. Lewis[143], D.J. Lewis[4], L. Lewitt[144], A. Li[30], B. Li[64b], C. Li[109], C-Q. Li[113], H. Li[64a], H. Li[64b], H. Li[115a], H. Li[15], H. Li[64b], J. Li[64c], K. Li[14], L. Li[64c], M. Li[14,115c], R. Li[177], S. Li[14,115c], S. Li[64d,64c,d], T. Li[5], X. Li[107], Z. Li[158], Z. Li[14,115c], Z. Li[64a], S. Liang[14,115c], Z. Liang[14], M. Liberatore[139], B. Liberti[78a], K. Lie[66c], J. Lieber Marin[85e], H. Lien[70], H. Lin[109], K. Lin[110], L. Linden[112], R.E. Lindley[7], J.H. Lindon[2], J. Ling[63], E. Lipeles[132], A. Lipniacka[17], A. Lister[169], J.D. Little[70], B. Liu[14], B.X. Liu[115b], D. Liu[64d,64c], E.H.L. Liu[21], J.B. Liu[64a], J.K.K. Liu[33], K. Liu[64d], K. Liu[64d,64c], M. Liu[64a], M.Y. Liu[64a], P. Liu[14], Q. Liu[64d,143,64c], X. Liu[64a], X. Liu[64b], Y. Liu[115b,115c], Y.L. Liu[64b], Y.W. Liu[64a], S.L. Lloyd[97], E.M. Lobodzinska[50], P. Loch[7], E. Lodhi[159], T. Lohse[19], K. Lohwasser[144], E. Loiacono[50], J.D. Lomas[21], J.D. Long[43], I. Longarini[163], R. Longo[167], I. Lopez Paz[69], A. Lopez Solis[50], N.A. Lopez-canelas[7], N. Lorenzo Martinez[4], A.M. Lory[112], M. Losada[120a], G. Löschcke Centeno[151], O. Loseva[39], X. Lou[49a,49b], X. Lou[14,115c], A. Lounis[68], P.A. Love[94], G. Lu[14,115c], M. Lu[68], S. Lu[132], Y.J. Lu[153], H.J. Lubatti[143], C. Luci[77a,77b], F.L. Lucio Alves[115a], F. Luehring[70], O. Lukianchuk[68], B.S. Lunday[132], O. Lundberg[149], B. Lund-Jensen[149,*], N.A. Luongo[6], M.S. Lutz[37], A.B. Lux[26], D. Lynn[30], R. Lysak[135], E. Lytken[101], V. Lyubushkin[40],

JHEP05(2025)038

T. Lyubushkina[40], M.M. Lyukova[150], M.Firdaus M. Soberi[54], H. Ma[30], K. Ma[64a], L.L. Ma[64b], W. Ma[64a], Y. Ma[125], J.C. MacDonald[103], P.C. Machado De Abreu Farias[85e], R. Madar[42], T. Madula[99], J. Maeda[87], T. Maeno[30], P.T. Mafa[34c,k], H. Maguire[144], V. Maiboroda[139], A. Maio[134a,134b,134d], K. Maj[88a], O. Majersky[50], S. Majewski[127], N. Makovec[68], V. Maksimovic[16], B. Malaescu[131], Pa. Malecki[89], V.P. Maleev[39], F. Malek[62,o], M. Mali[96], D. Malito[98], U. Mallik[82,*], S. Maltezos[10], S. Malyukov[40], J. Mamuzic[13], G. Mancini[55], M.N. Mancini[27], G. Manco[75a,75b], J.P. Mandalia[97], S.S. Mandarry[151], I. Mandić[96], L. Manhaes de Andrade Filho[85a], I.M. Maniatis[174], J. Manjarres Ramos[92], D.C. Mankad[174], A. Mann[112], S. Manzoni[37], L. Mao[64c], X. Mapekula[34c], A. Marantis[157,t], G. Marchiori[5], M. Marcisovsky[135], C. Marcon[73a], M. Marinescu[21], S. Marium[50], M. Marjanovic[124], A. Markhoos[56], M. Markovitch[68], M.K. Maroun[106], E.J. Marshall[94], Z. Marshall[18a], S. Marti-Garcia[168], J. Martin[99], T.A. Martin[138], V.J. Martin[54], B. Martin dit Latour[17], L. Martinelli[77a,77b], M. Martinez[13,w], P. Martinez Agullo[168], V.I. Martinez Outschoorn[106], P. Martinez Suarez[13], S. Martin-Haugh[138], G. Martinovicova[137], V.S. Martoiu[28b], A.C. Martyniuk[99], A. Marzin[37], D. Mascione[80a,80b], L. Masetti[103], J. Masik[104], A.L. Maslennikov[39], S.L. Mason[43], P. Massarotti[74a,74b], P. Mastrandrea[76a,76b], A. Mastroberardino[45b,45a], T. Masubuchi[128], T.T. Mathew[127], T. Mathisen[166], J. Matousek[137], D.M. Mattern[51], J. Maurer[28b], T. Maurin[61], A.J. Maury[68], B. Maček[96], D.A. Maximov[39], A.E. May[104], R. Mazini[34g], I. Maznas[119], M. Mazza[110], S.M. Mazza[140], E. Mazzeo[73a,73b], J.P. Mc Gowan[170], S.P. Mc Kee[109], C.A. Mc Lean[6], C.C. McCracken[169], E.F. McDonald[108], A.E. McDougall[118], L.F. Mcelhinney[94], J.A. Mcfayden[151], R.P. McGovern[132], R.P. Mckenzie[34g], T.C. Mclachlan[50], D.J. Mclaughlin[99], S.J. McMahon[138], C.M. Mcpartland[95], R.A. McPherson[170,aa], S. Mehlhase[112], A. Mehta[95], D. Melini[168], B.R. Mellado Garcia[34g], A.H. Melo[57], F. Meloni[50], A.M. Mendes Jacques Da Costa[104], H.Y. Meng[159], L. Meng[94], S. Menke[113], M. Mentink[37], E. Meoni[45b,45a], G. Mercado[119], S. Merianos[157], C. Merlassino[71a,71c], L. Merola[74a,74b], C. Meroni[73a,73b], J. Metcalfe[6], A.S. Mete[6], E. Meuser[103], C. Meyer[70], J-P. Meyer[139], R.P. Middleton[138], L. Mijović[54], G. Mikenberg[174], M. Mikestikova[135], M. Mikuž[96], H. Mildner[103], A. Milic[37], D.W. Miller[41], E.H. Miller[148], L.S. Miller[35], A. Milov[174], D.A. Milstead[49a,49b], T. Min[115a], A.A. Minaenko[39], I.A. Minashvili[154b], A.I. Mincer[121], B. Mindur[88a], M. Mineev[40], Y. Mino[90], L.M. Mir[13], M. Miralles Lopez[61], M. Mironova[18a], M.C. Missio[117], A. Mitra[172], V.A. Mitsou[168], Y. Mitsumori[114], O. Miu[159], P.S. Miyagawa[97], T. Mkrtchyan[65a], M. Mlinarevic[99], T. Mlinarevic[99], M. Mlynarikova[37], S. Mobius[20], P. Mogg[112], M.H. Mohamed Farook[116], A.F. Mohammed[14,115c], S. Mohapatra[43], G. Mokgatitswane[34g], L. Moleri[174], B. Mondal[146], S. Mondal[136], K. Mönig[50], E. Monnier[105], L. Monsonis Romero[168], J. Montejo Berlingen[13], A. Montella[49a,49b], M. Montella[123], F. Montereali[79a,79b], F. Monticelli[93], S. Monzani[71a,71c], A. Morancho Tarda[44], N. Morange[68], A.L. Moreira De Carvalho[50], M. Moreno Llácer[168], C. Moreno Martinez[58], J.M. Moreno Perez[23b], P. Morettini[59b], S. Morgenstern[37], M. Morii[63], M. Morinaga[158], M. Moritsu[91], F. Morodei[77a,77b], P. Moschovakos[37], B. Moser[130], M. Mosidze[154b], T. Moskalets[46], P. Moskvitina[117], J. Moss[32,l], P. Moszkowicz[88a], A. Moussa[36d], Y. Moyal[174], E.J.W. Moyse[106], O. Mtintsilana[34g], S. Muanza[105],

J. Mueller[133], D. Muenstermann[94], R. Müller[37], G.A. Mullier[166], A.J. Mullin[33], J.J. Mullin[132], A.E. Mulski[63], D.P. Mungo[159], D. Munoz Perez[168], F.J. Munoz Sanchez[104], M. Murin[104], W.J. Murray[172,138], M. Muškinja[96], C. Mwewa[30], A.G. Myagkov[39,a], A.J. Myers[8], G. Myers[109], M. Myska[136], B.P. Nachman[18a], K. Nagai[130], K. Nagano[86], R. Nagasaka[158], J.L. Nagle[30,ah], E. Nagy[105], A.M. Nairz[37], Y. Nakahama[86], K. Nakamura[86], K. Nakkalil[5], H. Nanjo[128], E.A. Narayanan[46], Y. Narukawa[158], I. Naryshkin[39], L. Nasella[73a,73b], S. Nasri[120b], C. Nass[25], G. Navarro[23a], J. Navarro-Gonzalez[168], A. Nayaz[19], P.Y. Nechaeva[39], S. Nechaeva[24b,24a], F. Nechansky[135], L. Nedic[130], T.J. Neep[21], A. Negri[75a,75b], M. Negrini[24b], C. Nellist[118], C. Nelson[107], K. Nelson[109], S. Nemecek[135], M. Nessi[37,h], M.S. Neubauer[167], F. Neuhaus[103], J. Neundorf[50], J. Newell[95], P.R. Newman[21], C.W. Ng[133], Y.W.Y. Ng[50], B. Ngair[120a], H.D.N. Nguyen[111], R.B. Nickerson[130], R. Nicolaidou[139], J. Nielsen[140], M. Niemeyer[57], J. Niermann[37], N. Nikiforou[37], V. Nikolaenko[39,a], I. Nikolic-Audit[131], K. Nikolopoulos[21], P. Nilsson[30], I. Ninca[50], G. Ninio[156], A. Nisati[77a], N. Nishu[2], R. Nisius[113], N. Nitika[71a,71c], J-E. Nitschke[52], E.K. Nkadimeng[34g], T. Nobe[158], T. Nommensen[152], M.B. Norfolk[144], B.J. Norman[35], M. Noury[36a], J. Novak[96], T. Novak[96], L. Novotny[136], R. Novotny[116], L. Nozka[126], K. Ntekas[163], N.M.J. Nunes De Moura Junior[85b], J. Ocariz[131], A. Ochi[87], I. Ochoa[134a], S. Oerdek[50,x], J.T. Offermann[41], A. Ogrodnik[137], A. Oh[104], C.C. Ohm[149], H. Oide[86], R. Oishi[158], M.L. Ojeda[37], Y. Okumura[158], L.F. Oleiro Seabra[134a], I. Oleksiyuk[58], S.A. Olivares Pino[141d], G. Oliveira Correa[13], D. Oliveira Damazio[30], J.L. Oliver[163], Ö.O. Öncel[56], A.P. O'Neill[20], A. Onofre[134a,134e], P.U.E. Onyisi[11], M.J. Oreglia[41], D. Orestano[79a,79b], N. Orlando[13], R.S. Orr[159], L.M. Osojnak[132], Y. Osumi[114], G. Otero y Garzon[31], H. Otono[91], P.S. Ott[65a], G.J. Ottino[18a], M. Ouchrif[36d], F. Ould-Saada[129], T. Ovsiannikova[143], M. Owen[61], R.E. Owen[138], V.E. Ozcan[22a], F. Ozturk[89], N. Ozturk[8], S. Ozturk[84], H.A. Pacey[130], A. Pacheco Pages[13], C. Padilla Aranda[13], G. Padovano[77a,77b], S. Pagan Griso[18a], G. Palacino[70], A. Palazzo[72a,72b], J. Pampel[25], J. Pan[177], T. Pan[66a], D.K. Panchal[11], C.E. Pandini[118], J.G. Panduro Vazquez[138], H.D. Pandya[1], H. Pang[15], P. Pani[50], G. Panizzo[71a,71c], L. Panwar[131], L. Paolozzi[58], S. Parajuli[167], A. Paramonov[6], C. Paraskevopoulos[55], D. Paredes Hernandez[66b], A. Pareti[75a,75b], K.R. Park[43], T.H. Park[159], M.A. Parker[33], F. Parodi[59b,59a], V.A. Parrish[54], J.A. Parsons[43], U. Parzefall[56], B. Pascual Dias[111], L. Pascual Dominguez[102], E. Pasqualucci[77a], S. Passaggio[59b], F. Pastore[98], P. Patel[89], U.M. Patel[53], J.R. Pater[104], T. Pauly[37], F. Pauwels[137], C.I. Pazos[162], M. Pedersen[129], R. Pedro[134a], S.V. Peleganchuk[39], O. Penc[37], E.A. Pender[54], S. Peng[15], G.D. Penn[177], K.E. Penski[112], M. Penzin[39], B.S. Peralva[85d], A.P. Pereira Peixoto[143], L. Pereira Sanchez[148], D.V. Perepelitsa[30,ah], G. Perera[106], E. Perez Codina[160a], M. Perganti[10], H. Pernegger[37], S. Perrella[77a,77b], O. Perrin[42], K. Peters[50], R.F.Y. Peters[104], B.A. Petersen[37], T.C. Petersen[44], E. Petit[105], V. Petousis[136], C. Petridou[157,e], T. Petru[137], A. Petrukhin[146], M. Pettee[18a], A. Petukhov[84], K. Petukhova[37], R. Pezoa[141f], L. Pezzotti[37], G. Pezzullo[177], A.J. Pfleger[37], T.M. Pham[175], T. Pham[108], P.W. Phillips[138], G. Piacquadio[150], E. Pianori[18a], F. Piazza[127], R. Piegaia[31], D. Pietreanu[28b], A.D. Pilkington[104], M. Pinamonti[71a,71c], J.L. Pinfold[2], B.C. Pinheiro Pereira[134a], J. Pinol Bel[13],

JHEP05(2025)038

A.E. Pinto Pinoargote[139,139], L. Pintucci[71a,71c], K.M. Piper[151], A. Pirttikoski[58], D.A. Pizzi[35], L. Pizzimento[66b], A. Pizzini[118], M.-A. Pleier[30], V. Pleskot[137], E. Plotnikova[40], G. Poddar[97], R. Poettgen[101], L. Poggioli[131], S. Polacek[137], G. Polesello[75a], A. Poley[147,160a], A. Polini[24b], C.S. Pollard[172], Z.B. Pollock[123], E. Pompa Pacchi[124], N.I. Pond[99], D. Ponomarenko[70], L. Pontecorvo[37], S. Popa[28a], G.A. Popeneciu[28d], A. Poreba[37], D.M. Portillo Quintero[160a], S. Pospisil[136], M.A. Postill[144], P. Postolache[28c], K. Potamianos[172], P.A. Potepa[88a], I.N. Potrap[40], C.J. Potter[33], H. Potti[152], J. Poveda[168], M.E. Pozo Astigarraga[37], A. Prades Ibanez[78a,78b], J. Pretel[170], D. Price[104], M. Primavera[72a], L. Primomo[71a,71c], M.A. Principe Martin[102], R. Privara[126], T. Procter[61], M.L. Proffitt[143], N. Proklova[132], K. Prokofiev[66c], G. Proto[113], J. Proudfoot[6], M. Przybycien[88a], W.W. Przygoda[88b], A. Psallidas[48], J.E. Puddefoot[144], D. Pudzha[56], D. Pyatiizbyantseva[39], J. Qian[109], R. Qian[110], D. Qichen[104], Y. Qin[13], T. Qiu[54], A. Quadt[57], M. Queitsch-Maitland[104], G. Quetant[58], R.P. Quinn[169], G. Rabanal Bolanos[63], D. Rafanoharana[56], F. Raffaeli[78a,78b], F. Ragusa[73a,73b], J.L. Rainbolt[41], J.A. Raine[58], S. Rajagopalan[30], E. Ramakoti[39], L. Rambelli[59b,59a], I.A. Ramirez-Berend[35], K. Ran[50,115c], D.S. Rankin[132], N.P. Rapheeha[34g], H. Rasheed[28b], V. Raskina[131], D.F. Rassloff[65a], A. Rastogi[18a], S. Rave[103], S. Ravera[59b,59a], B. Ravina[57], I. Ravinovich[174], M. Raymond[37], A.L. Read[129], N.P. Readioff[144], D.M. Rebuzzi[75a,75b], G. Redlinger[30], A.S. Reed[113], K. Reeves[27], J.A. Reidelsturz[176], D. Reikher[127], A. Rej[51], C. Rembser[37], H. Ren[64a], M. Renda[28b], F. Renner[50], A.G. Rennie[163], A.L. Rescia[50], S. Resconi[73a], M. Ressegotti[59b,59a], S. Rettie[37], W.F. Rettie[35], J.G. Reyes Rivera[110], E. Reynolds[18a], O.L. Rezanova[39], P. Reznicek[137], H. Riani[36d], N. Ribaric[53], E. Ricci[80a,80b], R. Richter[113], S. Richter[49a,49b], E. Richter-Was[88b], M. Ridel[131], S. Ridouani[36d], P. Rieck[121], P. Riedler[37], E.M. Riefel[49a,49b], J.O. Rieger[118], M. Rijssenbeek[150], M. Rimoldi[37], L. Rinaldi[24b,24a], P. Rincke[57,166], T.T. Rinn[30], M.P. Rinnagel[112], G. Ripellino[166], I. Riu[13], J.C. Rivera Vergara[170], F. Rizatdinova[125], E. Rizvi[97], B.R. Roberts[18a], S.S. Roberts[140], S.H. Robertson[107,aa], D. Robinson[33], M. Robles Manzano[103], A. Robson[61], A. Rocchi[78a,78b], C. Roda[76a,76b], S. Rodriguez Bosca[37], Y. Rodriguez Garcia[23a], A.M. Rodríguez Vera[119], S. Roe[37], J.T. Roemer[37], O. Røhne[129], R.A. Rojas[106], C.P.A. Roland[131], J. Roloff[30], A. Romaniouk[81], E. Romano[75a,75b], M. Romano[24b], A.C. Romero Hernandez[167], N. Rompotis[95], L. Roos[131], S. Rosati[77a], B.J. Rosser[41], E. Rossi[130], E. Rossi[74a,74b], L.P. Rossi[63], L. Rossini[56], R. Rosten[123], M. Rotaru[28b], B. Rottler[56], C. Rougier[92], D. Rousseau[68], D. Rousso[50], A. Roy[167], S. Roy-Garand[159], A. Rozanov[105], Z.M.A. Rozario[61], Y. Rozen[155], A. Rubio Jimenez[168], V.H. Ruelas Rivera[19], T.A. Ruggeri[1], A. Ruggiero[130], A. Ruiz-Martinez[168], A. Rummler[37], Z. Rurikova[56], N.A. Rusakovich[40], H.L. Russell[170], G. Russo[77a,77b], J.P. Rutherfoord[7], S. Rutherford Colmenares[33], M. Rybar[137], E.B. Rye[129], A. Ryzhov[46], J.A. Sabater Iglesias[58], H.F-W. Sadrozinski[140], F. Safai Tehrani[77a], B. Safarzadeh Samani[138], S. Saha[1], M. Sahinsoy[84], A. Saibel[168], M. Saimpert[139], M. Saito[158], T. Saito[158], A. Sala[73a,73b], D. Salamani[37], A. Salnikov[148], J. Salt[168], A. Salvador Salas[156], D. Salvatore[45b,45a], F. Salvatore[151], A. Salzburger[37], D. Sammel[56], E. Sampson[94], D. Sampsonidis[157,e], D. Sampsonidou[127], J. Sánchez[168], V. Sanchez Sebastian[168],

H. Sandaker[129], C.O. Sander[50], J.A. Sandesara[106], M. Sandhoff[176], C. Sandoval[23b], L. Sanfilippo[65a], D.P.C. Sankey[138], T. Sano[90], A. Sansoni[55], L. Santi[37,77b], C. Santoni[42], H. Santos[134a,134b], A. Santra[174], E. Sanzani[24b,24a], K.A. Saoucha[165], J.G. Saraiva[134a,134d], J. Sardain[7], O. Sasaki[86], K. Sato[161], C. Sauer[37], E. Sauvan[4], P. Savard[159,af], R. Sawada[158], C. Sawyer[138], L. Sawyer[100], C. Sbarra[24b], A. Sbrizzi[24b,24a], T. Scanlon[99], J. Schaarschmidt[143], U. Schäfer[103], A.C. Schaffer[68,46], D. Schaile[112], R.D. Schamberger[150], C. Scharf[19], M.M. Schefer[20], V.A. Schegelsky[39], D. Scheirich[137], M. Schernau[141e], C. Scheulen[58], C. Schiavi[59b,59a], M. Schioppa[45b,45a], B. Schlag[148], S. Schlenker[37], J. Schmeing[176], M.A. Schmidt[176], K. Schmieden[103], C. Schmitt[103], N. Schmitt[103], S. Schmitt[50], L. Schoeffel[139], A. Schoening[65b], P.G. Scholer[35], E. Schopf[130], M. Schott[25], J. Schovancova[37], S. Schramm[58], T. Schroer[58], H-C. Schultz-Coulon[65a], M. Schumacher[56], B.A. Schumm[140], Ph. Schune[139], H.R. Schwartz[140], A. Schwartzman[148], T.A. Schwarz[109], Ph. Schwemling[139], R. Schwienhorst[110], F.G. Sciacca[20], A. Sciandra[30], G. Sciolla[27], F. Scuri[76a], C.D. Sebastiani[95], K. Sedlaczek[119], S.C. Seidel[116], A. Seiden[140], B.D. Seidlitz[43], C. Seitz[50], J.M. Seixas[85b], G. Sekhniaidze[74a], L. Selem[62], N. Semprini-Cesari[24b,24a], A. Semushin[178,39], D. Sengupta[58], V. Senthilkumar[168], L. Serin[68], M. Sessa[78a,78b], H. Severini[124], F. Sforza[59b,59a], A. Sfyrla[58], Q. Sha[14], E. Shabalina[57], A.H. Shah[33], R. Shaheen[149], J.D. Shahinian[132], D. Shaked Renous[174], L.Y. Shan[14], M. Shapiro[18a], A. Sharma[37], A.S. Sharma[169], P. Sharma[30], P.B. Shatalov[39], K. Shaw[151], S.M. Shaw[104], Q. Shen[64c], D.J. Sheppard[147], P. Sherwood[99], L. Shi[99], X. Shi[14], S. Shimizu[86], C.O. Shimmin[177], I.P.J. Shipsey[130,*], S. Shirabe[91], M. Shiyakova[40,y], M.J. Shochet[41], D.R. Shope[129], B. Shrestha[124], S. Shrestha[123,aj], I. Shreyber[39], M.J. Shroff[170], P. Sicho[135], A.M. Sickles[167], E. Sideras Haddad[34g,164], A.C. Sidley[118], A. Sidoti[24b], F. Siegert[52], Dj. Sijacki[16], F. Sili[93], J.M. Silva[54], I. Silva Ferreira[85b], M.V. Silva Oliveira[30], S.B. Silverstein[49a], S. Simion[68], R. Simoniello[37], E.L. Simpson[104], H. Simpson[151], L.R. Simpson[109], S. Simsek[84], S. Sindhu[57], P. Sinervo[159], S. Singh[30], S. Sinha[50], S. Sinha[104], M. Sioli[24b,24a], I. Siral[37], E. Sitnikova[50], J. Sjölin[49a,49b], A. Skaf[57], E. Skorda[21], P. Skubic[124], M. Slawinska[89], I. Slazyk[17], V. Smakhtin[174], B.H. Smart[138], S.Yu. Smirnov[39], Y. Smirnov[39], L.N. Smirnova[39,a], O. Smirnova[101], A.C. Smith[43], D.R. Smith[163], E.A. Smith[41], J.L. Smith[104], R. Smith[148], H. Smitmanns[103], M. Smizanska[94], K. Smolek[136], A.A. Snesarev[39], H.L. Snoek[118], S. Snyder[30], R. Sobie[170,aa], A. Soffer[156], C.A. Solans Sanchez[37], E.Yu. Soldatov[39], U. Soldevila[168], A.A. Solodkov[39], S. Solomon[27], A. Soloshenko[40], K. Solovieva[56], O.V. Solovyanov[42], P. Sommer[52], A. Sonay[13], W.Y. Song[160b], A. Sopczak[136], A.L. Sopio[54], F. Sopkova[29b], J.D. Sorenson[116], I.R. Sotarriva Alvarez[142], V. Sothilingam[65a], O.J. Soto Sandoval[141c,141b], S. Sottocornola[70], R. Soualah[165], Z. Soumaimi[36e], D. South[50], N. Soybelman[174], S. Spagnolo[72a,72b], M. Spalla[113], D. Sperlich[56], G. Spigo[37], B. Spisso[74a,74b], D.P. Spiteri[61], M. Spousta[137], E.J. Staats[35], R. Stamen[65a], A. Stampekis[21], E. Stanecka[89], W. Stanek-Maslouska[50], M.V. Stange[52], B. Stanislaus[18a], M.M. Stanitzki[50], B. Stapf[50], E.A. Starchenko[39], G.H. Stark[140], J. Stark[92], P. Staroba[135], P. Starovoitov[165], S. Stärz[107], R. Staszewski[89], G. Stavropoulos[48], A. Stefl[37], P. Steinberg[30], B. Stelzer[147,160a], H.J. Stelzer[133], O. Stelzer-Chilton[160a], H. Stenzel[60], T.J. Stevenson[151], G.A. Stewart[37], J.R. Stewart[125], M.C. Stockton[37], G. Stoicea[28b], M. Stolarski[134a], S. Stonjek[113], A. Straessner[52], J. Strandberg[149], S. Strandberg[49a,49b], M. Stratmann[176], M. Strauss[124], T. Strebler[105], P. Strizenec[29b], R. Ströhmer[171], D.M. Strom[127], R. Stroynowski[46], A. Strubig[49a,49b], S.A. Stucci[30], B. Stugu[17], J. Stupak[124], N.A. Styles[50], D. Su[148], S. Su[64a], W. Su[64d], X. Su[64a], D. Suchy[29a], K. Sugizaki[158], V.V. Sulin[39], M.J. Sullivan[95], D.M.S. Sultan[130], L. Sultanaliyeva[39], S. Sultansoy[3b], S. Sun[175], W. Sun[14], O. Sunneborn Gudnadottir[166], N. Sur[105], M.R. Sutton[151], H. Suzuki[161], M. Svatos[135], M. Swiatlowski[160a], T. Swirski[171], I. Sykora[29a], M. Sykora[137], T. Sykora[137], D. Ta[103], K. Tackmann[50,x], A. Taffard[163], R. Tafirout[160a], J.S. Tafoya Vargas[68], Y. Takubo[86], M. Talby[105], A.A. Talyshev[39], K.C. Tam[66b], N.M. Tamir[156], A. Tanaka[158], J. Tanaka[158], R. Tanaka[68], M. Tanasini[150], Z. Tao[169], S. Tapia Araya[141f], S. Tapprogge[103], A. Tarek Abouelfadl Mohamed[110], S. Tarem[155], K. Tariq[14], G. Tarna[28b], G.F. Tartarelli[73a], M.J. Tartarin[92], P. Tas[137], M. Tasevsky[135], E. Tassi[45b,45a], A.C. Tate[167], G. Tateno[158], Y. Tayalati[36e,z], G.N. Taylor[108], W. Taylor[160b], P. Teixeira-Dias[98], J.J. Teoh[159], K. Terashi[158], J. Terron[102], S. Terzo[13], M. Testa[55], R.J. Teuscher[159,aa], A. Thaler[81], O. Theiner[58], T. Theveneaux-Pelzer[105], O. Thielmann[176], D.W. Thomas[98], J.P. Thomas[21], E.A. Thompson[18a], P.D. Thompson[21], E. Thomson[132], R.E. Thornberry[46], C. Tian[64a], Y. Tian[58], V. Tikhomirov[39,a], Yu.A. Tikhonov[39], S. Timoshenko[39], D. Timoshyn[137], E.X.L. Ting[1], P. Tipton[177], A. Tishelman-Charny[30], S.H. Tlou[34g], K. Todome[142], S. Todorova-Nova[137], S. Todt[52], L. Toffolin[71a,71c], M. Togawa[86], J. Tojo[91], S. Tokár[29a], K. Tokushuku[86], O. Toldaiev[70], G. Tolkachev[105], M. Tomoto[86,114], L. Tompkins[148,n], E. Torrence[127], H. Torres[92], E. Torró Pastor[168], M. Toscani[31], C. Tosciri[41], M. Tost[11], D.R. Tovey[144], I.S. Trandafir[28b], T. Trefzger[171], A. Tricoli[30], I.M. Trigger[160a], S. Trincaz-Duvoid[131], D.A. Trischuk[27], B. Trocmé[62], A. Tropina[40], L. Truong[34c], M. Trzebinski[89], A. Trzupek[89], F. Tsai[150], M. Tsai[109], A. Tsiamis[157], P.V. Tsiareshka[40], S. Tsigaridas[160a], A. Tsirigotis[157,t], V. Tsiskaridze[159], E.G. Tskhadadze[154a], M. Tsopoulou[157], Y. Tsujikawa[90], I.I. Tsukerman[39], V. Tsulaia[18a], S. Tsuno[86], K. Tsuri[122], D. Tsybychev[150], Y. Tu[66b], A. Tudorache[28b], V. Tudorache[28b], A.N. Tuna[63], S. Turchikhin[59b,59a], I. Turk Cakir[3a], R. Turra[73a], T. Turtuvshin[40], P.M. Tuts[43], S. Tzamarias[157,e], E. Tzovara[103], F. Ukegawa[161], P.A. Ulloa Poblete[141c,141b], E.N. Umaka[30], G. Unal[37], A. Undrus[30], G. Unel[163], J. Urban[29b], P. Urrejola[141a], G. Usai[8], R. Ushioda[142], M. Usman[111], F. Ustuner[54], Z. Uysal[84], V. Vacek[136], B. Vachon[107], T. Vafeiadis[37], A. Vaitkus[99], C. Valderanis[112], E. Valdes Santurio[49a,49b], M. Valente[160a], S. Valentinetti[24b,24a], A. Valero[168], E. Valiente Moreno[168], A. Vallier[92], J.A. Valls Ferrer[168], D.R. Van Arneman[118], T.R. Van Daalen[143], A. Van Der Graaf[51], P. Van Gemmeren[6], M. Van Rijnbach[37], S. Van Stroud[99], I. Van Vulpen[118], P. Vana[137], M. Vanadia[78a,78b], U.M. Vande Voorde[149], W. Vandelli[37], E.R. Vandewall[125], D. Vannicola[156], L. Vannoli[55], R. Vari[77a], E.W. Varnes[7], C. Varni[18b], D. Varouchas[68], L. Varriale[168], K.E. Varvell[152], M.E. Vasile[28b], L. Vaslin[86], A. Vasyukov[40], L.M. Vaughan[125], R. Vavricka[103], T. Vazquez Schroeder[37], J. Veatch[32], V. Vecchio[104], M.J. Veen[106], I. Veliscek[30], L.M. Veloce[159], F. Veloso[134a,134c], S. Veneziano[77a], A. Ventura[72a,72b], S. Ventura Gonzalez[139], A. Verbytskyi[113], M. Verducci[76a,76b], C. Vergis[97], M. Verissimo De Araujo[85b], W. Verkerke[118], J.C. Vermeulen[118],

C. Vernieri[148], M. Vessella[163], M.C. Vetterli[147,af], A. Vgenopoulos[103], N. Viaux Maira[141f], T. Vickey[144], O.E. Vickey Boeriu[144], G.H.A. Viehhauser[130], L. Vigani[65b], M. Vigl[113], M. Villa[24b,24a], M. Villaplana Perez[168], E.M. Villhauer[54], E. Vilucchi[55], M.G. Vincter[35], A. Visibile[118], C. Vittori[37], I. Vivarelli[24b,24a], E. Voevodina[113], F. Vogel[112], J.C. Voigt[52], P. Vokac[136], Yu. Volkotrub[88b], E. Von Toerne[25], B. Vormwald[37], V. Vorobel[137], K. Vorobev[39], M. Vos[168], K. Voss[146], M. Vozak[118], L. Vozdecky[124], N. Vranjes[16], M. Vranjes Milosavljevic[16], M. Vreeswijk[118], N.K. Vu[64d,64c], R. Vuillermet[37], O. Vujinovic[103], I. Vukotic[41], I.K. Vyas[35], S. Wada[161], C. Wagner[148], J.M. Wagner[18a], W. Wagner[176], S. Wahdan[176], H. Wahlberg[93], C.H. Waits[124], J. Walder[138], R. Walker[112], W. Walkowiak[146], A. Wall[132], E.J. Wallin[101], T. Wamorkar[18a], A.Z. Wang[140], C. Wang[103], C. Wang[11], H. Wang[18a], J. Wang[66c], P. Wang[104], P. Wang[99], R. Wang[63], R. Wang[6], S.M. Wang[153], S. Wang[14], T. Wang[64a], W.T. Wang[82], W. Wang[14], X. Wang[167], X. Wang[64c], Y. Wang[64d], Y. Wang[115a], Y. Wang[64a], Z. Wang[109], Z. Wang[64d,53,64c], Z. Wang[109], A. Warburton[107], R.J. Ward[21], N. Warrack[61], S. Waterhouse[98], A.T. Watson[21], H. Watson[54], M.F. Watson[21], E. Watton[61,138], G. Watts[143], B.M. Waugh[99], J.M. Webb[56], C. Weber[30], H.A. Weber[19], M.S. Weber[20], S.M. Weber[65a], C. Wei[64a], Y. Wei[56], A.R. Weidberg[130], E.J. Weik[121], J. Weingarten[51], C. Weiser[56], C.J. Wells[50], T. Wenaus[30], B. Wendland[51], T. Wengler[37], N.S. Wenke[113], N. Wermes[25], M. Wessels[65a], A.M. Wharton[94], A.S. White[63], A. White[8], M.J. White[1], D. Whiteson[163], L. Wickremasinghe[128], W. Wiedenmann[175], M. Wielers[138], C. Wiglesworth[44], D.J. Wilbern[124], H.G. Wilkens[37], J.J.H. Wilkinson[33], D.M. Williams[43], H.H. Williams[132], S. Williams[33], S. Willocq[106], B.J. Wilson[104], D.J. Wilson[104], P.J. Windischhofer[41], F.I. Winkel[31], F. Winklmeier[127], B.T. Winter[56], M. Wittgen[148], M. Wobisch[100], T. Wojtkowski[62], Z. Wolffs[118], J. Wollrath[37], M.W. Wolter[89], H. Wolters[134a,134c], M.C. Wong[140], E.L. Woodward[43], S.D. Worm[50], B.K. Wosiek[89], K.W. Woźniak[89], S. Wozniewski[57], K. Wraight[61], C. Wu[21], M. Wu[115b], M. Wu[117], S.L. Wu[175], X. Wu[58], X. Wu[64a], Y. Wu[64a], Z. Wu[4], J. Wuerzinger[113,ad], T.R. Wyatt[104], B.M. Wynne[54], S. Xella[44], L. Xia[115a], M. Xia[15], M. Xie[64a], A. Xiong[127], J. Xiong[18a], D. Xu[14], H. Xu[64a], L. Xu[64a], R. Xu[132], T. Xu[109], Y. Xu[143], Z. Xu[54], Z. Xu[115a], B. Yabsley[152], S. Yacoob[34a], Y. Yamaguchi[86], E. Yamashita[158], H. Yamauchi[161], T. Yamazaki[18a], Y. Yamazaki[87], S. Yan[61], Z. Yan[106], H.J. Yang[64c,64d], H.T. Yang[64a], S. Yang[64a], T. Yang[66c], X. Yang[37], X. Yang[14], Y. Yang[46], Y. Yang[64a], W-M. Yao[18a], H. Ye[57], J. Ye[14], S. Ye[30], X. Ye[64a], Y. Yeh[99], I. Yeletskikh[40], B. Yeo[18b], M.R. Yexley[99], T.P. Yildirim[130], P. Yin[43], K. Yorita[173], S. Younas[28b], C.J.S. Young[37], C. Young[148], C. Yu[14,115c], Y. Yu[64a], J. Yuan[14,115c], M. Yuan[109], R. Yuan[64d,64c], L. Yue[99], M. Zaazoua[64a], B. Zabinski[89], I. Zahir[36a], E. Zaid[54], Z.K. Zak[89], T. Zakareishvili[168], S. Zambito[58], J.A. Zamora Saa[141d,141b], J. Zang[158], D. Zanzi[56], R. Zanzottera[73a,73b], O. Zaplatilek[136], C. Zeitnitz[176], H. Zeng[14], J.C. Zeng[167], D.T. Zenger Jr[27], O. Zenin[39], T. Ženiš[29a], S. Zenz[97], S. Zerradi[36a], D. Zerwas[68], M. Zhai[14,115c], D.F. Zhang[144], J. Zhang[64b], J. Zhang[6], K. Zhang[14,115c], L. Zhang[64a], L. Zhang[115a], P. Zhang[14,115c], R. Zhang[175], S. Zhang[109], S. Zhang[92], T. Zhang[158], X. Zhang[64c], Y. Zhang[143], Y. Zhang[99], Y. Zhang[115a], Z. Zhang[18a], Z. Zhang[64b], Z. Zhang[68], H. Zhao[143], T. Zhao[64b], Y. Zhao[140], Z. Zhao[64a], Z. Zhao[64a],

A. Zhemchugov[40], J. Zheng[115a], K. Zheng[167], X. Zheng[64a], Z. Zheng[148], D. Zhong[167], B. Zhou[109], H. Zhou[7], N. Zhou[64c], Y. Zhou[15], Y. Zhou[115a], Y. Zhou[7], C.G. Zhu[64b], J. Zhu[109], X. Zhu[64d], Y. Zhu[64c], Y. Zhu[64a], X. Zhuang[14], K. Zhukov[70], N.I. Zimine[40], J. Zinsser[65b], M. Ziolkowski[146], L. Živković[16], A. Zoccoli[24b,24a], K. Zoch[63], T.G. Zorbas[144], O. Zormpa[48], W. Zou[43], L. Zwalinski[37]

[1] *Department of Physics, University of Adelaide, Adelaide, Australia*
[2] *Department of Physics, University of Alberta, Edmonton AB, Canada*
[3] [(a)] *Department of Physics, Ankara University, Ankara;* [(b)] *Division of Physics, TOBB University of Economics and Technology, Ankara, Türkiye*
[4] *LAPP, Université Savoie Mont Blanc, CNRS/IN2P3, Annecy, France*
[5] *APC, Université Paris Cité, CNRS/IN2P3, Paris, France*
[6] *High Energy Physics Division, Argonne National Laboratory, Argonne IL, United States of America*
[7] *Department of Physics, University of Arizona, Tucson AZ, United States of America*
[8] *Department of Physics, University of Texas at Arlington, Arlington TX, United States of America*
[9] *Physics Department, National and Kapodistrian University of Athens, Athens, Greece*
[10] *Physics Department, National Technical University of Athens, Zografou, Greece*
[11] *Department of Physics, University of Texas at Austin, Austin TX, United States of America*
[12] *Institute of Physics, Azerbaijan Academy of Sciences, Baku, Azerbaijan*
[13] *Institut de Física d'Altes Energies (IFAE), Barcelona Institute of Science and Technology, Barcelona, Spain*
[14] *Institute of High Energy Physics, Chinese Academy of Sciences, Beijing, China*
[15] *Physics Department, Tsinghua University, Beijing, China*
[16] *Institute of Physics, University of Belgrade, Belgrade, Serbia*
[17] *Department for Physics and Technology, University of Bergen, Bergen, Norway*
[18] [(a)] *Physics Division, Lawrence Berkeley National Laboratory, Berkeley CA;* [(b)] *University of California, Berkeley CA, United States of America*
[19] *Institut für Physik, Humboldt Universität zu Berlin, Berlin, Germany*
[20] *Albert Einstein Center for Fundamental Physics and Laboratory for High Energy Physics, University of Bern, Bern, Switzerland*
[21] *School of Physics and Astronomy, University of Birmingham, Birmingham, United Kingdom*
[22] [(a)] *Department of Physics, Bogazici University, Istanbul;* [(b)] *Department of Physics Engineering, Gaziantep University, Gaziantep;* [(c)] *Department of Physics, Istanbul University, Istanbul, Türkiye*
[23] [(a)] *Facultad de Ciencias y Centro de Investigaciónes, Universidad Antonio Nariño, Bogotá;* [(b)] *Departamento de Física, Universidad Nacional de Colombia, Bogotá, Colombia*
[24] [(a)] *Dipartimento di Fisica e Astronomia A. Righi, Università di Bologna, Bologna;* [(b)] *INFN Sezione di Bologna, Italy*
[25] *Physikalisches Institut, Universität Bonn, Bonn, Germany*
[26] *Department of Physics, Boston University, Boston MA, United States of America*
[27] *Department of Physics, Brandeis University, Waltham MA, United States of America*
[28] [(a)] *Transilvania University of Brasov, Brasov;* [(b)] *Horia Hulubei National Institute of Physics and Nuclear Engineering, Bucharest;* [(c)] *Department of Physics, Alexandru Ioan Cuza University of Iasi, Iasi;* [(d)] *National Institute for Research and Development of Isotopic and Molecular Technologies, Physics Department, Cluj-Napoca;* [(e)] *National University of Science and Technology Politechnica, Bucharest;* [(f)] *West University in Timisoara, Timisoara;* [(g)] *Faculty of Physics, University of Bucharest, Bucharest, Romania*
[29] [(a)] *Faculty of Mathematics, Physics and Informatics, Comenius University, Bratislava;* [(b)] *Department of Subnuclear Physics, Institute of Experimental Physics of the Slovak Academy of Sciences, Kosice, Slovak Republic*
[30] *Physics Department, Brookhaven National Laboratory, Upton NY, United States of America*
[31] *Universidad de Buenos Aires, Facultad de Ciencias Exactas y Naturales, Departamento de Física, y CONICET, Instituto de Física de Buenos Aires (IFIBA), Buenos Aires, Argentina*
[32] *California State University, CA, United States of America*

JHEP05(2025)038

[33] Cavendish Laboratory, University of Cambridge, Cambridge, United Kingdom
[34] [(a)] Department of Physics, University of Cape Town, Cape Town; [(b)] iThemba Labs, Western Cape; [(c)] Department of Mechanical Engineering Science, University of Johannesburg, Johannesburg; [(d)] National Institute of Physics, University of the Philippines Diliman (Philippines); [(e)] University of South Africa, Department of Physics, Pretoria; [(f)] University of Zululand, KwaDlangezwa; [(g)] School of Physics, University of the Witwatersrand, Johannesburg, South Africa
[35] Department of Physics, Carleton University, Ottawa ON, Canada
[36] [(a)] Faculté des Sciences Ain Chock, Université Hassan II de Casablanca; [(b)] Faculté des Sciences, Université Ibn-Tofail, Kénitra; [(c)] Faculté des Sciences Semlalia, Université Cadi Ayyad, LPHEA-Marrakech; [(d)] LPMR, Faculté des Sciences, Université Mohamed Premier, Oujda; [(e)] Faculté des sciences, Université Mohammed V, Rabat; [(f)] Institute of Applied Physics, Mohammed VI Polytechnic University, Ben Guerir, Morocco
[37] CERN, Geneva, Switzerland
[38] Affiliated with an institute formerly covered by a cooperation agreement with CERN
[39] Affiliated with an institute covered by a cooperation agreement with CERN
[40] Affiliated with an international laboratory covered by a cooperation agreement with CERN
[41] Enrico Fermi Institute, University of Chicago, Chicago IL, United States of America
[42] LPC, Université Clermont Auvergne, CNRS/IN2P3, Clermont-Ferrand, France
[43] Nevis Laboratory, Columbia University, Irvington NY, United States of America
[44] Niels Bohr Institute, University of Copenhagen, Copenhagen, Denmark
[45] [(a)] Dipartimento di Fisica, Università della Calabria, Rende; [(b)] INFN Gruppo Collegato di Cosenza, Laboratori Nazionali di Frascati, Italy
[46] Physics Department, Southern Methodist University, Dallas TX, United States of America
[47] Physics Department, University of Texas at Dallas, Richardson TX, United States of America
[48] National Centre for Scientific Research "Demokritos", Agia Paraskevi, Greece
[49] [(a)] Department of Physics, Stockholm University; [(b)] Oskar Klein Centre, Stockholm, Sweden
[50] Deutsches Elektronen-Synchrotron DESY, Hamburg and Zeuthen, Germany
[51] Fakultät Physik, Technische Universität Dortmund, Dortmund, Germany
[52] Institut für Kern- und Teilchenphysik, Technische Universität Dresden, Dresden, Germany
[53] Department of Physics, Duke University, Durham NC, United States of America
[54] SUPA - School of Physics and Astronomy, University of Edinburgh, Edinburgh, United Kingdom
[55] INFN e Laboratori Nazionali di Frascati, Frascati, Italy
[56] Physikalisches Institut, Albert-Ludwigs-Universität Freiburg, Freiburg, Germany
[57] II. Physikalisches Institut, Georg-August-Universität Göttingen, Göttingen, Germany
[58] Département de Physique Nucléaire et Corpusculaire, Université de Genève, Genève, Switzerland
[59] [(a)] Dipartimento di Fisica, Università di Genova, Genova; [(b)] INFN Sezione di Genova, Italy
[60] II. Physikalisches Institut, Justus-Liebig-Universität Giessen, Giessen, Germany
[61] SUPA - School of Physics and Astronomy, University of Glasgow, Glasgow, United Kingdom
[62] LPSC, Université Grenoble Alpes, CNRS/IN2P3, Grenoble INP, Grenoble, France
[63] Laboratory for Particle Physics and Cosmology, Harvard University, Cambridge MA, United States of America
[64] [(a)] Department of Modern Physics and State Key Laboratory of Particle Detection and Electronics, University of Science and Technology of China, Hefei; [(b)] Institute of Frontier and Interdisciplinary Science and Key Laboratory of Particle Physics and Particle Irradiation (MOE), Shandong University, Qingdao; [(c)] School of Physics and Astronomy, Shanghai Jiao Tong University, Key Laboratory for Particle Astrophysics and Cosmology (MOE), SKLPPC, Shanghai; [(d)] Tsung-Dao Lee Institute, Shanghai; [(e)] School of Physics, Zhengzhou University, China
[65] [(a)] Kirchhoff-Institut für Physik, Ruprecht-Karls-Universität Heidelberg, Heidelberg; [(b)] Physikalisches Institut, Ruprecht-Karls-Universität Heidelberg, Heidelberg, Germany
[66] [(a)] Department of Physics, Chinese University of Hong Kong, Shatin, N.T., Hong Kong; [(b)] Department of Physics, University of Hong Kong, Hong Kong; [(c)] Department of Physics and Institute for Advanced Study, Hong Kong University of Science and Technology, Clear Water Bay, Kowloon, Hong Kong, China
[67] Department of Physics, National Tsing Hua University, Hsinchu, Taiwan

JHEP05(2025)038

[68] *IJCLab, Université Paris-Saclay, CNRS/IN2P3, 91405, Orsay, France*
[69] *Centro Nacional de Microelectrónica (IMB-CNM-CSIC), Barcelona, Spain*
[70] *Department of Physics, Indiana University, Bloomington IN, United States of America*
[71] [(a)] *INFN Gruppo Collegato di Udine, Sezione di Trieste, Udine;* [(b)] *ICTP, Trieste;* [(c)] *Dipartimento Politecnico di Ingegneria e Architettura, Università di Udine, Udine, Italy*
[72] [(a)] *INFN Sezione di Lecce;* [(b)] *Dipartimento di Matematica e Fisica, Università del Salento, Lecce, Italy*
[73] [(a)] *INFN Sezione di Milano;* [(b)] *Dipartimento di Fisica, Università di Milano, Milano, Italy*
[74] [(a)] *INFN Sezione di Napoli;* [(b)] *Dipartimento di Fisica, Università di Napoli, Napoli, Italy*
[75] [(a)] *INFN Sezione di Pavia;* [(b)] *Dipartimento di Fisica, Università di Pavia, Pavia, Italy*
[76] [(a)] *INFN Sezione di Pisa;* [(b)] *Dipartimento di Fisica E. Fermi, Università di Pisa, Pisa, Italy*
[77] [(a)] *INFN Sezione di Roma;* [(b)] *Dipartimento di Fisica, Sapienza Università di Roma, Roma, Italy*
[78] [(a)] *INFN Sezione di Roma Tor Vergata;* [(b)] *Dipartimento di Fisica, Università di Roma Tor Vergata, Roma, Italy*
[79] [(a)] *INFN Sezione di Roma Tre;* [(b)] *Dipartimento di Matematica e Fisica, Università Roma Tre, Roma, Italy*
[80] [(a)] *INFN-TIFPA;* [(b)] *Università degli Studi di Trento, Trento, Italy*
[81] *Universität Innsbruck, Department of Astro and Particle Physics, Innsbruck, Austria*
[82] *University of Iowa, Iowa City IA, United States of America*
[83] *Department of Physics and Astronomy, Iowa State University, Ames IA, United States of America*
[84] *Istinye University, Sariyer, Istanbul, Türkiye*
[85] [(a)] *Departamento de Engenharia Elétrica, Universidade Federal de Juiz de Fora (UFJF), Juiz de Fora;* [(b)] *Universidade Federal do Rio De Janeiro COPPE/EE/IF, Rio de Janeiro;* [(c)] *Instituto de Física, Universidade de São Paulo, São Paulo;* [(d)] *Rio de Janeiro State University, Rio de Janeiro;* [(e)] *Federal University of Bahia, Bahia, Brazil*
[86] *KEK, High Energy Accelerator Research Organization, Tsukuba, Japan*
[87] *Graduate School of Science, Kobe University, Kobe, Japan*
[88] [(a)] *AGH University of Krakow, Faculty of Physics and Applied Computer Science, Krakow;* [(b)] *Marian Smoluchowski Institute of Physics, Jagiellonian University, Krakow, Poland*
[89] *Institute of Nuclear Physics Polish Academy of Sciences, Krakow, Poland*
[90] *Faculty of Science, Kyoto University, Kyoto, Japan*
[91] *Research Center for Advanced Particle Physics and Department of Physics, Kyushu University, Fukuoka, Japan*
[92] *L2IT, Université de Toulouse, CNRS/IN2P3, UPS, Toulouse, France*
[93] *Instituto de Física La Plata, Universidad Nacional de La Plata and CONICET, La Plata, Argentina*
[94] *Physics Department, Lancaster University, Lancaster, United Kingdom*
[95] *Oliver Lodge Laboratory, University of Liverpool, Liverpool, United Kingdom*
[96] *Department of Experimental Particle Physics, Jožef Stefan Institute and Department of Physics, University of Ljubljana, Ljubljana, Slovenia*
[97] *School of Physics and Astronomy, Queen Mary University of London, London, United Kingdom*
[98] *Department of Physics, Royal Holloway University of London, Egham, United Kingdom*
[99] *Department of Physics and Astronomy, University College London, London, United Kingdom*
[100] *Louisiana Tech University, Ruston LA, United States of America*
[101] *Fysiska institutionen, Lunds universitet, Lund, Sweden*
[102] *Departamento de Física Teorica C-15 and CIAFF, Universidad Autónoma de Madrid, Madrid, Spain*
[103] *Institut für Physik, Universität Mainz, Mainz, Germany*
[104] *School of Physics and Astronomy, University of Manchester, Manchester, United Kingdom*
[105] *CPPM, Aix-Marseille Université, CNRS/IN2P3, Marseille, France*
[106] *Department of Physics, University of Massachusetts, Amherst MA, United States of America*
[107] *Department of Physics, McGill University, Montreal QC, Canada*
[108] *School of Physics, University of Melbourne, Victoria, Australia*
[109] *Department of Physics, University of Michigan, Ann Arbor MI, United States of America*
[110] *Department of Physics and Astronomy, Michigan State University, East Lansing MI, United States of America*
[111] *Group of Particle Physics, University of Montreal, Montreal QC, Canada*

JHEP05(2025)038

[112] *Fakultät für Physik, Ludwig-Maximilians-Universität München, München, Germany*
[113] *Max-Planck-Institut für Physik (Werner-Heisenberg-Institut), München, Germany*
[114] *Graduate School of Science and Kobayashi-Maskawa Institute, Nagoya University, Nagoya, Japan*
[115] [(a)] *Department of Physics, Nanjing University, Nanjing;* [(b)] *School of Science, Shenzhen Campus of Sun Yat-sen University;* [(c)] *University of Chinese Academy of Science (UCAS), Beijing, China*
[116] *Department of Physics and Astronomy, University of New Mexico, Albuquerque NM, United States of America*
[117] *Institute for Mathematics, Astrophysics and Particle Physics, Radboud University/Nikhef, Nijmegen, Netherlands*
[118] *Nikhef National Institute for Subatomic Physics and University of Amsterdam, Amsterdam, Netherlands*
[119] *Department of Physics, Northern Illinois University, DeKalb IL, United States of America*
[120] [(a)] *New York University Abu Dhabi, Abu Dhabi;* [(b)] *United Arab Emirates University, Al Ain, United Arab Emirates*
[121] *Department of Physics, New York University, New York NY, United States of America*
[122] *Ochanomizu University, Otsuka, Bunkyo-ku, Tokyo, Japan*
[123] *Ohio State University, Columbus OH, United States of America*
[124] *Homer L. Dodge Department of Physics and Astronomy, University of Oklahoma, Norman OK, United States of America*
[125] *Department of Physics, Oklahoma State University, Stillwater OK, United States of America*
[126] *Palacký University, Joint Laboratory of Optics, Olomouc, Czech Republic*
[127] *Institute for Fundamental Science, University of Oregon, Eugene, OR, United States of America*
[128] *Graduate School of Science, Osaka University, Osaka, Japan*
[129] *Department of Physics, University of Oslo, Oslo, Norway*
[130] *Department of Physics, Oxford University, Oxford, United Kingdom*
[131] *LPNHE, Sorbonne Université, Université Paris Cité, CNRS/IN2P3, Paris, France*
[132] *Department of Physics, University of Pennsylvania, Philadelphia PA, United States of America*
[133] *Department of Physics and Astronomy, University of Pittsburgh, Pittsburgh PA, United States of America*
[134] [(a)] *Laboratório de Instrumentação e Física Experimental de Partículas - LIP, Lisboa;* [(b)] *Departamento de Física, Faculdade de Ciências, Universidade de Lisboa, Lisboa;* [(c)] *Departamento de Física, Universidade de Coimbra, Coimbra;* [(d)] *Centro de Física Nuclear da Universidade de Lisboa, Lisboa;* [(e)] *Departamento de Física, Universidade do Minho, Braga;* [(f)] *Departamento de Física Teórica y del Cosmos, Universidad de Granada, Granada (Spain);* [(g)] *Departamento de Física, Instituto Superior Técnico, Universidade de Lisboa, Lisboa, Portugal*
[135] *Institute of Physics of the Czech Academy of Sciences, Prague, Czech Republic*
[136] *Czech Technical University in Prague, Prague, Czech Republic*
[137] *Charles University, Faculty of Mathematics and Physics, Prague, Czech Republic*
[138] *Particle Physics Department, Rutherford Appleton Laboratory, Didcot, United Kingdom*
[139] *IRFU, CEA, Université Paris-Saclay, Gif-sur-Yvette, France*
[140] *Santa Cruz Institute for Particle Physics, University of California Santa Cruz, Santa Cruz CA, United States of America*
[141] [(a)] *Departamento de Física, Pontificia Universidad Católica de Chile, Santiago;* [(b)] *Millennium Institute for Subatomic physics at high energy frontier (SAPHIR), Santiago;* [(c)] *Instituto de Investigación Multidisciplinario en Ciencia y Tecnología, y Departamento de Física, Universidad de La Serena;* [(d)] *Universidad Andres Bello, Department of Physics, Santiago;* [(e)] *Instituto de Alta Investigación, Universidad de Tarapacá, Arica;* [(f)] *Departamento de Física, Universidad Técnica Federico Santa María, Valparaíso, Chile*
[142] *Department of Physics, Institute of Science, Tokyo, Japan*
[143] *Department of Physics, University of Washington, Seattle WA, United States of America*
[144] *Department of Physics and Astronomy, University of Sheffield, Sheffield, United Kingdom*
[145] *Department of Physics, Shinshu University, Nagano, Japan*
[146] *Department Physik, Universität Siegen, Siegen, Germany*
[147] *Department of Physics, Simon Fraser University, Burnaby BC, Canada*
[148] *SLAC National Accelerator Laboratory, Stanford CA, United States of America*

[149] Department of Physics, Royal Institute of Technology, Stockholm, Sweden
[150] Departments of Physics and Astronomy, Stony Brook University, Stony Brook NY, United States of America
[151] Department of Physics and Astronomy, University of Sussex, Brighton, United Kingdom
[152] School of Physics, University of Sydney, Sydney, Australia
[153] Institute of Physics, Academia Sinica, Taipei, Taiwan
[154] [(a)] E. Andronikashvili Institute of Physics, Iv. Javakhishvili Tbilisi State University, Tbilisi; [(b)] High Energy Physics Institute, Tbilisi State University, Tbilisi; [(c)] University of Georgia, Tbilisi, Georgia
[155] Department of Physics, Technion, Israel Institute of Technology, Haifa, Israel
[156] Raymond and Beverly Sackler School of Physics and Astronomy, Tel Aviv University, Tel Aviv, Israel
[157] Department of Physics, Aristotle University of Thessaloniki, Thessaloniki, Greece
[158] International Center for Elementary Particle Physics and Department of Physics, University of Tokyo, Tokyo, Japan
[159] Department of Physics, University of Toronto, Toronto ON, Canada
[160] [(a)] TRIUMF, Vancouver BC; [(b)] Department of Physics and Astronomy, York University, Toronto ON, Canada
[161] Division of Physics and Tomonaga Center for the History of the Universe, Faculty of Pure and Applied Sciences, University of Tsukuba, Tsukuba, Japan
[162] Department of Physics and Astronomy, Tufts University, Medford MA, United States of America
[163] Department of Physics and Astronomy, University of California Irvine, Irvine CA, United States of America
[164] University of West Attica, Athens, Greece
[165] University of Sharjah, Sharjah, United Arab Emirates
[166] Department of Physics and Astronomy, University of Uppsala, Uppsala, Sweden
[167] Department of Physics, University of Illinois, Urbana IL, United States of America
[168] Instituto de Física Corpuscular (IFIC), Centro Mixto Universidad de Valencia - CSIC, Valencia, Spain
[169] Department of Physics, University of British Columbia, Vancouver BC, Canada
[170] Department of Physics and Astronomy, University of Victoria, Victoria BC, Canada
[171] Fakultät für Physik und Astronomie, Julius-Maximilians-Universität Würzburg, Würzburg, Germany
[172] Department of Physics, University of Warwick, Coventry, United Kingdom
[173] Waseda University, Tokyo, Japan
[174] Department of Particle Physics and Astrophysics, Weizmann Institute of Science, Rehovot, Israel
[175] Department of Physics, University of Wisconsin, Madison WI, United States of America
[176] Fakultät für Mathematik und Naturwissenschaften, Fachgruppe Physik, Bergische Universität Wuppertal, Wuppertal, Germany
[177] Department of Physics, Yale University, New Haven CT, United States of America
[178] Yerevan Physics Institute, Yerevan, Armenia

[a] Also Affiliated with an institute covered by a cooperation agreement with CERN
[b] Also at An-Najah National University, Nablus, Palestine
[c] Also at Borough of Manhattan Community College, City University of New York, New York NY, United States of America
[d] Also at Center for High Energy Physics, Peking University, China
[e] Also at Center for Interdisciplinary Research and Innovation (CIRI-AUTH), Thessaloniki, Greece
[f] Also at CERN, Geneva, Switzerland
[g] Also at CMD-AC UNEC Research Center, Azerbaijan State University of Economics (UNEC), Azerbaijan
[h] Also at Département de Physique Nucléaire et Corpusculaire, Université de Genève, Genève, Switzerland
[i] Also at Departament de Fisica de la Universitat Autonoma de Barcelona, Barcelona, Spain
[j] Also at Department of Financial and Management Engineering, University of the Aegean, Chios, Greece
[k] Also at Department of Mathematical Sciences, University of South Africa, Johannesburg, South Africa
[l] Also at Department of Physics, California State University, Sacramento, United States of America
[m] Also at Department of Physics, King's College London, London, United Kingdom
[n] Also at Department of Physics, Stanford University, Stanford CA, United States of America
[o] Also at Department of Physics, Stellenbosch University, South Africa

JHEP05(2025)038

[p] *Also at Department of Physics, University of Fribourg, Fribourg, Switzerland*
[q] *Also at Department of Physics, University of Thessaly, Greece*
[r] *Also at Department of Physics, Westmont College, Santa Barbara, United States of America*
[s] *Also at Faculty of Physics, Sofia University, 'St. Kliment Ohridski', Sofia, Bulgaria*
[t] *Also at Hellenic Open University, Patras, Greece*
[u] *Also at Henan University, China*
[v] *Also at Imam Mohammad Ibn Saud Islamic University, Saudi Arabia*
[w] *Also at Institucio Catalana de Recerca i Estudis Avancats, ICREA, Barcelona, Spain*
[x] *Also at Institut für Experimentalphysik, Universität Hamburg, Hamburg, Germany*
[y] *Also at Institute for Nuclear Research and Nuclear Energy (INRNE) of the Bulgarian Academy of Sciences, Sofia, Bulgaria*
[z] *Also at Institute of Applied Physics, Mohammed VI Polytechnic University, Ben Guerir, Morocco*
[aa] *Also at Institute of Particle Physics (IPP), Canada*
[ab] *Also at Institute of Physics, Azerbaijan Academy of Sciences, Baku, Azerbaijan*
[ac] *Also at National Institute of Physics, University of the Philippines Diliman (Philippines), Philippines*
[ad] *Also at Technical University of Munich, Munich, Germany*
[ae] *Also at The Collaborative Innovation Center of Quantum Matter (CICQM), Beijing, China*
[af] *Also at TRIUMF, Vancouver BC, Canada*
[ag] *Also at Università di Napoli Parthenope, Napoli, Italy*
[ah] *Also at University of Colorado Boulder, Department of Physics, Colorado, United States of America*
[ai] *Also at University of the Western Cape, South Africa*
[aj] *Also at Washington College, Chestertown, MD, United States of America*
[ak] *Also at Yeditepe University, Physics Department, Istanbul, Türkiye*
[*] *Deceased*

JHEP05(2025)038